EVALUATION OF TESTS PERFORMED ON ENERGY ABSORBING MATERIAL FOR PIPE WHIP RESTRAINTS

Commonwealth Edison Company
Byron and Braidwood Stations, Units 1 and 2
Project 4391/4392/4583/4684

A. K. Singh

Nuclear Safety Related
SAD File Index 8.15.1

Rev. 0 September 1984

Report No.
SAD-443

SARGENT & LUNDY ENGINEERS

Structural Analytical Division

Report Issue Summary

Project I.D.	Project Name	Byron/Braidwood	Number	4391/4392 4683/4684
	Client	Commonwealth Edison Company		
Document I.D.	Report Title	Evaluation of Tests Performed on Energy Absorbing Material for Pipe Whip Restraints		
	Report Number	SAD-443	Nuclear Safety Related	Yes [X] No [ ]

Revision No.&Date	Signatures	Date	Identification of Revised Pages
Rev. 0 9/24/84	Prepared by: AKSingh Reviewed by: M. Yang Approved by: [illegible]	9/24/84 9/24/84 9/24/84	

TABLE OF CONTENTS

LIST OF TABLES

LIST OF FIGURES

LIST OF FIGURES (continued)

LIST OF FIGURES (continued)

I. INTRODUCTION AND SUMMARY

In a meeting between NRC/NRR, NRC/Region III, CECo and Sargent & Lundy held on August 29, 1984 at the NRC/Region III offices in Glen Ellyn on the subject of Byron pipe whip restraint energy absorbing material, the NRC staff requested CECo to provide the following:

"Demonstrate how the qualification efforts to date bound all of the installed pipe whip restraint configurations. Provide a detailed discussion of all completed testing including testing for vertical stacking, precrushing and height-to-length and width ratio. The discussion should include an evaluation by a party other than the vendor of such things as the repeatability of precrushing test data and plots of vertical load versus displacement and vertical load versus energy absorbed. The discussion should also provide a comparison of the crush strengths of the materials tested and the crush strength of the installed material and the basis for concluding that the test results are applicable."

In addition, the NRC staff has requested clarification on the Byron angular configuration test results presented in S&L Report SAD-431, Revision 1. This includes justification for any measured data discarded, the significance of the larger than normal load oscillations on the load versus time plots and the justification for the 30% reduction in force magnitude for force measurements made using the new one million pound tup.

This report provides the requested information.

Section II presents the evaluation of the bounding tests used for qualification of the Energy Absorbing Material (EAM). For this evaluation, the 59 active pipe whip

restraints using the EAM are categorized into four broad categories based on the restraint configuration and pipe whip loading angularity on the EAM. For all the restraints in each of these four categories, the critical design parameters and the bounding test results are identified. Based on this analysis, it is concluded that the EAM qualification is bounded by available test results.

Section II also presents the bounding qualification analysis for the twelve field-cut EAMs. It is recognized that field cutting of EAMs requires added consideration for the qualification analysis, including consideration of field dimensional tolerance, a possible loss of precrush, a height-to-width ratio greater than two, stacking of EAMs vertically and stacking of EAMs side by side. It is shown that the available test data bounds the EAM qualification for the twelve field-cut EAMs. However, to confirm our judgment, additional confirmatory tests are recommended.

The available test data on EAM is evaluated to determine the conformance of the tests to the NRC Safety Review Plan (SRP) Section 3.6.2 requirements. The applicability of the test data to Byron EAMs and the need for additional tests to confirm our judgment are also presented. The available test data includes:

1. Byron Production Tests
2. Byron Angular Configuration Tests
3. Height Greater Than Width Tests
4. Tests on Vertically Stacked Specimens
5. Tests to Determine Effect of Precrush
6. Tests to Determine Material Variability

Sections III through VIII present Sargent & Lundy's evaluation of these test data. It is concluded that the results from these tests are applicable to Byron EAM. To the extent practical, the tests also meet the SRP requirements.

To provide added assurance, it is recommended that additional confirmatory tests be conducted. These additional tests include one axial compression test, one test for field dimensional tolerance effect, one test for height-to-width ratio of 2.10, one test on vertically stacked specimen and one test to determine the effect of the lack of precrush on peak crushing load of EAM. All tests will be conducted at design temperatures using Byron type 6000 psi EAM and the test parameters will meet the SRP requirements.

Section IV summarizes the Byron angular configuration test results. An evaluation of the measured data is provided to show that no measured data was discarded, only erroneous computed data was discarded. It is shown that the observed load oscillations are very high frequency oscillations (greater than 500 Hz) and thus not significant to structural design. Also, load oscillations due to load frequencies of 200 Hz or less are small and can be accommodated by the inherent restraint design margins. The rationale for the 30% reduction in force magnitude issue for the new tup is discussed. Our analysis shows that the tup calibration constant for the new tup is most likely too high and thus the 30% reduction in computed force magnitude is appropriate. To confirm our judgment, we will recalibrate the 1,000,000 lb. new tup and, if necessary, revise S&L Report No. SAD-431 to account for the new calibration constant.

II. BOUNDING TESTS FOR EAM QUALIFICATIONS

This section describes the various types of pipe whip restraints which have been used on the Byron project and the available applicable test data on the energy absorbing material under various loading conditions. An analysis of how the available test data bounds all the whip restraint EAM loading conditions is also presented. Based on this evaluation, it is concluded that the available test data bounds all loading conditions for all the pipe whip restraint EAMs at Byron.

A. Types of Pipe Whip Restraints

The purpose of pipe whip restraints is to stop the moving pipe once a break occurrs. This condition is realized when the total energy absorbed by the pipe and the restraint equals the external work done by the break force. The restraints can be designed to remain elastic or they can be designed to absorb the energy through plastic deformation. Due to the large reaction transferred to the structure by elastic restraint, the pipe whip restraints are generally designed to absorb the energy through plastic deformation. When this is done, the yielding member is sized to minimize the reaction transferred to the structure consistent with the maximum permissible deflection of the pipe.

The commonly used material for energy absorption for tensile loads is a yielding tension member, whereas for energy absorption for compressive loads it is a block of crushable energy absorption material (EAM). In the simplest application, when the pipe whip loading is unidirectional and the supporting primary structure is nearby, a single tension rod or an EAM block can be used to absorb the pipe break energy. These simple

restraint systems are shown in Figure II-1. Other possible variations of these restraint systems using the concept of unidirectional crushing of the EAM are shown in Figures II-2 and II-3.

When several break directions are feasible or the arrangement of the supporting structure is such that the above-described simple arrangements are not possible, pipe whip restraints (PWR) of the types shown in Figures II-4 and II-5 are used. The restraint shown in Figure II-4 has two compression legs. Each leg is composed of a compression structural member and an EAM block. The restraints of the type shown in Figure II-5 have one tension and one compression leg. For these two-legged restraints, the tension rod and EAM block can be sized to let the PWR absorb the pipe whip energy in tension or compression yielding. When energy absorption in tension yielding is desired, the EAM is sized not to crush, whereas the tension rod is sized to yield. When compression energy absorption is desired, the tension rod is sized not to yield, whereas the EAM is sized to be crushed.

A total of 79 pipe whip restraints which use the EAM to absorb the pipe whip energy have been designed for the Byron project by Sargent & Lundy. Of these 79 restraints, 20 have been deleted because the associated postulated pipe breaks have been eliminated. The remaining 59 restraints where EAM is utilized can be classified into four broad categories based on the energy absorbing mechanism and the resulting loading on the EAM.

Restraint Type Description	Type Category	Total Number in Category
Pipe whip restraints of the type shown in Figures II-2 and II-3 utilizing uniaxial crushing of the EAM	A	39
Two-legged compression pipe whip restraints of the type shown in Figure II-4 when the load direction is such that both legs are in compression	B	4
Two-legged tension/compression pipe whip restraints of the type shown in Figure II-5 utilizing crushing of the EAM	C	10
Two-legged tension/compression pipe whip restraints of the type shown in Figure II-5 utilizing yielding of the tension rod	D	6

Note that in the above table and for the discussion presented in this section restraints with multiple breaks (FWR-31 and RH-R1) have been placed in the more critical category. FWR-31 has been placed in Category C even though one of the breaks would put it in Category D. RH-R1 is also placed in C even though two of the three breaks would place it in Category A.

Table II-1 lists the 20 pipe whip restraints which are no longer required because the postulated pipe breaks associated with them have been eliminated. As shown in Table II-1, these deleted restraints are fairly evenly divided among the above four categories as follows.

Restraint Type Category	Number of Deleted Restraints in Category
A	6
B	4
C	4
D	6

No bounding test data analysis for these 20 deleted pipe whip restraints is provided because these restraints are no longer required to perform any safety functions.

B. Available Test Data

Several series of tests have been conducted on the Hexcel/Solarib EAM to determine its properties and behavior under different loading conditions and deformations. Test data and results from the following series have been used to support the design assumptions used in the design of Byron pipe whip restraints using the EAM:

1. Byron production dynamic and static tests conducted on specimens cut from each core block of EAM used to fabricate Byron pipe whip restraint. These tests are further discussed in Section III.

2. Byron angular configuration tests conducted to evaluate the reduction in energy absorbing capacity of the EAM when loaded in combined axial compression and lateral shear. These tests are further described in Section IV.

3. Tests conducted to determine the effect of height-to-width ratio on the energy absorbing capacity of the Hexcel/Solarib EAM. These tests are further discussed in Section V.

4. Tests performed to determine the effect of two or more vertically stacked EAM specimens on the energy absorbing capacity of Hexcel/Solarib EAM. These tests are described in Section VI.

5. Tests conducted to determine the effect of various degrees of precrush on the peak crush loads during impact loading of Hexcel/Solarib EAM. These tests are discussed in Section VII.

6. Tests conducted to determine the variability in the energy absorbing capacity and crush strength of Hexcel/Solariz EAM within a single core block of material. These tests are described in Section VIII.

The Byron production tests, mentioned in paragraph 1, were required by the EAM procurement specification. The Byron angular configuration tests were conducted at the request of the NRC staff to confirm the design assumption that no significant loss of energy absorbing capacity occurs when the EAM is loaded in both shear and direct compression. Tests mentioned in paragraphs

3 through 6 were performed by Hexcel/MCI to study the behavior of the Hexcel/Solarib EAM under various conditions of use.

C. Bounding Tests for EAM Qualification

As described in paragraph A above, the 59 pipe whip restraints still required by design, can be categorized into four different categories based on the mechanism of energy absorption and the resulting loading on the EAM. The bounding tests for pipe whip restraints in each of the four categories are discussed in the following paragraphs.

Bounding Tests for Type A Restraints

These types of restraints account for 39 of the 59 pipe whip restraints using EAM.

The typical restraints of this type are shown in Figures II-2 and II-3. For the restraint in Figure II-2, the pipe whip energy is absorbed in compression by pure axial crushing of the EAM. For the restraint of Figure II-3, again the pipe whip energy is absorbed in compression by pure axial crushing of the EAM. However, the crushing is due to the plunger type action of the tension member.

For the Type A restraint, the critical EAM parameter is its dynamic crush strength and the height-to-width (H/W) ratio of the EAM. The Byron production tests described in Section III establish that the dynamic crush strength of the EAM meets the design requirements. The height-to-width ratio tests

described in Section V show that up to a height to minimum width ratio of 2.0 there is no buckling or loss of the energy absorbing capacity of the EAM.

Table II-2 lists the 39 Type A restraints including their controlling height-to-width ratios. Observe that all H/W ratios are less than 2.0 except for Restraint RC3-4, for which the ratio is 2.09. This ratio is only marginally above the limiting ratio of 2.0 and, in our judgment, is acceptable. Thus for all practical purposes, the test data bounds the EAM configuration and loadings for all 39 Type A restraints. To confirm our judgment on restraint RC3-4 with a H/W ratio of 2.09, an additional test is planned with a H/W ratio of 2.10 as described in Section V.

Bounding Tests For Type B Restraints

Type B restraints account for four of the 59 restraints. The typical restraint configuration is shown in Figure II-4. For this type of restraint design, the pipe whip energy is absorbed by crushing the EAM in the two legs.

The typical deformation of these restraints under a pipe whip load inducing compression in both legs is shown in Figure II-6. To conservatively estimate the maximum lateral shear deformations of the EAMs, it is assumed here that all deformations are localized within the EAMs. For this postulated restraint behavior, the EAM is loaded in combined lateral shear and axial compression. In general, the bending of the pipe collar assembly and the compression legs will permit rotation of the legs and this will result in a more axial compression of the EAM.

When the deformed shape of the EAM in Figure II-6 is compared to those in the Byron angular configuration tests (see Figure IV-1, Section IV), it can be observed that the EAM deformation is identical. In the test setup, the anvil forces the EAM to crush at an angle offset from the axial direction. This offset causes lateral shear and axial compression in the EAM similar to that in the pipe whip restraints. Thus it is concluded that the test results are directly applicable to these Type B restraints.

In the Byron angular configuration tests, the EAM was loaded to 125% of design energy in 90° and 120° anvil configurations. The test was set up to prove that the EAM is functional at the following EAM load angularities.

Anvil Angle	Load Angularity
90°	45°
120°	60°

Table II-3 presents the computed EAM load angularities for four Type B restraints. The table also presents the included angles between the two compression legs. Based on Table II-3, it is concluded that the Byron angular configuration tests bound the design of these four Type B restraints, both in terms of the EAM load angularities and the included leg angle.

Table II-3 also lists the H/W ratios for the EAMs in these four restraints. These H/W ratios are all less than 2.0, thus the height greater than width test data bound the qualification of these EAM for H/W ratios.

Bounding Tests for Type C Restraints

Type C restraints account for ten of the 59 restraints using EAM. The typical Type C restraint is shown in Figure II-5. The pipe whip loading causes tension in one leg and compression in the other. In Type C restraints, the tension leg yield capacity is large so that yielding does not occur. The pipe whip energy is absorbed by crushing the EAM in the compression leg.

For the Type C restraints, two alternate loading/deformation conditions for the EAM may be postulated. When the pipe whip restraint is idealized as a two-leg truss where restraint leg rotation is possible at the structural connections and the pipe collar, the EAM deformation is purely axial as shown in Figure II-7. In this figure the solid lines denote the restraint in the initial undeformed shape, whereas the dotted lines show the deformed shape of the restraint and EAM. For this postulated behavior the EAM is loaded in pure compression. The Byron production tests bound this EAM loading and deformation. Note that "hinges" are not necessarily required to permit this behavior because the required rotations are small (generally less than 10^{o}). Flexibility of the whip restraint legs and the pipe collar are enough to accommodate these small rotations.

Alternatively, when we postulate that the restraint legs and the pipe collar are rigid, no joint rotations are possible. For this case, the restraint deformed shape is shown in Figure II-8. In this figure the solid lines denote the initial shape of the restraint, whereas the dotted lines show the restraint and the EAM in its deformed shape. For this postulated restraint behavior, the EAM is loaded in combined lateral shear

and axial compression. As the tension rod remains elastic (by design), it can only move normal to its length. The EAM crushes at an angle α to satisfy compatibility. The load angularity, α, is given by

$$\alpha = (\theta_1 + \theta_2 - 90^\circ)$$

where θ_1 and θ_2 define the orientation of the compression and tension leg, respectively. When this EAM deformed shape is compared to those induced in the Byron angular configuration tests (see Figure IV-1, Section IV), the deformed EAM shapes are the same. In the test setup, the anvil forces the EAM to crush at an angle offset from the axial direction. This offset causes lateral shear and axial compression in the EAM similar to that in the pipe whip restraint.

In the Byron angular configuration tests, the EAM was loaded to 125% of its design capacity in the 90° and 120° anvil angle configuration. The test setup was to prove that the EAM is functional for the following EAM load angularities:

Anvil Angle	Load Angularity
90°	45°
120°	60°

Table II-4 presents all Type C restraints and the computed load angularities for the EAM under the postulated pipe whip loading. Based on Table II-4, it is concluded that the Byron angular configuration tests bound the EAM design of these ten Type C restraints, even when the more conservative assumption that restraint legs and pipe collar are rigid is made.

The nonlinear large deflection finite element analysis of Type C pipe whip restraints SI3R-640A, FWR-35 and FWR-16, presented in S&L report SAD-442, dated September 1984 and being submitted to the NRC, shows that the actual deformation of the EAM is closer to the behavior predicted by the truss model of Figure II-7 than by the rigid plastic model of Figure II-8. The maximum EAM strain in the finite element analysis was computed to be only 21% and the deformation was predominantly axial. The design allowable EAM strain is 50%.

Based on the above evaluation, it is concluded that the design of the EAM for Type C restraints is bounded by the Byron production tests and by the Byron angular configuration tests.

Table II-4 also lists the H/W ratios for the EAMs. These H/W ratios are all less than 2.0, thus the height greater than width tests bound the qualification of these EAM for H/W ratios.

Bounding Tests for Type D Restraints

Type D restraints account for six of the 59 restraints using EAM. These six restraints are listed in Table II-5. The typical Type D restraint is shown in Figure II-5. For Type D restraints, the pipe whip loading causes tension in one leg and compression in the other leg. In Type D restraints, the EAM crushing capacity is large so that crushing does not occur. The pipe whip energy is absorbed by yielding of the tension rod. Under these conditions, there was no need to provide the EAM in the compression leg. However, the EAM was provided for a break which has been deleted.

As the pipe whip energy is being absorbed by yielding of the tension rod, the restraint function is unaffected by the crushing behavior of the EAM. The Byron production test on the EAM assures us that premature crushing of the EAM will not occur and that the restraints will perform their intended function.

D. Bounding Tests for Field Cut EAM

During the final stages of construction on Byron Unit 1, it became necessary to modify the EAM of twelve active pipe whip restraints due to field interference problems, final as-built analysis, and larger than predicted pipe thermal movement during the hot functional testing. These twelve restraints and the reasons for the modifications are listed below:

Restraint	Reasons for Field Cut
MS-R4X	As-built analysis
MS-R12X	As-built analysis
MS-R18	Hot functional modification
MS-R19	Hot functional modification
MS-P26	As-built analysis
FWR-8	Resolution of field problem
FWR-14	As-built analysis
RH-R1	Redesign because of field problems
SI1R-35B	Resolution of field problem
SI3R-660B	Redesign because of field problems
MS-R16	Hot functional modification
MS-R44	Resolution of field problems

Due to schedule constraints and lack of available EAM material at Hexcel, it was not possible to get the revised EAM pieces fabricated at the Hexcel shop. Instead the EAM pieces were fabricated at the Byron

site using EAM from deleted restraints and restraints from Byron Unit 2 and Braidwood Units 1 and 2. This field fabrication involved field cutting of the EAM.

The isometric view of the field-fabricated EAM for these twelve restraints is shown in Figures II-9 through II-20. These figures show the direction of loading, the sides of the EAM which were field-cut (marked by ✓) and the net effect of the field fabrication on the EAM. These effects include the possible loss of precrush, H/W ratio greater than 2.0, vertical (one on top of the other) stacking and horizontal (side by side) stacking. The figures also list the restraint design margins. The restraint design margins for restraints where a loss of precrush has occurred have been reduced by a factor of 1.17 to account for the increase in force due to the loss of precrush. Note that for restraints MSR-18, the 4" x 4" vertically stacked pieces are not needed per design and thus are not addressed in this report.

The field cutting of the EAMs requires that the additional effects be considered in the bounding test analysis presented in paragraph C above. These effects include field-cut dimensional tolerances, H/W ratios larger than two, the possible loss of precrush, the effects of vertical stacking and the effects of side by side stacking of the EAM pieces. These effects are evaluated in the following paragraphs.

To determine the maximum dimensional tolerance of the field-cut EAM pieces, all accessible pieces were measured for skewness and concavity. Skewness is described in Figure II-21a and is defined as the difference between the top (w_t) and the bottom dimension (w_b) of the EAM piece. The concavity is

defined in Figure II-21b and is defined as the difference between the middle (w_m) and the average of the top and bottom dimensions of an EAM piece. Table II-6 presents the measurements for skewness for the 14 pieces of field-cut EAM where measurements were possible without disassembly. It is observed that the maximum skewness is 5/16 inches on a 12 inch wide EAM piece and 1/4 inch skewness on a 4-3/4 inch piece. For the nine pieces of field-cut EAM where concavity measurement was possible without disassembly, no concavity was observed. Based on these measurements, it is our judgment that existing tests conducted on 4 x 4 x 4 inch specimen with a dimensional tolerance of $\pm$1/8 inch bound the effect of field dimensional tolerance. To confirm this judgment, we will perform a test on a 4 x 4 x 4 inch specimen with a 1/4 inch skewness. The specimen will be cut from Byron type 6000 psi EAM.

The field cutting of the EAM resulted in a H/W ratio larger than 2.0 for EAMs in restraints MS-R19, MS-P26 and SI3R-660B. The field cut EAM for restraint MS-P26 will be fully encased in a structural box, thus buckling of the EAM would not be possible. Similarly for restraint MSR-19, the EAM will be supported by structural plates to limit the H/W ratio to 2.0 to avoid any possible buckling of the 2" piece. For restraint SI3R-660B, the stacked EAM pieces are separated by a braced structural plate to prevent buckling. The two individual pieces of EAM do not exceed the H/W ratio of 2.0.

For restraints MS-R18, MS-P26, SI3R-660B and MS-R44, the field fabrication resulted in stacking of EAM pieces vertically. For SI3R-660B, the stacked EAM pieces are separated by a structural plate. For

restraints MS-R18, MS-P26 and MS-R44, no separator plate is used between the stacked EAM pieces. The test results presented in Section VI show that vertical stacking has no significant effect on the ADCS of the EAM. However, in all the stacked EAM tests, a 0.02-inch separator plate was used between the EAM pieces. As the 0.02-inch separator plate was not used in MS-R18, MS-P26 and MS-R44, additional tests will be conducted to evaluate this effect as described in Section VI.

Field fabrication has resulted in side by side stacking in six of the twelve restraints. This side by side stacking does not in any way reduce the ADCS of the EAMs, provided the EAM crushing is axial and the critical H/W ratio for each of the stacked EAM pieces is less than 2.0. This H/W requirement is met for all the field-cut EAM pieces which are not laterally supported by a structural box as discussed previously. Thus, no additional tests are needed.

Field cutting of EAMs has resulted in a possible loss of precrush for EAMs in restraints MS-R19, MS-P26, RH-R1, SI1R-35B and MS-R16. The loss of precrush may result in a small increase in the peak crushing force of EAMs. Accounting for a nominal 17% increase in peak crush force for these four restraints, the restraint design margins were computed at 5.09, 2.40, 1.14, 1.84 and 4.23 for restraints MS-R19, MS-P26, RH-R1, SI1R-35B and MS-R16, respectively. Thus the EAM behavior is bounded by design margins. Section VII describes the precrush test results and proposed additional confirmatory tests.

Based on the above evaluation, we conclude that the existing tests bound the EAM behavior for the twelve field-cut EAMs. Additional confirmatory tests are planned to provide added assurance. Based on the results of the confirmatory tests, we will revise restraint drawings to provide guidance for all future field fabrication of EAM.

TABLE II-1: DELETED RESTRAINTS AND THEIR CLASSIFICATIONS

No.	Restraint	Type
1	MS-P6	B
2	MS-P14	B
3	MS-P21	B
4	MS-P29	B
5	FWR-4	C
6	FWR-6	C
7	FWR-7	A
8	FWR-13	D
9	FWR-16	D
10	FWR-17	A
11	FWR-25	D
12	FWR-26	A
13	FWR-27	D
14	FWR-28	A
15	FWR-30	D
16	FWR-35	C
17	FWR-36	D
18	FWR-38	C
19	FWR-40	A
20	SI1R-170A	A

TABLE II-2: HEIGHT-TO-WIDTH RATIOS FOR TYPE A RESTRAINTS

No.	Restraint	EAM H/W Ratio
1.	MS-R4X	1.40
2.	MS-R12X	1.20
3.	MS-R16	0.75
4.	MS-R18	0.92
5.	MS-R19	2.00 (*)
6.	MS-R28	1.33
7.	MS-R32	1.54
8.	MS-R34X	0.82
9.	MS-R35C	0.55
10.	MS-R36	0.73
11.	MS-R49X	2.08
12.	MS-R64X	0.82
13.	FWR-1	0.88
14.	FWR-8	0.80
15.	FWR-10	0.44
16.	FWR-11	0.58
17.	FWR-14	0.67
18.	FWR-15	1.20
19.	FWR-18	0.93
20.	FWR-29	0.62
21.	FWR-31	0.53
22.	FWR-37	0.62
23.	RY-2	1.21
24.	RY-3	0.78
25.	RY-4	1.03
26.	RY-5	0.98
27.	RY-6	0.46
28.	RY-7	0.52
29.	RY-8	1.29
30.	RC2-6	1.20
31.	RC3-4	2.09

Table II-2 (continued)

No.	Restraint	EAM H/W Ratio
32.	RC3-6	1.20
33.	RC4-4	1.17
34.	RC4-6	1.20
35.	SI1R-35B	1.67
36.	SI3R-660B	1.71
37.	MS-R44	1.00 (+)
38.	MS-P26	**
39.	RC2-4	1.60

** = No buckling is possible because the EAM will be fully encased by structural steel plates.

* = EAM will be structurally supported to limit the H/W ratio to 2.0.

+ = EAM is structurally supported to prevent lateral buckling in the other direction

TABLE II-3: TWO LEG COMPRESSION (TYPE B) RESTRAINTS

No.	Restraint	EAM Load Angularity *	Angle Between Legs	H/W Ratio
1.	MS-R4	20°	90°	0.83
2.	MS-R33	49°	90°	0.67
3.	MS-R48	45°	90°	1.40
4.	FWR-2	44°	60°	1.28

* Angle between the load direction and the EAM which is being crushed.

TABLE II-4: COMPRESSION YIELD TENSION-COMPRESSION (TYPE C) RESTRAINTS

No.	Restraint	EAM Load Angularity	H/W Ratio
1.	MS-R1	3°	0.53
2.	MS-R2	2°	0.84
3.	MS-R9	0°	1.24
4.	MS-R10	5°	0.84
5.	FWR-3	23°	0.24
6.	RH-R1	14°	1.02
7.	RH-R3	11°	0.50
8.	SI1R-10B	26°	0.75
9.	SI3R-640A	55°	0.75
10.	SI3R-15B	49°	0.75

TABLE II-5: TENSION YIELD TWO-LEG TENSION-COMPRESSION TYPE D RESTRAINTS (*)

No.	Restraint
1	MS-R11
2	MS-R49
3	MS-P10
4	MS-P25
5	FWR-12
6	FWR-39

* Restraint FWR-31 is not listed because it has multiple breaks and is listed under Type C.

TABLE II-6: MEASURED SKEWNESS IN ACCESSIBLE FIELD-CUT EAMS

Restraint #	Block #	Face #	EAM Dimensions (in) H	W_t	W_b	Skewness (in) $(W_t - W_b)$
MS-R18	1	1	8	*	*	
		2	8	11-15/16	11-15/16	0
		3	8	*	*	
		4	8-1/16	11-7/8	11-7/8	0
MS-R18	2	1	2-7/8	*	*	
		2	2-15/16	11-3/4	11-3/4	0
		3	2-13/16	*	*	
		4	2-7/8	11-7/8	11-13/16	1/16
MS-R18	3	1	8-1/16	*	*	
		2	7-15/16	11-15/16	11-15/16	0
		3	8	*	*	
		4	8	12	12	0
MS-R18	4	1	2-13/16	*	*	
		2	2-7/8	12	12	0
		3	2-15/16	*	*	
		4	2-3/4	12-1/8	11-13/16	5/16
MS-P26	5	1	8-3/16	13-15/16	13-15/16	0
		2	8-3/16	6-1/2	6-1/2	0
		3	8-3/16	13-15/16	13-15/16	0
		4	8-3/16	6-1/2	6-1/2	0
MS-P26	6	1	8-1/8	13-15/16	13-15/16	0
		2	8-1/8	6-7/16	6-7/16	0
		3	8-1/8	13-15/16	13-15/16	0
		4	8-1/8	6-7/16	6-7/16	0
MS-P26	7	1	3-15/16	13-15/16	13-15/16	0
		2	3-15/16	6-1/2	6-1/2	0
		3	3-15/16	13-15/16	13-15/16	0
		4	3-15/16	6-1/2	6-1/2	0
MS-P26	8	1	4-3/16	13-15/16	13-15/16	0
		2	4-3/16	6-3/8	6-3/8	0
		3	4-3/16	13-15/16	13-15/16	0
		4	4-3/16	6-3/8	6-3/8	0
FWR-8	9	1	7-11/16	8-3/4	8-3/4	0
		2	7-11/16	9-3/8	9-5/16	1/16
		3	7-5/8	*	*	
		4	7-11/16	*	*	

TABLE II-6 (continued)

Restraint #	Block #	Face #	EAM Dimensions (in) H	W_t	W_b	Skewness (in) $(W_t - W_b)$
FWR-14	10	1	4-1/8	8-15/16	8-15/16	0
		2	4-1/8	6-1/8	6-1/8	0
		3	4-1/8	9	9	0
		4	4-1/8	6-1/8	6-1/8	0
MS-R44	11	1	7-1/16	17	17	0
		2	7-1/16	5	5	0
		3	7-1/16	17	17	0
		4	7-1/16	5	5	0
MS-R44	12	1	10	17	17	0
		2	10-3/16	5-1/64	5	1/64
		3	10-3/16	17	17	0
		4	10	4-5/16	5	1/16
MS-R44	13	1	7-1/16	17	17	0
		2	7	5	5	0
		3	7	17	17	0
		4	7-1/16	5	5	0
MS-R44	14	1	10-1/16	17	17	0
		2	10-1/16	4-5/8	4-3/4	1/8
		3	10-1/16	17	17	0
		4	10-1/16	4-3/4	5	1/4

* Denotes dimension inaccessible.

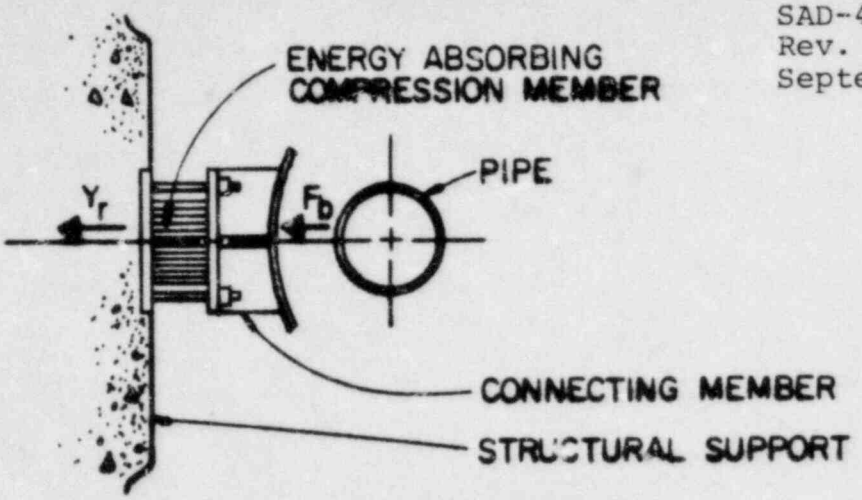

COMPRESSION RESTRAINT

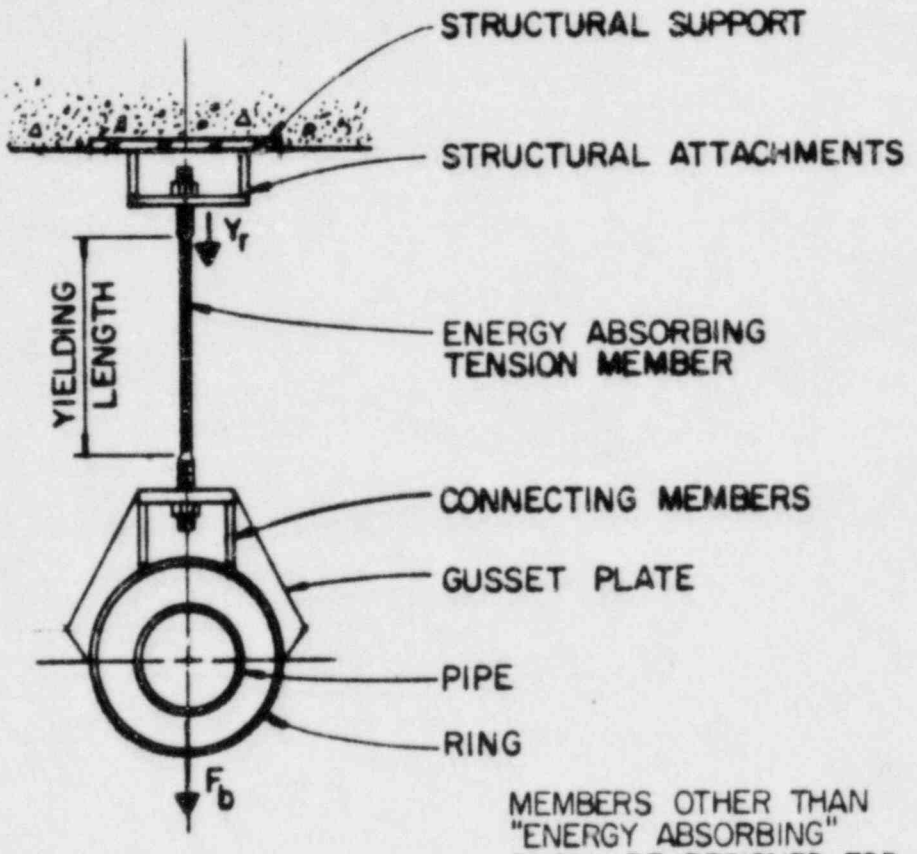

MEMBERS OTHER THAN "ENERGY ABSORBING" SHALL BE DESIGNED FOR 1.25R TO PREVENT THEIR YIELDING OR BUCKING. ($Yr = 1.25R$)

TENSION RESTRAINT

SIMPLE PIPE WHIP RESTRAINTS

FIGURE II-1

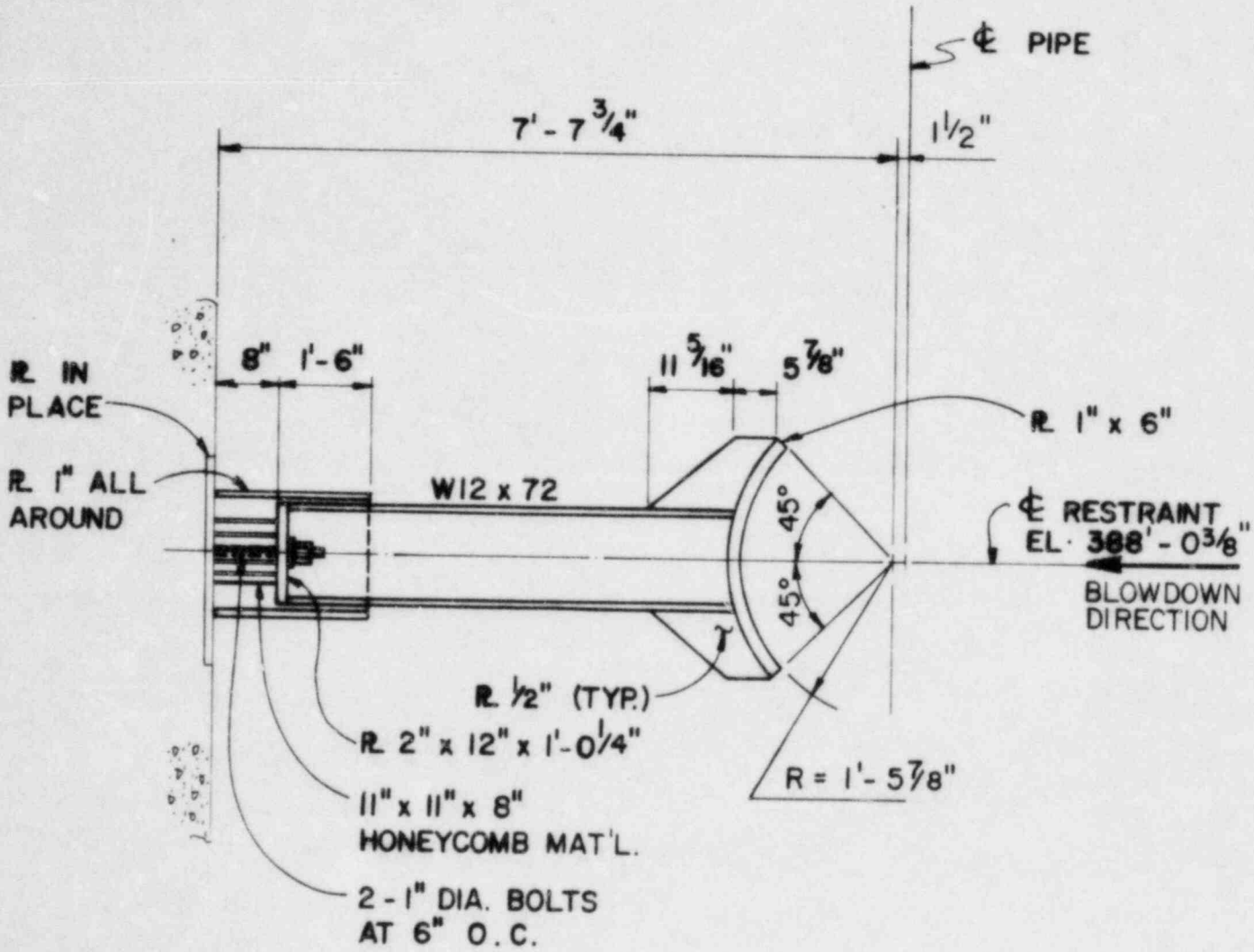

TYPICAL WHIP RESTRAINT UTILIZING SINGLE COMPRESSION MEMBER CONCEPT

FIGURE II-2

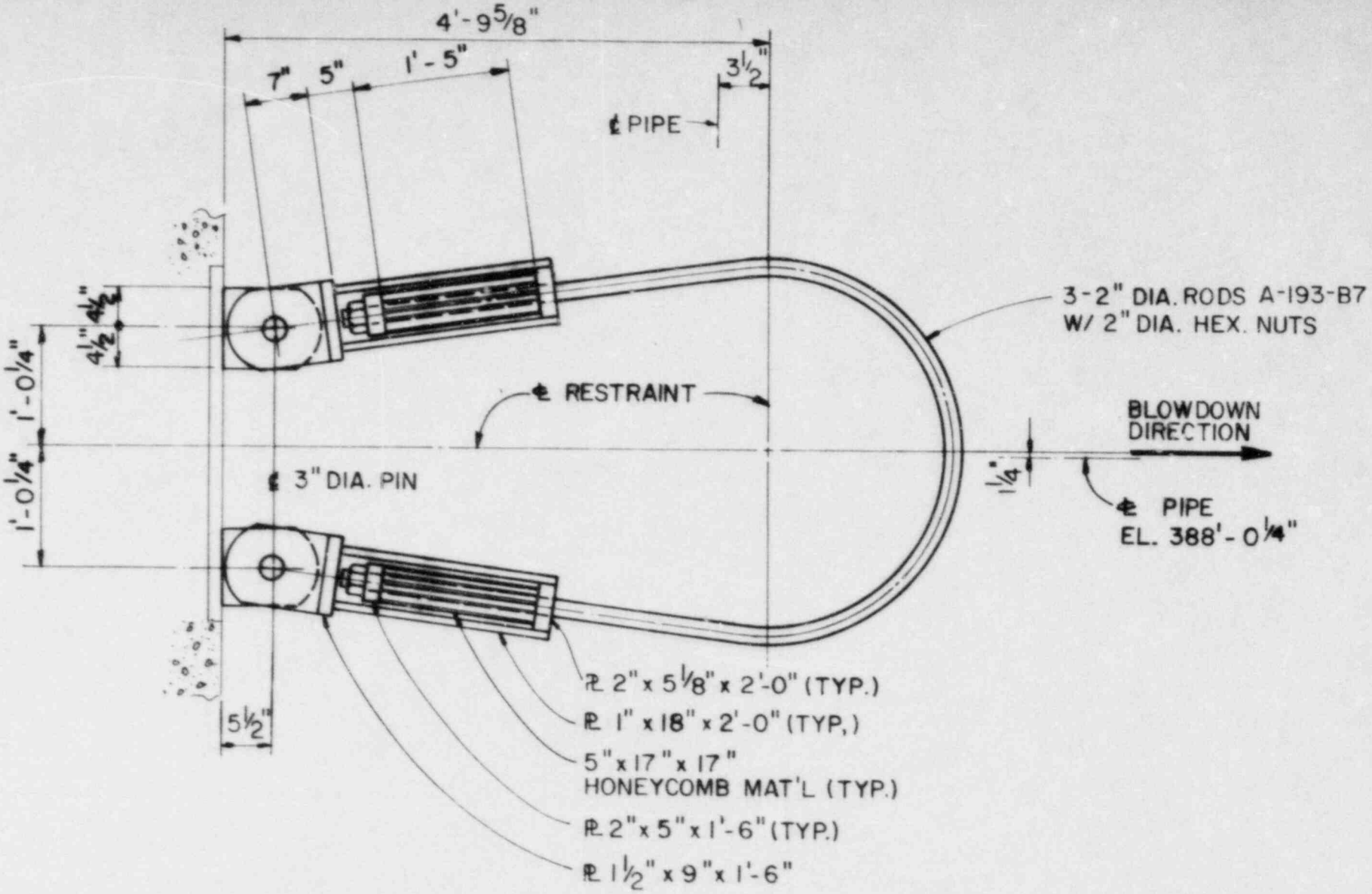

TYPICAL WHIP RESTRAINT UTILIZING PLUNGER TYPE CONCEPT

FIGURE II-3

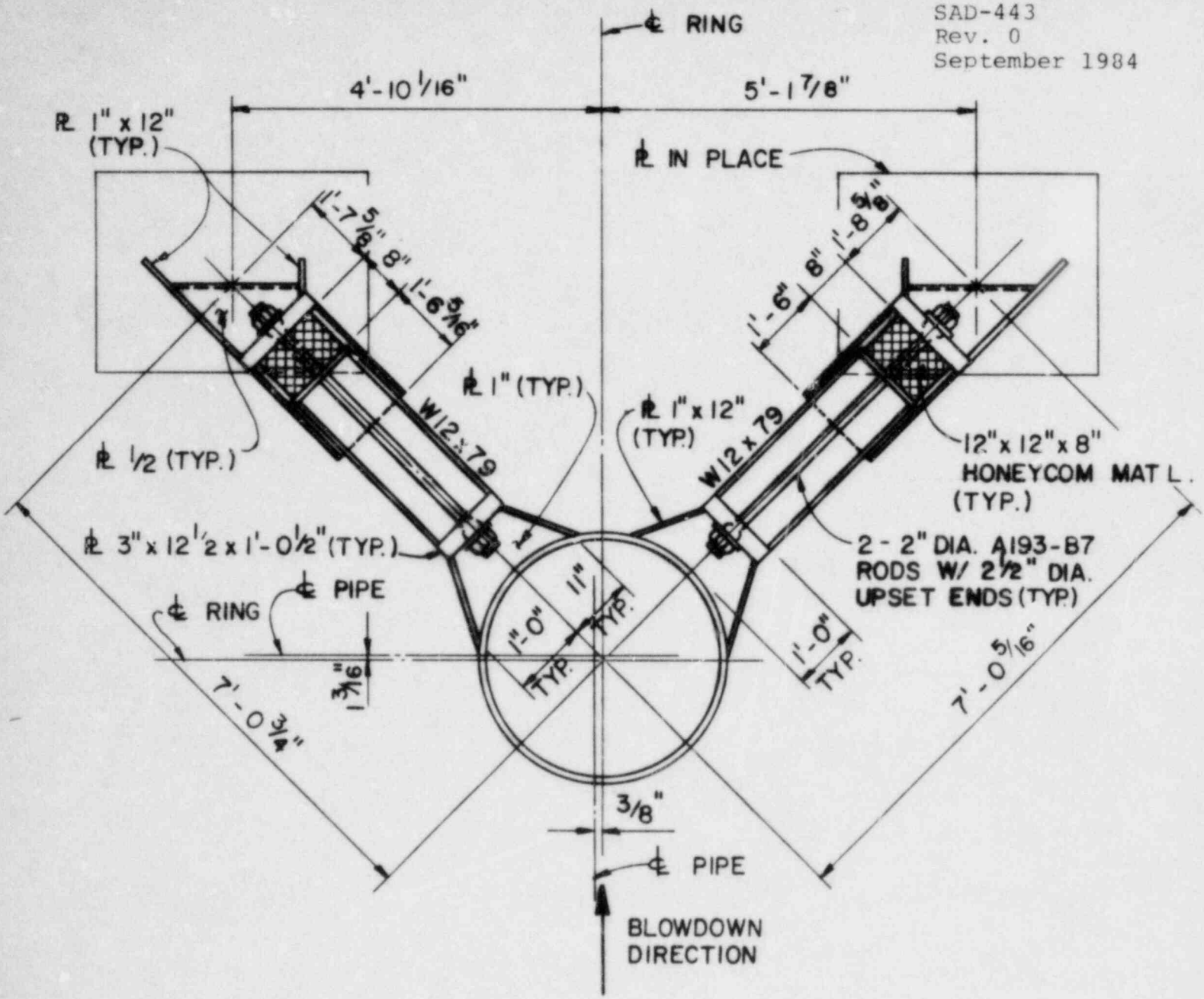

TYPICAL WHIP RESTRAINT UTILIZING TWO COMPRESSION MEMBERS CONCEPT

FIGURE II - 4

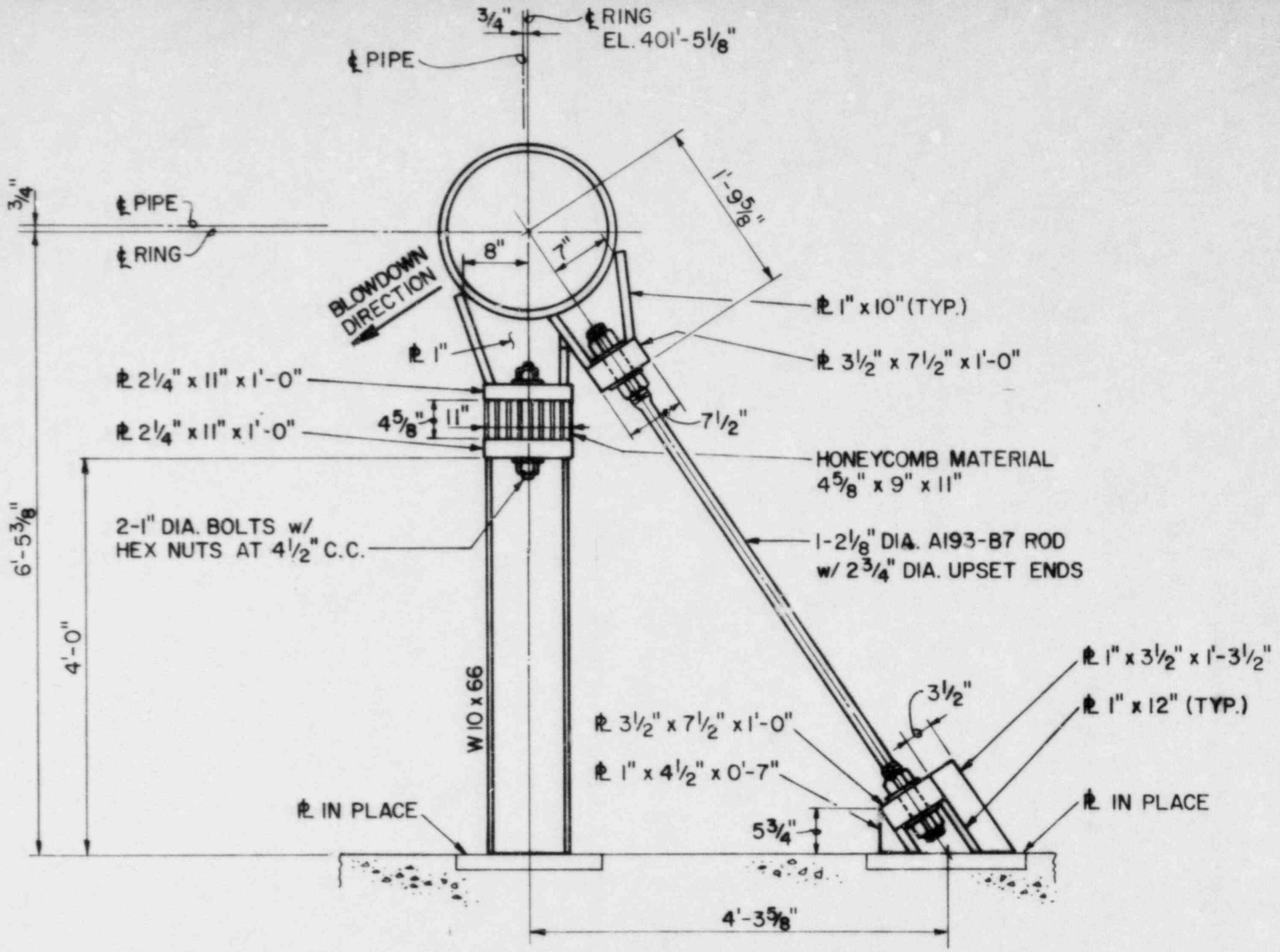

TYPICAL WHIP RESTRAINT UTILIZING
TENSION-COMPRESSION MEMBER CONCEPT

FIGURE II - 5

SAD-443
Rev. 0
September 1984

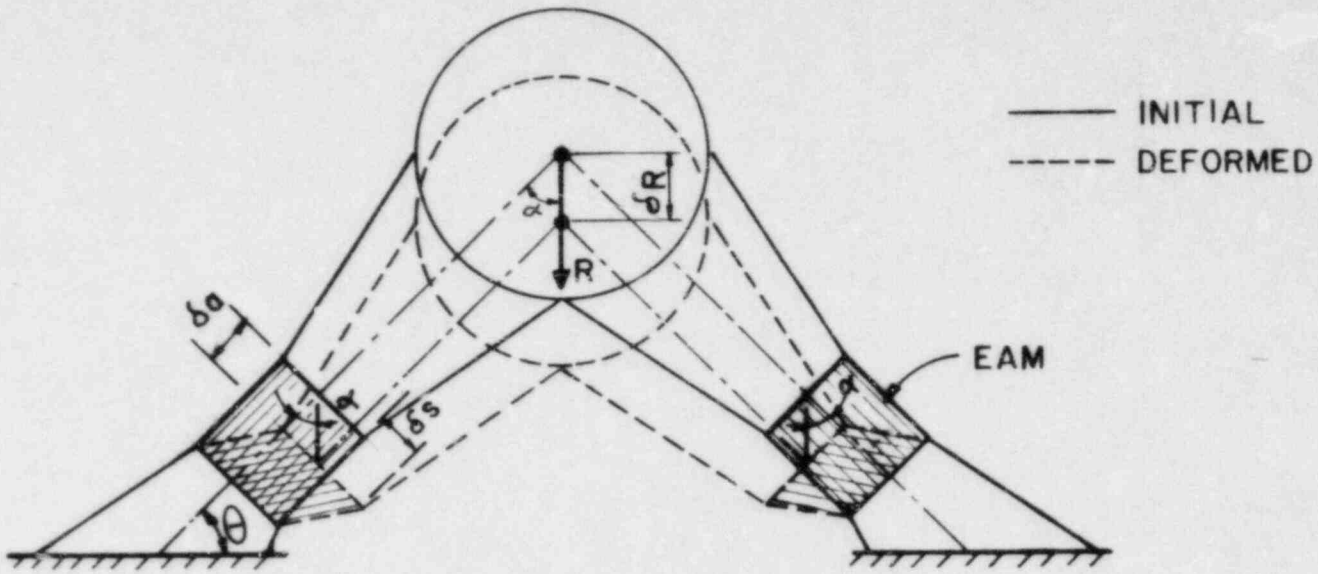

BEHAVIOR OF TWO-LEGGED RESTRAINT WHEN BOTH LEGS ARE IN COMPRESSION

FIGURE II-6

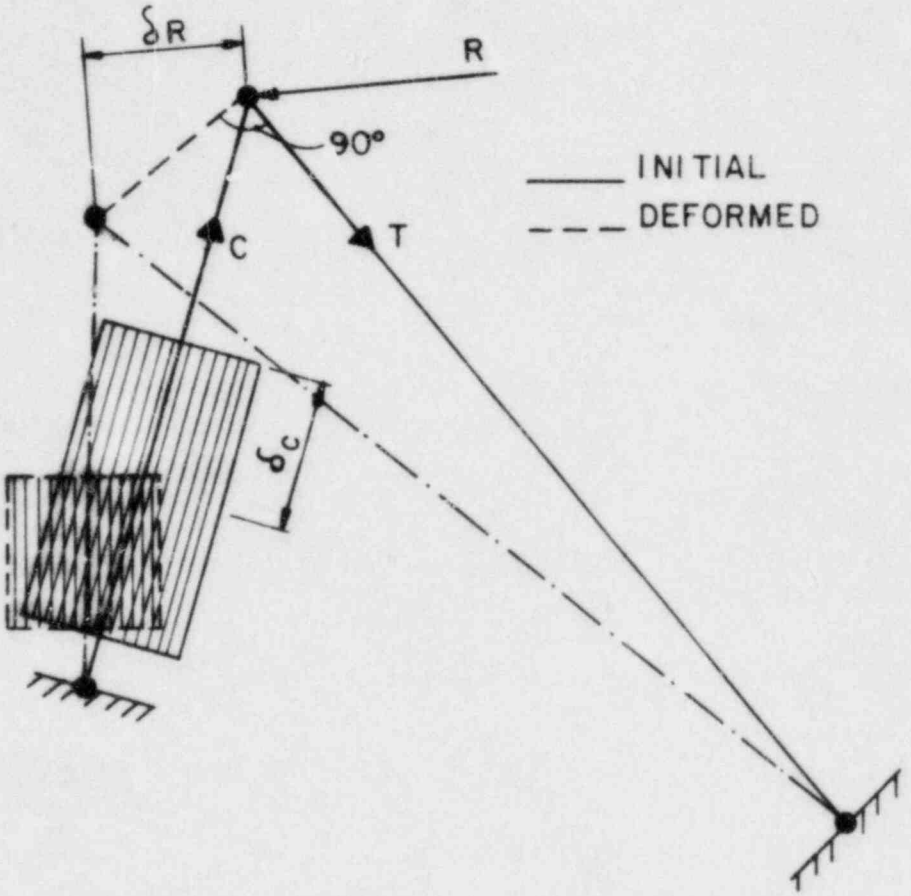

BEHAVIOR OF TENSION-COMPRESSION TWO LEGGED RESTRAINT WHEN COMPRESSION YIELDING ABSORBS THE ENERGY AND ROTATION AT PIPE RING AND SUPPORTS IS ASSUMED

FIGURE II-7

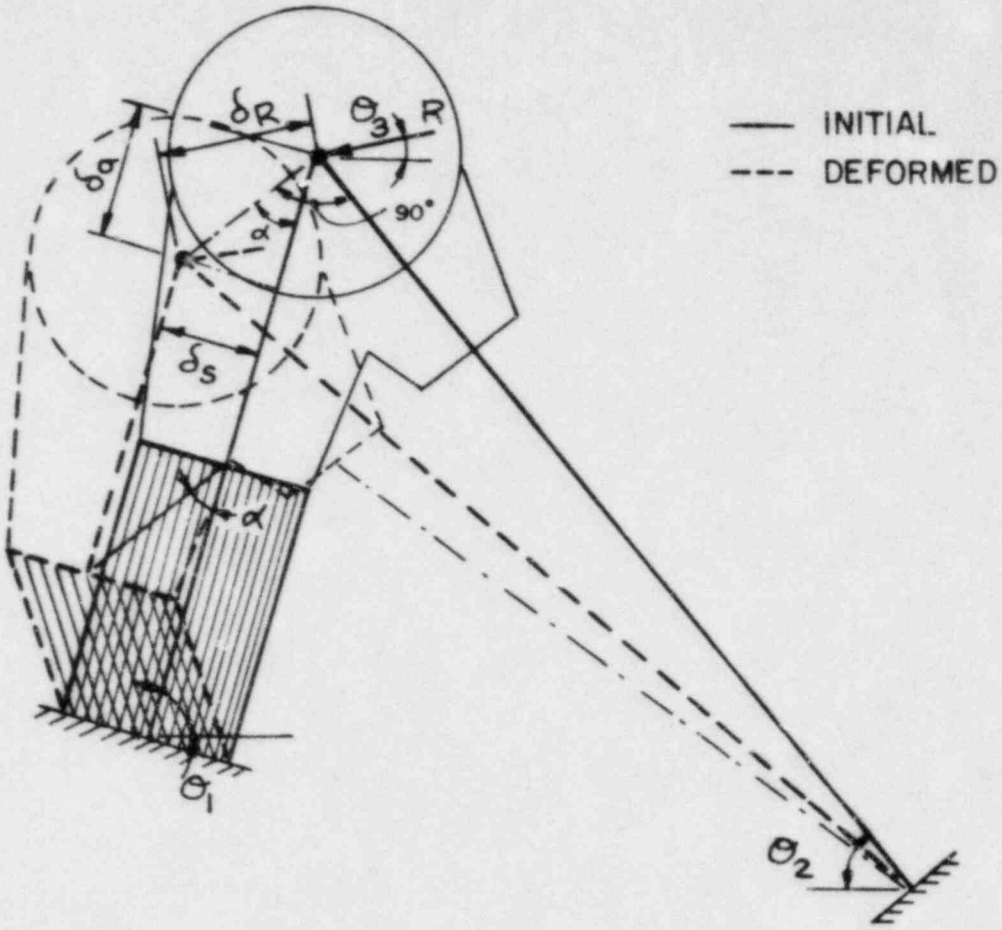

BEHAVIOR OF TENSION-COMPRESSION TWO-LEGGED RESTRAINT WHEN COMPRESSION YIELDING ABSORBS THE ENERGY AND NO ROTATION AT SUPPORT OR PIPE RING IS ASSUMED

FIGURE II-8

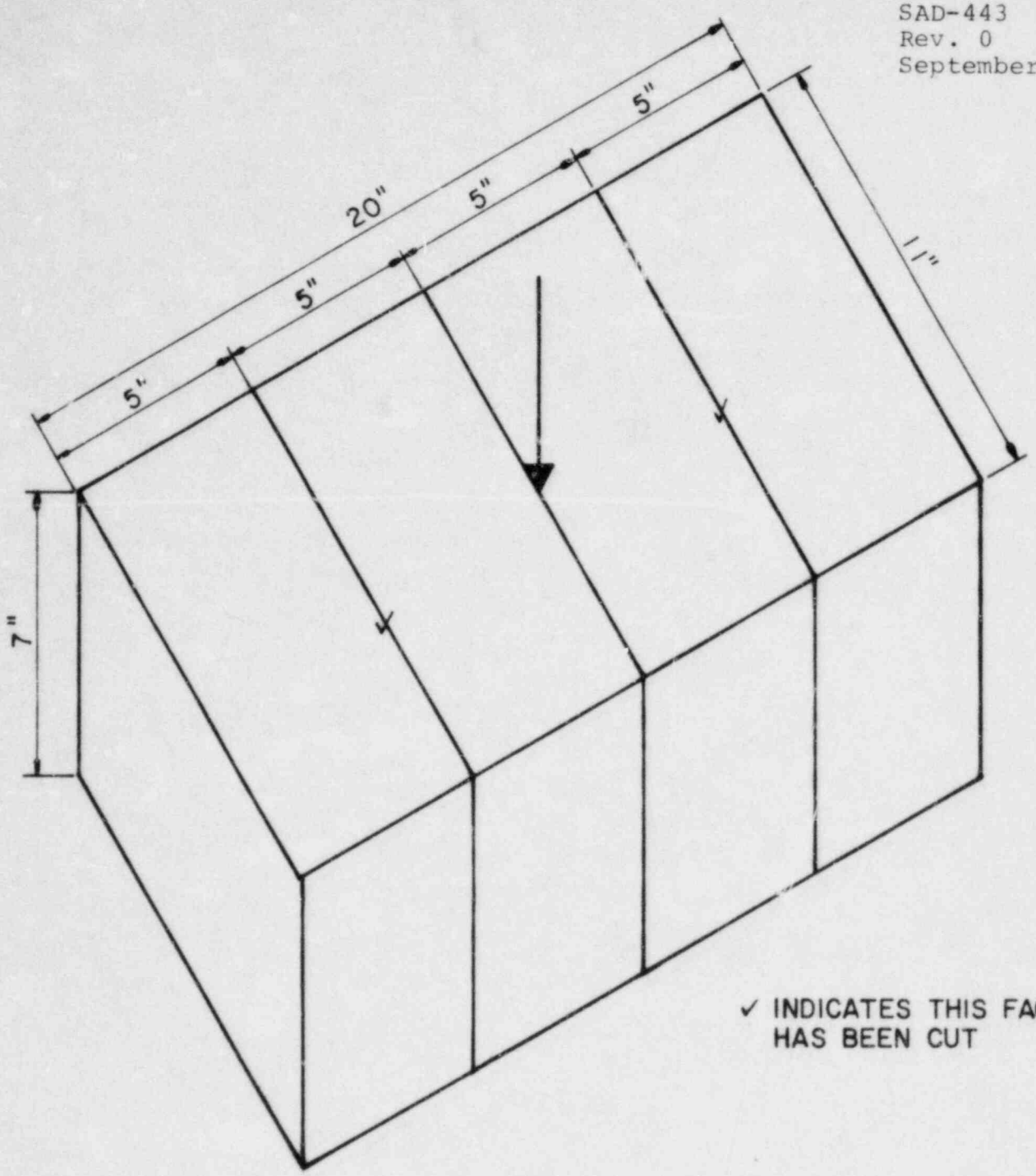

✓ INDICATES THIS FACE HAS BEEN CUT

	YES	NO
VERTICAL STACK		X
HORIZONTAL STACK	X	
VERTICAL CUT	X	
HORIZONTAL CUT		X
LOSS OF PRECRUSH		X

RESTRAINT DESIGN MARGIN = 1.40

FIELD CUT EAM FOR RESTRAINT MS-R4X

FIGURE II-9

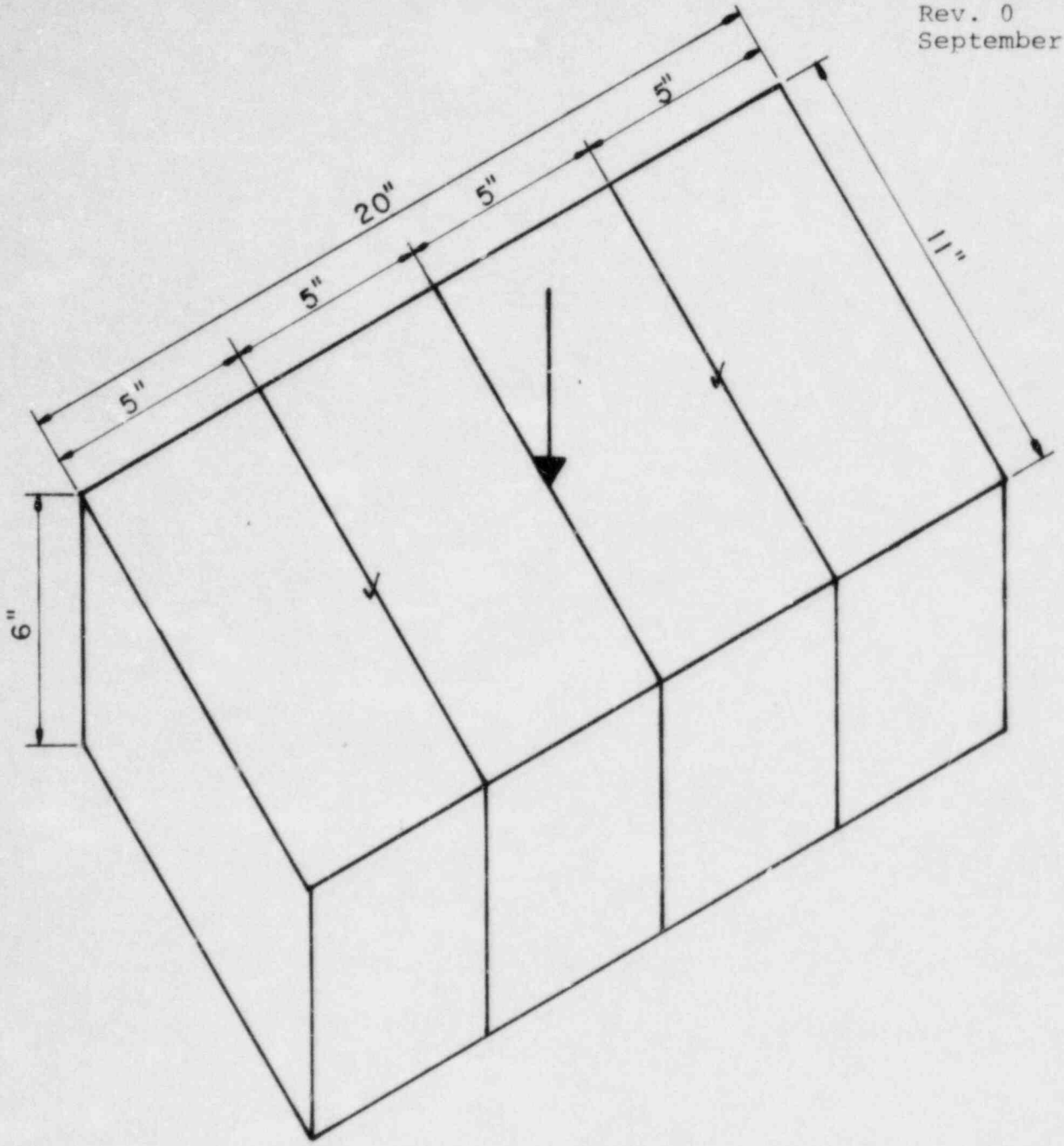

√ INDICATES THIS FACE HAS BEEN CUT

	YES	NO
VERTICAL STACK		×
HORIZONTAL STACK	×	
VERTICAL CUT	×	
HORIZONTAL CUT		×
LOSS OF PRECRUSH		×

RESTRAINT DESIGN MARGIN = 1.41

FIELD CUT EAM FOR RESTRAINT MS-R12X

FIGURE II-10

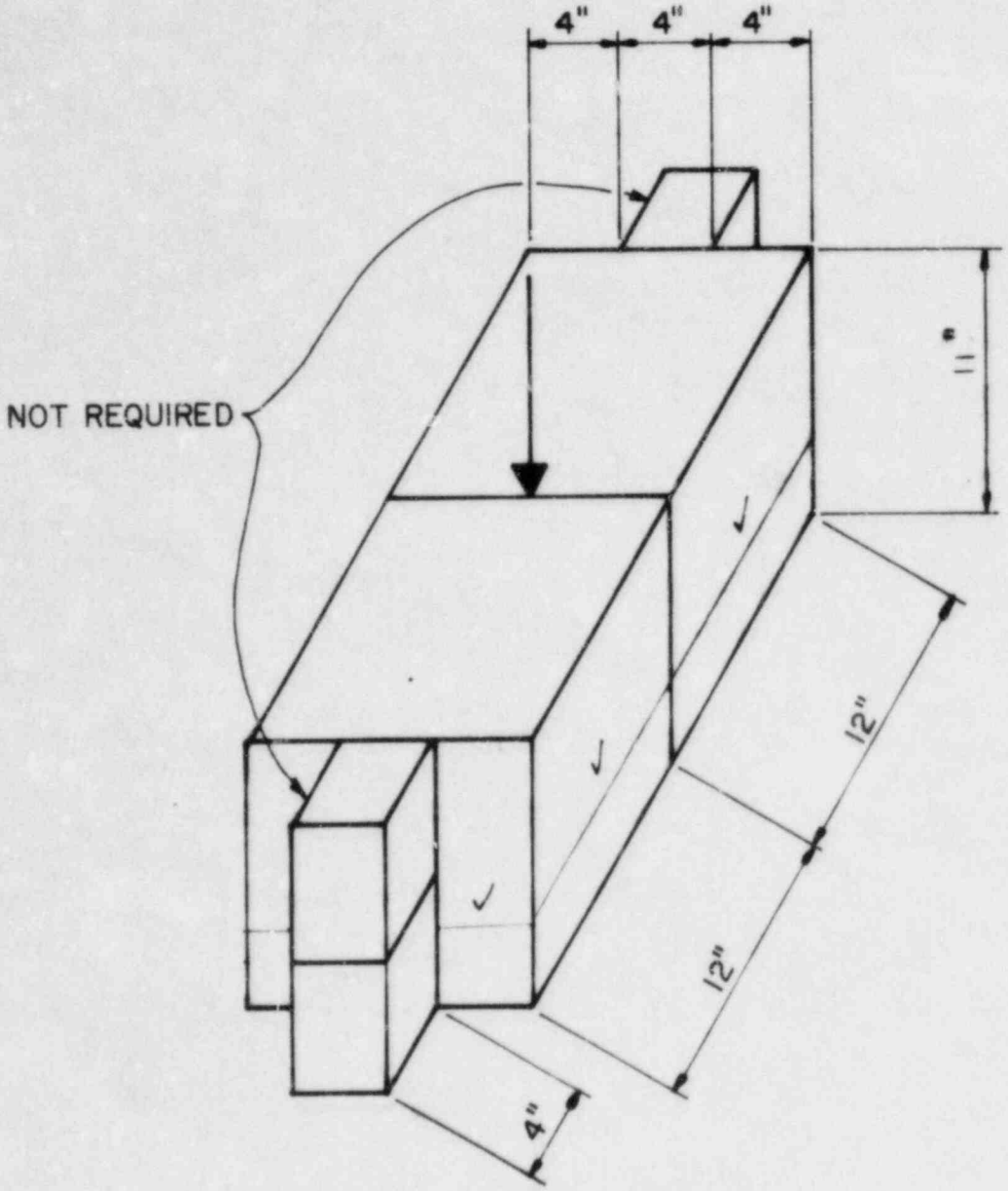

V INDICATES THIS FACE HAS BEEN CUT

	YES	NO
VERTICAL STACK	✗	
HORIZONTAL STACK	×	
VERTICAL CUT		×
HORIZONTAL CUT	×	
LOSS OF PRECRUSH		×

RESTRAINT DESIGN MARGIN = 1.91

FIELD CUT EAM FOR RESTRAINT MS-R18

FIGURE II-11

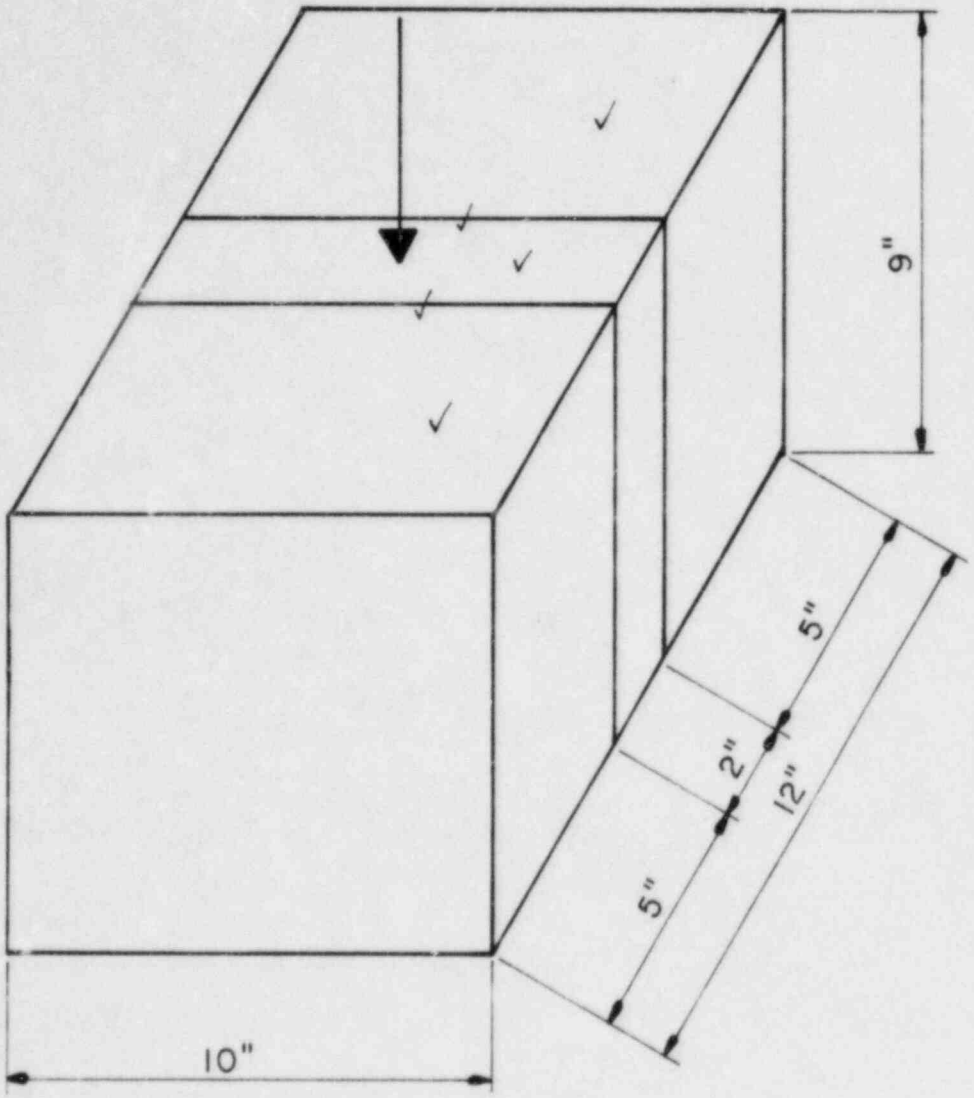

✓ INDICATES THIS FACE HAS BEEN CUT

NOTE: EAM WILL BE STRUCTURALLY SUPPORTED TO LIMIT H/W TO 2.0

	YES	NO
VERTICAL STACK		✓
HORIZONTAL STACK	×	
VERTICAL CUT	×	
HORIZONTAL CUT	×	
LOSS OF PRECRUSH	×	

RESTRAINT DESIGN MARGIN = 5.09

FIELD CUT EAM FOR RESTRAINT MS-R19

FIGURE II-12

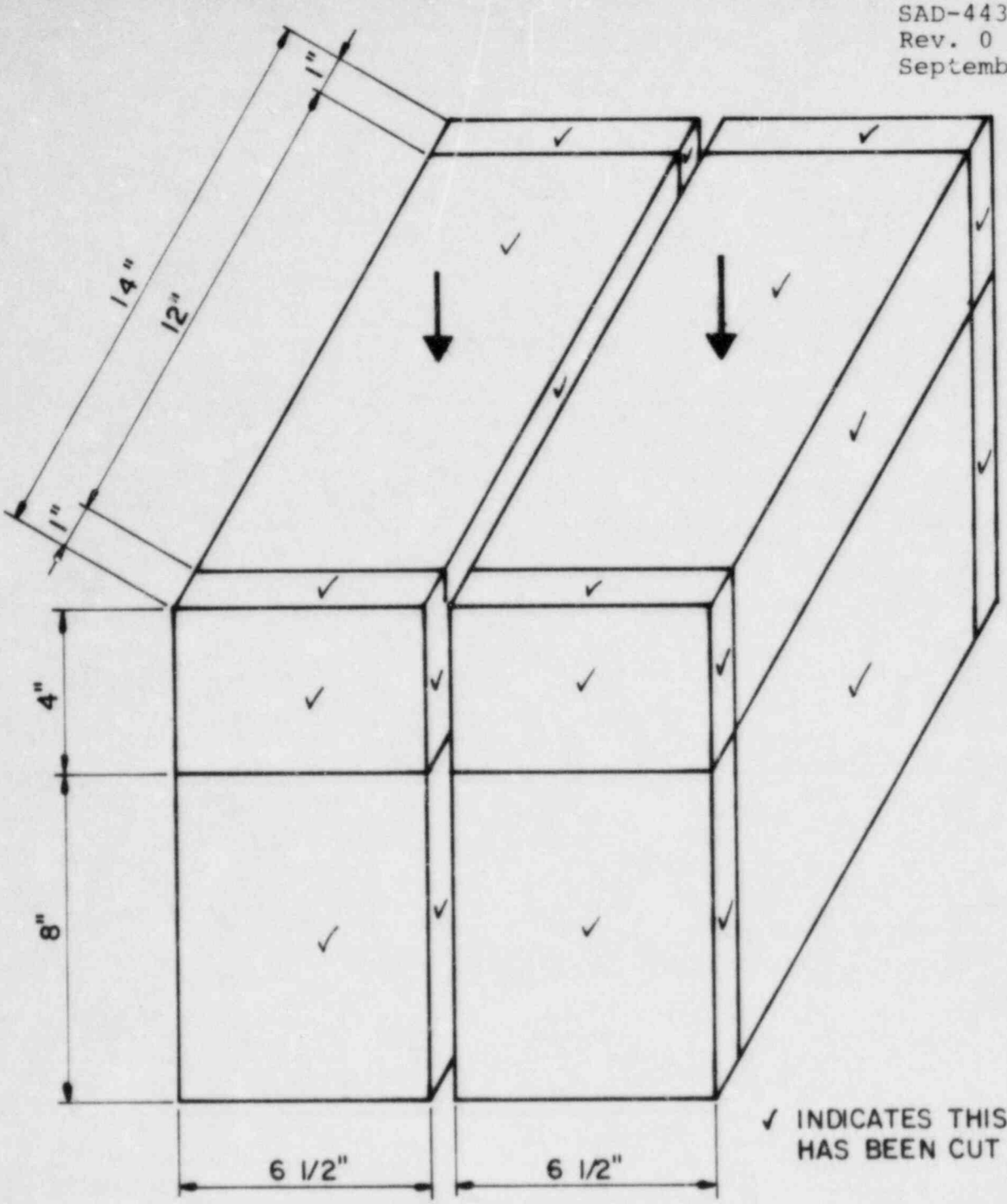

✓ INDICATES THIS FACE HAS BEEN CUT

	YES	NO
VERTICAL STACK	×	
HORIZONTAL STACK	×	
VERTICAL CUT	×	
HORIZONTAL CUT	×	
LOSS OF PRECRUSH	×	

RESTRAINT DESIGN MARGIN = 2.40

NOTE: EAM WILL BE FULLY ENCLOSED IN A STRUCTURAL BOX

FIELD CUT EAM FOR RESTRAINT MS-P26

FIGURE II-13

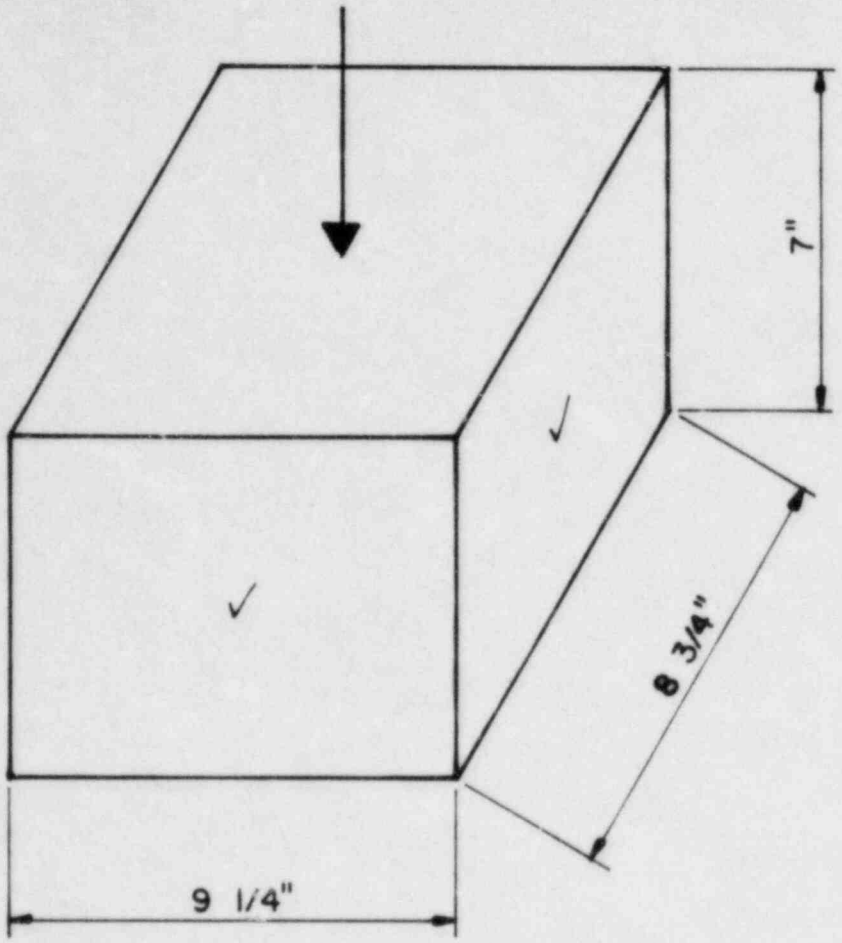

✓ INDICATES THIS FACE HAS BEEN CUT

	YES	NO
VERTICAL STACK		×
HORIZONTAL STACK		×
VERTICAL CUT	×	
HORIZONTAL CUT		×
LOSS OF PRECRUSH		×

RESTRAINT DESIGN MARGIN = 1.53

FIELD CUT EAM FOR RESTRAINT FWR-8

FIGURE II-14

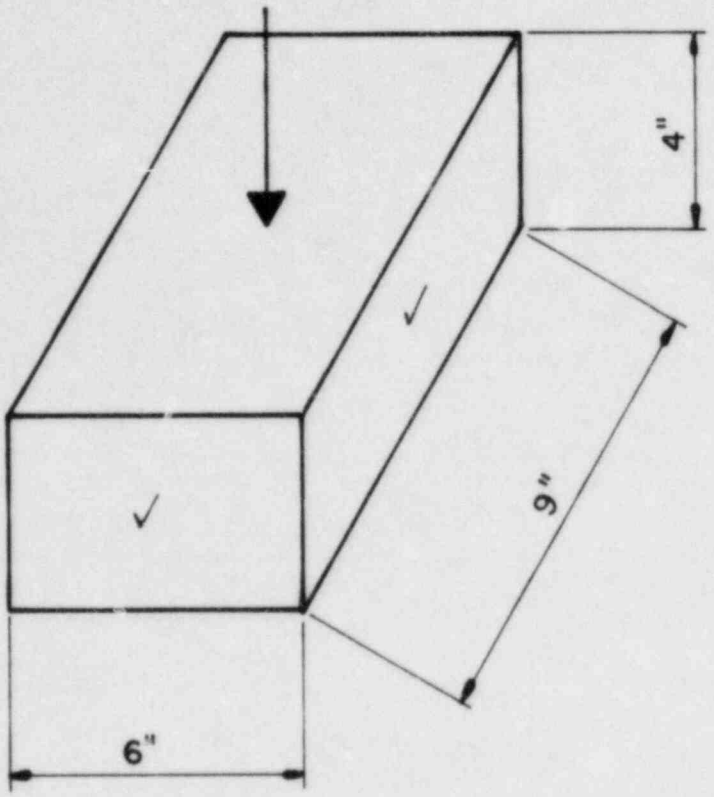

√ INDICATES THIS FACE HAS BEEN CUT

	YES	NO
VERTICAL STACK		×
HORIZONTAL STACK		×
VERTICAL CUT	×	
HORIZONTAL CUT		×
LOSS OF PRECRUSH		×

RESTRAINT DESIGN MARGIN = 1.86

FIELD CUT EAM FOR RESTRAINT FWR-14

FIGURE II-15

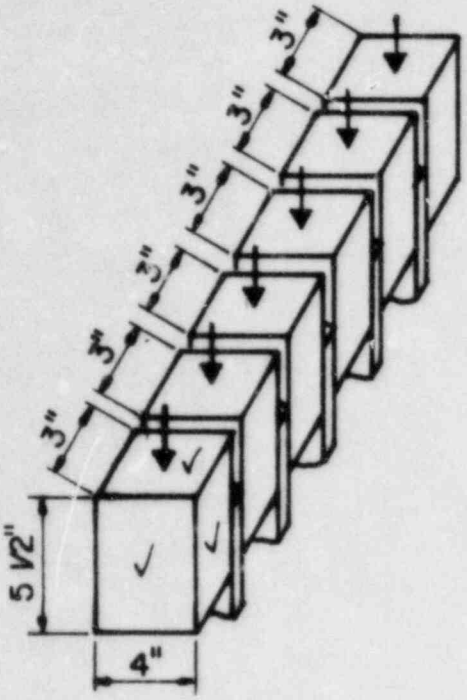

SECTION

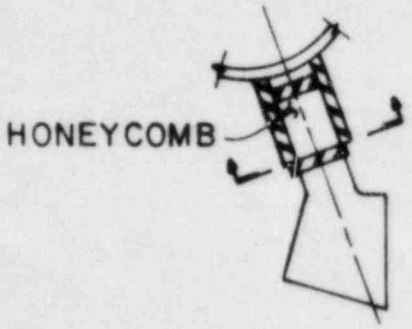

PLAN

√ INDICATES THIS FACE HAS BEEN CUT

	YES	NO
VERTICAL STACK		X
HORIZONTAL STACK		X
VERTICAL CUT	X	
HORIZONTAL CUT	X	
LOSS OF PRECRUSH	X	

RESTRAINT DESIGN MARGIN = 1.14

FIELD CUT EAM FOR RESTRAINT RH-R1

FIGURE II - 16

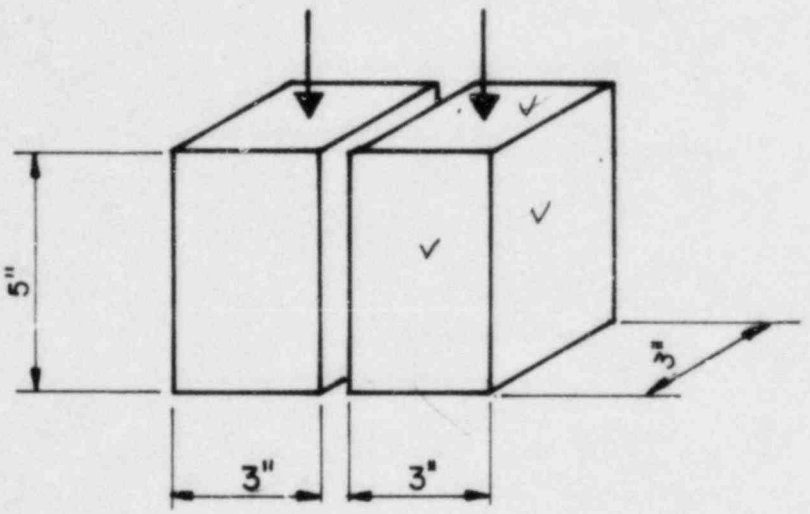

V INDICATES THIS FACE HAS BEEN CUT

	YES	NO
VERTICAL STACK		×
HORIZONTAL STACK	×	
VERTICAL CUT	×	
HORIZONTAL CUT	×	
LOSS OF PRECRUSH	×	

RESTRAINT DESIGN MARGIN = 1.84

FIELD CUT EAM FOR RESTRAINT SIIR-35B

FIGURE II-17

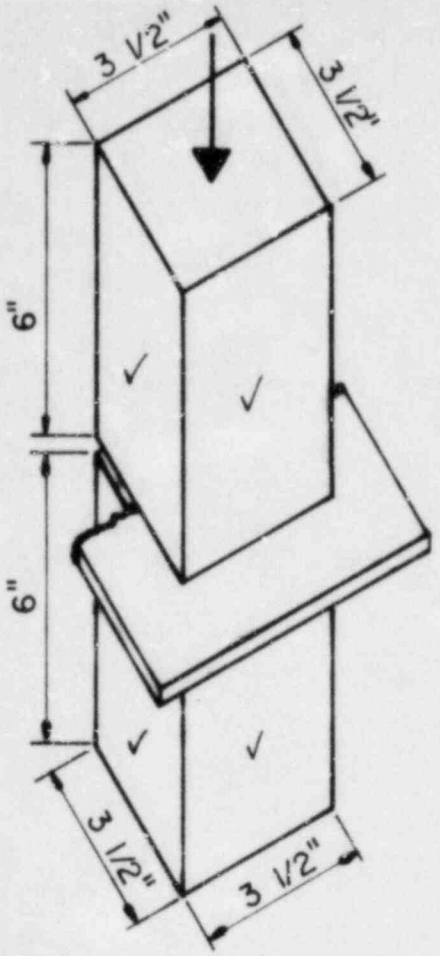

√ INDICATES THIS FACE HAS BEEN CUT

	YES	NO
VERTICAL STACK	X	
HORIZONTAL STACK		X
VERTICAL CUT	X	
HORIZONTAL CUT		X
LOSS OF PRECRUSH		X

RESTRAINT DESIGN MARGIN = 2.0

FIELD CUT EAM FOR RESTRAINT SI3R-660B

FIGURE II-18

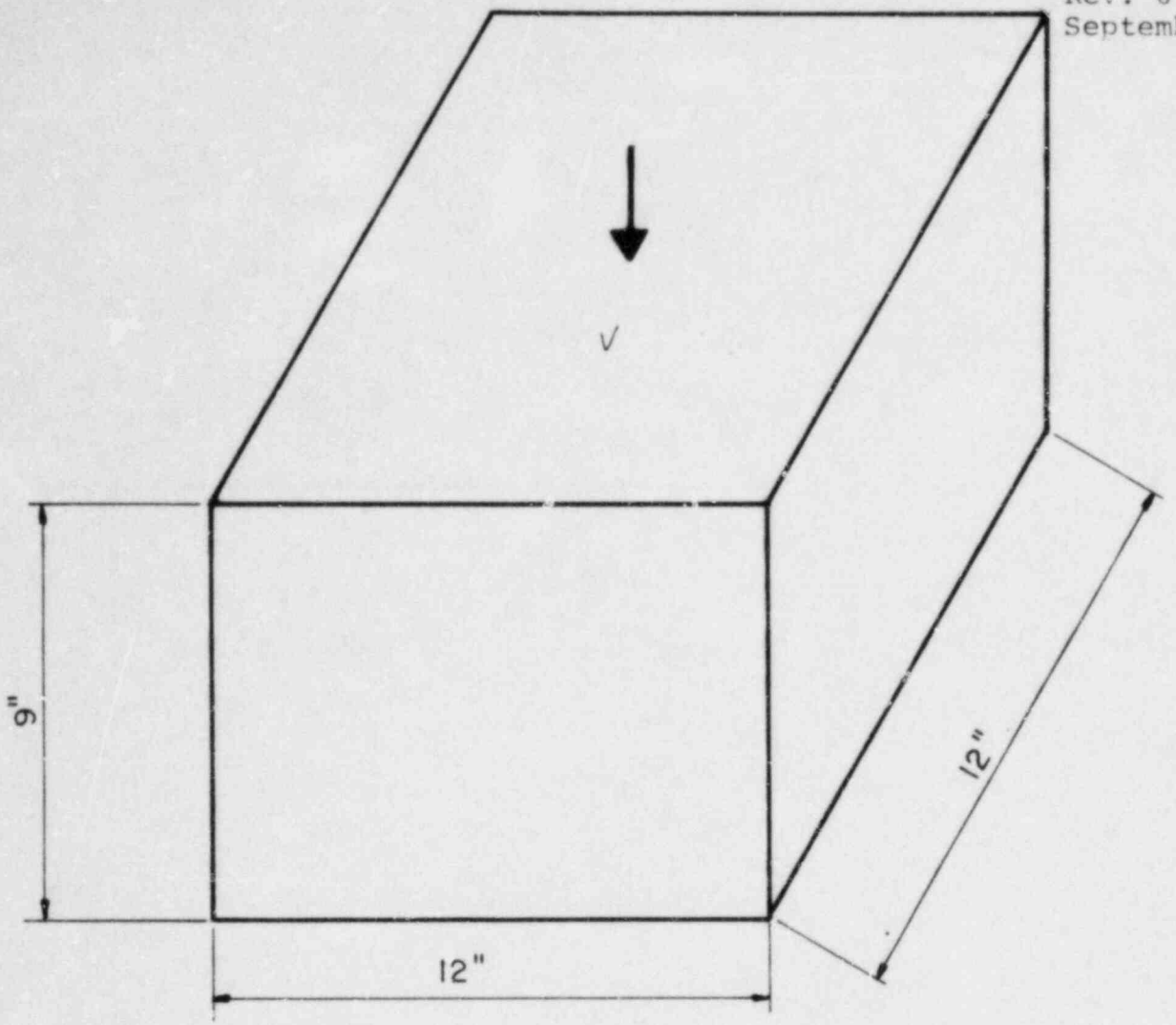

v INDICATES THIS FACE HAS BEEN CUT

	YES	NO
VERTICAL STACK		X
HORIZONTAL STACK		X
VERTICAL CUT		X
HORIZONTAL CUT	X	
LOSS OF PRECRUSH	X	

RESTRAINT DESIGN MARGIN = 4.23

FIELD CUT EAM FOR RESTRAINT MS-R16

FIGURE II-19

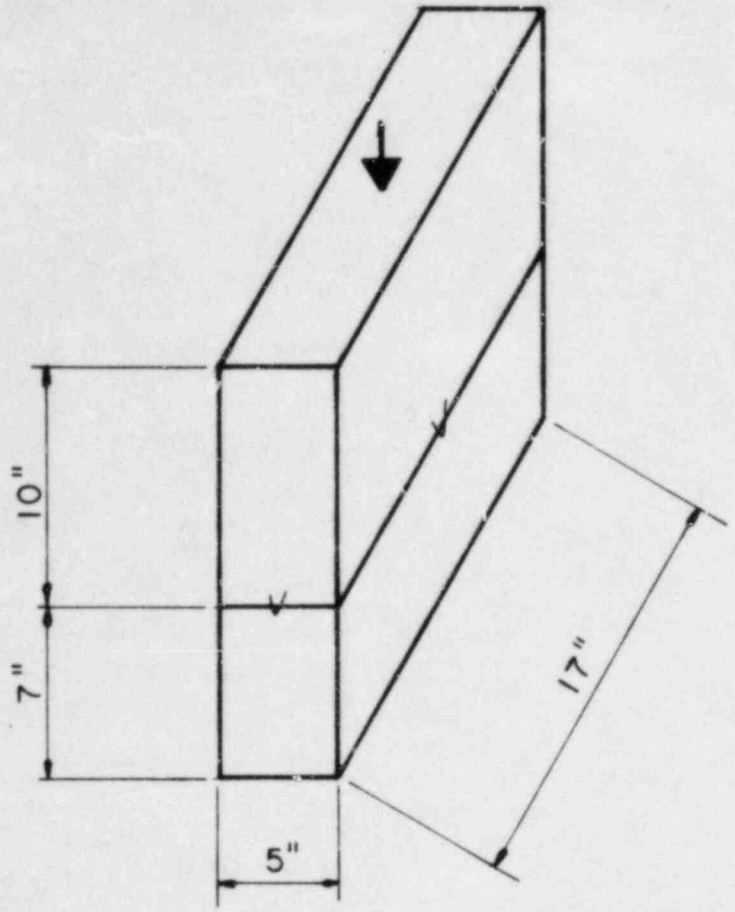

V INDICATES THIS FACE HAS BEEN CUT

	YES	NO
VERTICAL STACK	X	
HORIZONTAL STACK		X
VERTICAL CUT		X
HORIZONTAL CUT	X	
LOSS OF PRECRUSH		X

RESTRAINT DESIGN MARGIN = 1.66

FIELD CUT EAM FOR RESTRAINT MS-R44

FIGURE II-20

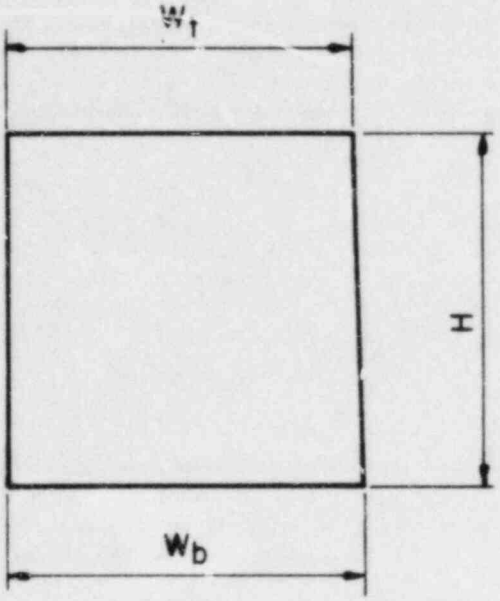

a) SKEWNESS

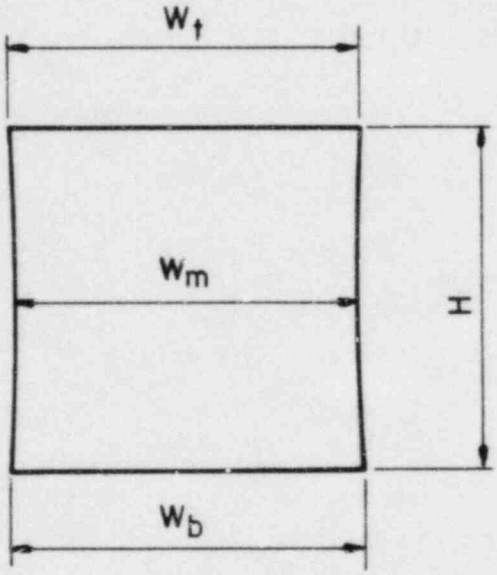

b) CONCAVITY

SKEWNESS AND CONCAVITY FOR FIELD CUT EAM PIECES

FIGURE II-21

III. BYRON PRODUCTION TESTS

This section describes the Byron production tests which include static and dynamic impact tests performed in 1978 and 1979 to control the properties of the EAM used in Byron.

A. Test Description

For each core block of EAM used to fabricate pipe whip restraints, one dynamic test was performed to establish the average dynamic crush strength (ADCS). In most cases, one static test was also conducted to determine the load deflection curve for the EAM. For these dynamic and static tests, the following is to be noted:

1. The EAM specimens were loaded in direct uniaxial compression.

2. The nominal specimen size for these tests was 3-3/4 x 3-3/4 x 4 inches, except for specimens from core blocks with a height of less than 4 inches, where the specimen had a height equal to the core block height. The tests were performed at the design temperature of $150^{\circ} \pm 10^{\circ}$ F.

3. The Byron production tests were performed during 1978-1979. Prior to 1980, Hexcel/MCI did not have the instrumentation capable of producing the load and energy versus deflection plots for dynamic tests. The average dynamic crush strength for each test specimen was computed by dividing the input energy by the change in specimen volume during crushing. Figure III-1 presents a typical work sheet reporting the dynamic test results.

4. The load versus deflection curves were obtained from the static tests. The specimens were, in general, crushed to approximately one-third of their original height. Figure III-2 shows a typical load deflection curve obtained. For this test the specimen was crushed to a strain of approximately 62%.

5. In the dynamic test, the specimens were crushed, in general, to approximately 40% to 60% strain. This maximum crushing was limited by the Hexcel test setup. The maximum hammer weight at the time of the test was limited to 4020 lbs. and the maximum hammer impact velocity was limited to 15.5 feet/seconds. This maximum weight and velocity was used in all dynamic tests.

B. Test Results

The average dynamic crush strength (ADCS) obtained for the 123 dynamic tests conducted as part of the Byron production tests is listed in Table III-1. This table shows that 95% of the specimens tested had ADCS within 10% of the specified value of 6000 psi. In this table, the core blocks used to fabricate the presently required 59 Byron Unit 1 restraints are marked by an asterisk (*).

C. Conformance to SRP Requirements

As stated earlier, the Byron production tests were conducted during 1978 and 1979. The then current NRC Safety Review Plan Section 3.6.2 (SRP) did not contain any specific requirements for testing of EAM. The SRP requirements for testing of EAM were first published in 1981. The 1981 revision of the SRP Section 3.6.2

requires that "...the capacity of the crushable material shall be limited to 80% of its rated energy dissipating capacity as determined by dynamic testing, at loading rates within ±50% of the specified design loading rate..."

In the Byron production tests, the energy dissipating capacity was determined using dynamic impact tests. The test velocity for the impact tests was 15.5 feet/second. The pipe whip impact velocity for the Byron pipe whip restraints using EAM is listed in Table III-2. Note that for a great majority of these restraints (71 out of 79), the test velocity of 15.5 feet per second is within ±50% of design impact velocity.

The dynamic tests were performed with impact energy close to the design values. The rated capacity of the EAM was not established using the dynamic tests because the test equipment to measure the dynamic load and energy versus displacements was not available at the time the tests were performed. The maximum crushing had to be limited to approximately 50% of the specimen height to avoid any unconservative bias in the computed ADCS. This condition arises because the crush strength of the EAM increases at strain levels exceeding 60%. If this strain hardening portion of the load deflection curve was also used in computing ADCS, it would lead to a higher ADCS. To establish that no significant increase in crush strength occurs as the EAM is crushed, static tests were performed. In the static tests the specimen load deflection curves were determined. These static test load deflection curves show that the load deflection curves are essentially flat (show an elastic-plastic behavior) up to the

design strain limit of 50%. Some strain hardening occurs beyond 50% strain, but this strain hardening is very gradual as shown in Figure III-2.

Based on the above, it is concluded that to the extent possible in 1978-1979, the Byron production test met the requirements of the current SRP (1981). The then current SRP did not have any specific test requirements. Also, based on the dynamic test data, the static load deflection curves, and recent dynamic tests performed on EAM similar to Byron 6000 psi EAM, it is our judgment that the Byron EAM meets the requirements of the current SRP 3.6.2 (1981 revision).

D. Additional Tests

To confirm our judgment and to provide a benchmark for other tests recommended later, we will conduct two additional dynamic tests which fully meet the current SRP requirements on specimens cut from Byron type 6000 psi EAM. The test will be conducted at the design temperature and with a test impact velocity of approximately 20 feet/second. The 4" x 4" x 4" specimens will be cut either at the Byron site or at Hexcel's shop and precrushed 0.02" to 0.09" at Hexcel's shop prior to testing. A 0.02" to 0.09" precrush was used in fabrication of Byron EAM. This value of precrush was based on information supplied by Solar Turbine International (STI) who have licensed Hexcel/MCI to fabricate the EAM. STI had indicated in 1978 that any amount of precrush, however small, results in eliminating the initial peak during crushing.

Table III-1

Byron Production Test Results
for Dynamic Crush Tests

Core Block Identification	Average Dynamic Crush Strength (PSI)	Maximum Strain (in/in)
SK206 *	5897	0.517
SK209 *	5446	0.516
SK211 *	5446	0.517
SK210 *	5842	0.568
SK204 *	5760	0.513
SK243 *	6095	0.501
SK244 *	6403	0.469
SK221	5842	0.550
SK289 *	6449	0.516
SK291 *	6008	0.500
SK205 *	6403	0.469
SK247 *	6403	0.476
SK294 *	6162	0.500
SK295 *	6030	0.525
SK208 *	5683	0.550
SK297 *	6469	0.477
SK248	6162	0.488
SK250	5802	0.499
SK268 *	6432	0.500
SK226 *	6388	0.328
SK222	5590	0.375
SK300 *	6320	0.462
SK312 *	6162	0.500
SK311 *	6162	0.475
SK302 *	6377	0.475
SK252	5822	0.500
SK292 *	6162	0.500

Table III-1 (continued)

Byron Production Test Results
for Dynamic Crush Tests

Core Block Identification	Average Dynamic Crush Strength (PSI)	Maximum Strain (in/in)
SK231 *	6324	0.668
SK343 *	6540	0.424
SK341 *	6450	0.450
SK344 *	6371	0.480
SK257	6405	0.450
SK298 *	6570	0.474
SK319 *	6330	0.474
SK212 *	5610	0.500
SK331 *	6440	0.446
SK330 *	6280	0.459
SK323 *	5500	0.502
SK228 *	5723	0.650
SK218	6140	0.468
SK217 *	6595	0.440
SK301	6469	0.46[illegible]
SK353 *	6595	0.440
SK320 *	6120	0.484
SK322 *	5974	0.517
SK255 *	6030	0.471
SK219	6350	0.424
SK237	6250	0.613
SK245 *	6570	0.434
SK253	6350	0.465
SK331 *	6440	0.446
SK227	6520	0.602
SK235 *	6350	0.629

Table III-1 (continued)

Byron Production Test Results
for Dynamic Crush Tests

Core Block Identification	Average Dynamic Crush Strength (PSI)	Maximum Strain (in/in)
SK223 *	6544	0.590
SK299 *	6730	0.446
SK239	6780	0.437
SK332 *	6280	0.456
SK213 *	5410	0.566
SK251	7035	0.394
SK251	6780	0.402
SK269	6350	0.433
SK271	6010	0.456
SK271	7674	0.364
SK271	5482	0.525
SK271	6009	0.493
SK340 *	5890	0.496
SK344	6371	0.480
SK283 *	5450	0.602
SK283 *	6220	0.493
SK283 *	6090	0.500
SK286	6550	0.452
SK255	6030	0.471
SK342	6117	0.470
SK244	6403	0.470
SK320	6120	0.484
SK310 *	6730	0.424
SK333 *	6194	0.472
SK333 *	5674	0.516
SK333 *	6240	0.482
SK238	5650	0.559

Table III-1 (continued)

Byron Production Test Results
for Dynamic Crush Tests

Core Block Identification	Average Dynamic Crush Strength (PSI)	Maximum Strain (in/in)
SK240 *	6519	0.462
SK241 *	6370	0.445
SK216	6580	0.478
SK281 *	5430	0.549
SK487	6600	0.468
SK487	6980	0.418
SK495 *	5780	0.488
SK464 *	5970	0.482
SK313	5640	0.523
SK313	5880	0.535
SK313	5760	0.563
SK306	6480	0.484
SK306	6480	0.463
SK328 *	6440	0.483
SK328 *	6440	0.481
SK328 *	7000	0.429
SK489	6400	0.460
SK489	6300	0.460
SK489	6520	0.464
SK490	5920	0.507
SK490	6320	0.493
SK490	6320	0.459
SK273	6370	0.455
SK273	6620	0.436
SK326 *	5430	0.566
SK326 *	5540	0.544
SK326 *	5410	0.550

Table III-1 (continued)

Byron Production Test Results
for Dynamic Crush Tests

Core Block Identification	Average Dynamic Crush Strength (PSI)	Maximum Strain (in/in)
SK337 *	5430	0.517
SK337 *	5410	0.531
SK337 *	5880	0.481
SK469 *	6600	0.463
SK339 *	6010	0.505
SK339 *	5680	0.534
SK339 *	5670	0.520
SK273	6620	0.436
SK273	6370	0.456
SK476	6160	0.470
SK476	5540	0.546
SK476	5500	0.507
SK284	6070	0.501
SK284	5410	0.553
SK336 *	5460	0.537
SK336 *	5680	0.500

* Used on presently required restraints.

Table III-2: SUMMARY OF PIPE IMPACT VELOCITIES

Restraint	Velocity in/sec	Restraint	Velocity in/sec	Restraint	Velocity in/sec
MS-R1	21.4	+ MS-P25	19.8	* FWR-36	21.5
MS-R2	26.8	MS-P26	21.3	FWR-37	21.9
MS-R4	16.3	* MS-P29	33.4	* FWR-38	23.0
MS-R4X	40.3	FWR-1	18.8	+ FWR-39	27.4
MS-R9	34.8	FWR-2	46.5	* FWR-40	12.9
MS-R10	26.9	FWR-3	16.9	RC2-4	25.3
+ MS-R11	9.9	* FWR-4	15.3	RC2-6	26.9
MS-R12X	32.8	* FWR-6	12.0	RC3-4	13.2
MS-R16	19.0	* FWR-7	16.0	RC3-6	31.0
MS-R18	22.3	FWR-8	22.4	RC4-4	11.5
MS-R19	19.3	FWR-10	13.4	RC4-6	32.3
MS-R28	19.9	FWR-11	2.2	RH-R1	38.7
MS-R32	25.4	+ FWR-12	14.6	RH-R3	30.9
MS-R33	19.4	* FWR-13	13.8	SI1R-10B	12.6
MS-R34X	16.1	FWR-14	16.0	SI1R-35B	8.9
MS-R35C	18.3	FWR-15	20.2	* SI1R-170A	7.0
MS-R36	9.9	* FWR-16	12.3	SI1R-640A	16.6
MS-R44	25.0	* FWR-17	12.4	SI1R-660B	11.4
MS-R48	22.5	FWR-18	29.3	SI4R-15B	6.3
+ MS-R49	16.8	* FWR-25	9.9	RY-2	30.6
MS-R49x	25.3	* FWR-26	18.4	RY-3	30.6
MS-R64X	13.6	* FWR-27	16.6	RY-4	30.6
* MS-P6	23.4	* FWR-28	24.5	RY-5	30.6
+ MS-P10	26.7	FWR-29	19.3	RY-6	30.6
* MS-P14	27.6	* FWR-30	14.8	RY-7	30.6
* MS-P21	34.0	FWR-31	25.2	RY-8	30.6
		* FWR-35	13.5		

* Deleted Restraints
\+ Tension Controlled Restraints

DYNAMIC CRUSH TEST REPORT

WORK ORDER No. CW-8[illegible]
CORE BLOCK No. SK-255
TEST DATE 3/7/79
TEST PERFORMED BY [signature]
TEST TEMPERATURE 150° F.

CUSTOMER Chrysler Body & Frame
P.O. No. S-51864-83511

DIMEN ENT.	a INITIAL LENGTH (IN.)	b INITIAL WIDTH (IN.)	c INITIAL HEIGHT (IN.)	d INITIAL VOLUME (IN^3) abc	e FINAL HEIGHT (IN.)	f FINAL VOLUME (IN^3) abe	g VOLUME CHANGE (IN^3) d-f	h % CRUSH $\frac{d-f}{d}$	i LOAD WT. (LBS)	j DROP HEIGHT (IN.)	k IMPACT VELOCITY (FPS)	ENERGY (IN.LBS.) ij	CRUSH STRENGT (LBS/I $\frac{i}{g}$
SK255	3.80	3.90	4.01	59.4	2.12	31.4	28.0	47.1	4020	42.0	15.0	168840	6032

CHARGE AMPLIFIER OUTPUT (mV/g) 30.0
ACCELEROMETER OUTPUT (mV/g) 40.9
ACCELEROMETER CALIB. DATE 11/2/78
CHARGE AMPLIFIER CALIB. DATE 11/6/78
OSCILLOSCOPE CALIB. DATE 10/31/78
TEMPERATURE RECORDER CALIB. DATE 2/6/79

TIME → (50 MILLISEC/DIV.)

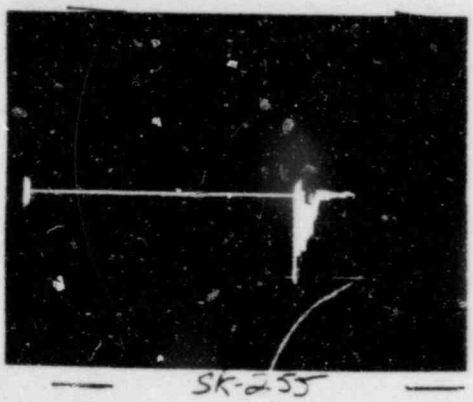

↑ (1 V/DIV.)
VOLTAGE

Q.A. ACCEPTANCE [signature]
DATE 3/8/79

Figure III-1: Typical Dynamic Crush Test Report

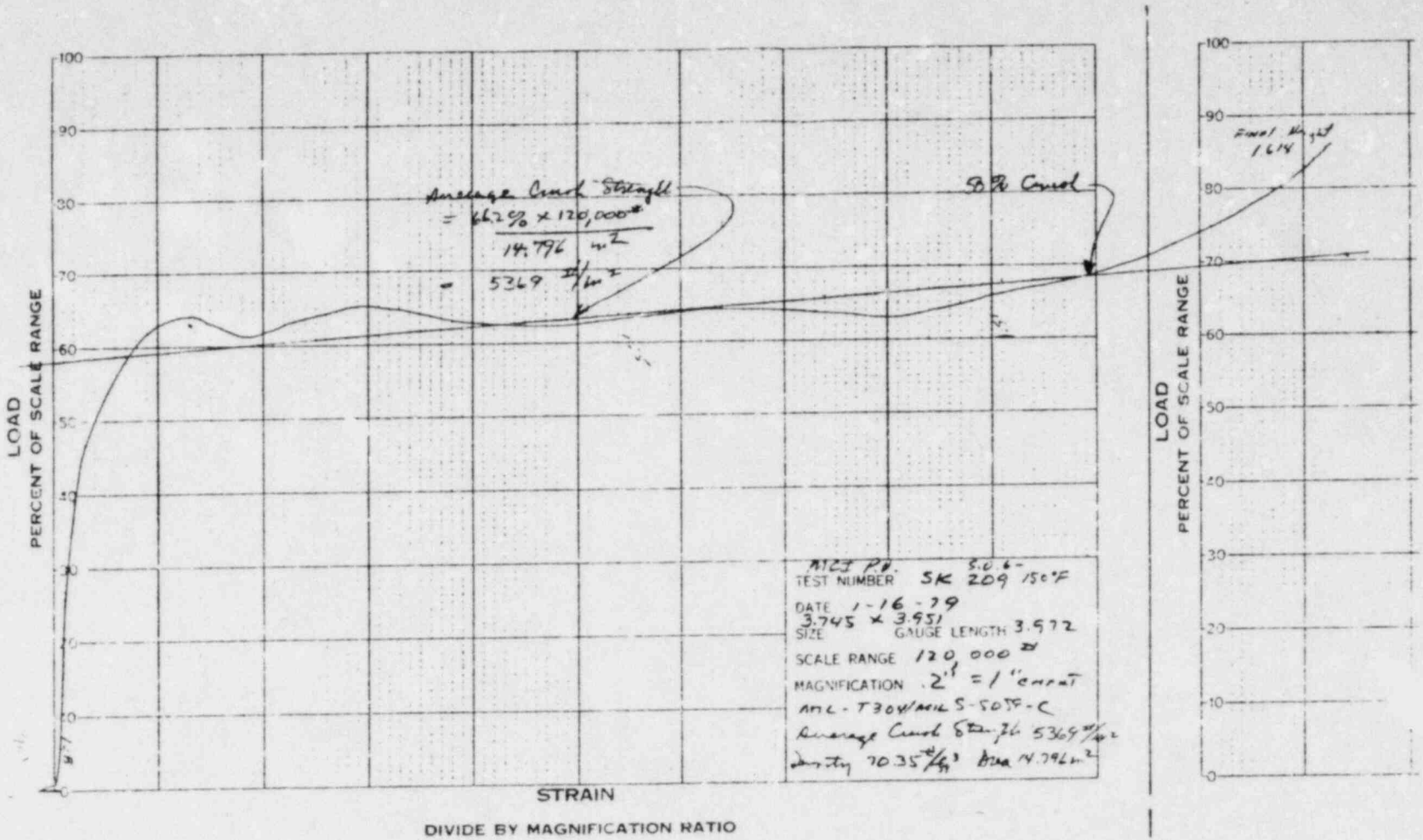

Figure III-2: Typical EAM Load Deflection Curve Obtained from Static Tests

IV. BYRON ANGULAR CONFIGURATION TESTS

A test program was conducted in 1983 to evaluate the possible reduction in the average dynamic crush strength of the EAM specimens when the EAM is subjected to the action of combined lateral shear and axial load. These tests were performed on the Byron project at the request of the NRC staff.

The test results were presented in Sargent & Lundy Report SAD-431 entitled, "Evaluation of Energy Absorbing For Pipe Whip Restraint," Revision 1, dated April 1984. The report was submitted to the NRC staff for review on the Byron/Braidwood docket. For a detailed discussion of these tests, the reader is directed to the above-mentioned report. The following provides a summary of the test setup and results.

The test setup is schematically shown in Figure IV-1. The solid lines show the shape of the EAM at impact and the dotted lines show the crushed shape of the EAM. In this test setup, the EAM specimens are impact-loaded by the impact hammer shaped like an anvil. The anvil forces the EAM to crush at an angle offset from the axial direction. This offset causes lateral shear and axial compression in the EAM. By varying the anvil angle θ, the relative magnitudes of the shear and the axial load on the EAM can be varied to bound the EAM design parameters.

The majority of the tests were conducted for the anvil angle of 90°. Two tests were conducted for the anvil angle of 120°. The 90° anvil results in EAM load angularity of 45°. The 120° anvil results in the EAM load angularity of 60°. The EAMs were impacted with a velocity of approximately 25 feet/second. The drop weight was

adjusted for each test to load each EAM to a minimum of 125% of the design energy. The following tests were conducted:

Test Specimen Size (inch)	Anvil Angle (degree)	Hammer Weight (lbs.)
3 x 3 x 3 WS	90°	1975
3 x 3 x 3 SS	90°	1975
4 x 4 x 2 WS	90°	1975
4 x 4 x 2 SS	90°	1975
4 x 4 x 2 5/16 WS	120°	2400
4 x 4 x 2 5/16 SS	120°	2400
4 x 4 x 3 WS	90°	3050
4 x 4 x 3 SS	90°	3050
4 x 4 x 4 WS	90°	4000
4 x 4 x 4 SS	90°	4150
4 x 4 x 4 BT	90°	4150
5 x 5 x 4 WS	90°	6550
5 x 5 x 4 SS	90°	6550
6 x 6 x 3 WS	90°	6925
6 x 6 x 3 SS	90°	6925

In the above table, WS refers to the orientation of the EAM specimens in the tests, where the shear load was applied in the weak shear direction of the EAM. SS refers to specimen orientation so that the shear load is applied in the strong shear direction of the EAM. BT refers to the test setup, where a bolt was threaded through the EAM to simulate field conditions of Type 3 restraints shown in Figure II-4.

The following conclusions were drawn from the tests.

1. There is no scaling effect on the behavior of the EAM. The test results are thus applicable to full-size EAM pieces in the pipe whip restraints.

2. There is no loss of energy absorbing capacity when the EAM is loaded under shear and direct compression. The EAM load angularity for the 90° tests was 45° and for the 120° tests was 60°.

3. There is no significant difference in the energy absorbing capacity of the EAM with or without bolts.

4. There is no significant difference in the energy absorbing capacity of the EAM whether it is loaded in the strong shear direction or the weak shear direction.

At the August 29, 1984 meeting between the NRC, CECo and S&L, the NRC staff requested further clarification of the results presented in the S&L Report No. SAD-431 including (i) the basis for discarding any data not used in the final EAM qualification assessment, (ii) apparent anomaly between generalized EAM peak-to-average force behavior and the tests data and (iii) the reduction of recorded force data by 30% for the new one million pound instrumented tup. The following paragraphs provide the requested information:

A. Basis for Discarding Data

In the initial Byron angular configuration tests program submitted to the NRC, it was proposed to use Hexcel's ETI-300 instrumented impact system to compute the average dynamic crush strength (ADCS) of the EAM specimens. The ETI-300 software was to be used to generate the load and energy versus displacement plots

to compute the ADCS. A brief description of the ETI-300 system and its validation testing is described in Appendix A. The validation testing showed that the ETI system software computed energy values within 2.5% of theoretical values. The displacement calculations were within 11% of measured values. This validation was performed for the EAM specimen loaded in direct compression. Given the impulsive nature of the load, this degree of accuracy is acceptable. The ETI-300 system has been used for dynamic testing of EAM at Hexcel since January 1980.

In the planning stages it was recognized that for the test setup shown in Figure IV-2, the ETI-300 system software had not been validated. To check the accuracy of the ETI-300 software for the Byron angularity test setup, four shake down tests were conducted prior to the production tests. The results from these shake down tests were used to develop the data measurement and reduction system for the production tests. The conclusions of the shake down tests were:

1. The physical data for each test should be recorded in a test log. This physical data will serve as a cross check for all computed quantities, including load versus displacements and energy versus displacement plots. The physical data includes

   - o Weight of the impact hammer
   - o Drop height of the hammer
   - o Specimen dimensions
   - o Impact angle

- o EAM crush distance

- o Vertical displacement of the saddle

The weight of the hammer and the drop height of the hammer provide the physical measure of the total crush energy. This can be used to check total energy computed from the force time history measurements. The drop height can be used to check the impact velocity measurements. The saddle vertical displacement gives a physical measure of the total displacement during the test. This can be used to check the maximum displacements computed from the tup voltage (force time history) measurements. The EAM crush distance and the impact angle measurements can be used to provide an independent check of the saddle displacement measurements.

2. The tup voltage (force time history) recordings on the TEAC-R71 recorder are accurate.

3. The accelerometer signals (acceleration time history) were not being recorded on the TEAC-R71 recorder due to saturation of the charge amplifier. Also, given the test schedule, there was no practical solution to the problem. The acceleration data could have been used to check the maximum displacements computed from the tup voltage (force time history) measurements. As the saddle displacement measurement could provide the same cross check, it was concluded that the acceleration time histories measurement were redundant and could be eliminated without loss of accuracy.

4. The load and energy versus displacement plots being generated by the ETI-300 system software were in error for the Byron Angularity test setup and could not be used to compute the ADCS.

Table IV-1 presents the summary of the data measured and computed for each test. It can be observed that all the measured and computed data was used in the test result assessment except the following:

1. Acceleration time histories that were never recorded due to saturation of the charge amplifiers. This was expected as a result of the shake down tests.

2. The load and energy versus displacement plots computed using the ETI-300 software were discarded because of erroneous results. As examples, Figures IV-3 and IV-4 show the load and energy versus displacement plots computed by the ETI-300 software for the 4 x 4 x 4 SS and the 5 x 5 x 4 SS specimen tests. The computed maximum displacements are 4.2 and 2.3 inches. The measured saddle displacements for the same tests were 3.52 and 3.23 inches, respectively. Note the ETI-300 computed displacements are in error. In addition, note that for the 5 x 5 x 4 SS specimen, the plot shows significant negative displacement ($\sim$ 0.5 inches) towards the end, which again is in

...rgy versus time plots, also
...I-300 system, were discarded
... displacement calculations

which are used to compute the energy. In addition, the load and energy versus time plots can not alone be used to compute the ADCS.

Note from the table that the tup voltage time history is the measured data. This must be multiplied by the tup calibration constant to obtain the load time history.

Based on the above evaluation, it is concluded that all accurately measured or computed data has been used in the final EAM qualification assessment. Only the erroneous data has been discarded.

B. Apparent Anomaly Between Peak-To-Average Load

The load time histories for the 4 x 4 x 4 SS and the 5 x 5 x 4 SS tests are shown in Figures IV-5 and IV-6. These plots show significant load oscillations. These load oscillations, in our judgment, are due to the dynamic response of the test setup under the impulsive load and are not representative of the crushing behavior of the EAM. However, if we were to postulate that these oscillations represent the EAM crushing load deflection curves, they are still not significant to the design of the pipe whip restraints or the supporting structure. This is because the load oscillations are of very high frequencies (greater than 500 Hz). Pipe whip restraints (Type B and C) and supporting structure frequencies are generally in the 10 to 50 Hz range. Thus these high frequency load oscillations are not design significant. When the high frequency content (greater than 200 Hz) is filtered out of these load time histories, the load oscillations are relatively small. Figures IV-7 and IV-8 present these filtered load time histories for

the 4 x 4 x 4 SS and the 5 x 5 x 4 SS tests, respectively. Observe that the load oscillations are small. Table IV-2 tabulates the peak load, the average load and the ratio of the peak-to-average load based on the 200 Hz filtered load time histories for all 14 tests. Both the peak load and the average loads are computed in the time domain for which test energy is less than or equal to the design energy. Observe that the peak-to-average ratios vary from 1.01 to 1.15.

Table IV-3 presents the design margin factor for the four Type B and the ten Type C restraints. Note that the design margins are greater than the ratio of the peak-to-average load measured. Based on the above evaluation, we conclude that the measured load oscillations are high frequency oscillations and not significant to design. The load oscillations when the high frequencies (greater than 200 Hz) are filtered are less than 15% of the average load magnitude. The inherent design margins for the Byron restraints are adequate to accommodate this increase in design load.

C. Reduction of Recorded Load Data by 30%

In Section 5 of the S&L Report No. SAD-431, Revision 1 dated April 1984, it was stated that for the 1,000,000 pound tup for EAM specimen 5 x 5 x 4, 6 x 6 x 3 and 4 x 4 x 4 (Bolt), it was necessary to reduce the levels of the recorded force data (voltage) by 30% so that the deviations in computed to measured displacement and energy could be brought in line with those using the 350,000 pound tup. The following paragraphs provide the rationale for the 30% reduction.

Table IV-1 presents all the measured and computed data for the angularity tests. Note that the load time history is a computed quantity. The tup voltage time history is the measured quantity. This voltage measurement must be multiplied by the tup calibration constant to obtain the load time history.

In the Byron angularity tests, the crush load measurements were made using the instrumented tup which is part of the ETI-300 system. The ETI-300 system tup is a strain gauge based load measuring device. The tup output is a voltage which is proportional to the applied load. The tup calibration determines the multiplication constant to convert the output voltage time history to a load time history. The ETI-300 system was equipped with a tup with a maximum load rating of 350,000 lbs. The validation testing for this tup is presented in Appendix A.

During the shake down testing, it became apparent that the maximum load for the 5 x 5 x 4 and the 6 x 6 x 3 specimen tests would exceed the capacity of the 350,000 lb. tup. For this reason, a new tup with a maximum rating of 1,000,000 lbs. was purchased. This new tup was used for the 5 x 5 x 4, 6 x 6 x 3 and the 4 x 4 x 4 BT tests. the 350,000 lb. tup was used for all other tests.

As described in S&L Report No. SAD-431, the measured voltage time history was used to compute the displacement time histories. The computed maximum displacement values were then compared to the measured saddle displacements. This comparison is presented in Table IV-4. As can be observed, the deviations between the measured and computed displacements for the 350,000 lb. tup is generally less than 5% and the

maximum error is 13.6%. These variations are consistent with the results of the validation testing for the 350,000 lb. tup presented in Appendix A. This validation testing showed that displacement computations based on the tup force measurements are accurate to within 11% of actual measurements. General Research, the tup manufacturer, has attributed these deviations to the cumulation of roundoff errors during digitization of the tup voltage signal and the integration of these voltage signals to obtain displacements. As the computed results for all the tests using the 350,000 lb. tup were within the expected error band, they were accepted and reported as measured.

Observe from Table IV-4 that for the 1,000,000 lb. tup, the deviations between the measured and the computed displacement are much greater compared to the corresponding deviations for the 350,000 lb. tup. For the 1,000,000 lb. tup, the percent error for computed displacement is generally greater than 15%. This error magnitude is outside the acceptable error band and indicates an error in interpretation of test measurements.

The test setup and the analytical procedures used to compute the displacements were identical for both the 350,000 and the 1,000,000 lb. tup. The tup calibration was the only variable. Thus the error was attributed to the tup calibration constant for the 1,000,000 lb. tup. In our judgment, the calibration constant provided by Hexcel was too high by 30%. This judgment was based on the following:

1. The analytical procedure used to compute the displacement and energy requires that at the end of the test

   Hammer velocity = 0.0
   Hammer displacement = measured displacement
   Energy absorbed = energy input

   In the analysis, the tup calibration constant is the only variable. As all the above three conditions must be simultaneously satisfied, the analysis provides an independent check for the calibration constant.

   When the calibration constant for the 1,000,000 lb. tup was reduced by 30% (equivalent to reducing measured force magnitudes also by 30%), the velocity, displacement and energy conditions described above were simultaneously satisfied. This is shown in Table IV-5 where the computed displacements are generally less than 3% and the maximum error is 10.4%. It was thus concluded that the 30% reduction in the calibration constant for the 1,000,000 lb. tup was appropriate.

2. As stated earlier, the tup output during the test is a voltage time history. This voltage must be multiplied by the calibration constant to obtain the force time history. The calibration constant for the 1,000,000 lb. tup was determined by statically loading it to 30,000 lbs. and measuring the voltage output. As the measured loads in the tests were an order of magnitude higher, it is possible that the calibration constant used is not representative of actual calibration constant at these higher loads.

Based on the above evaluation, it is our judgment that the 30% reduction in the computed force magnitude for the 1,000,000 lb. tup measurements was appropriate. To confirm our judgment, we will recalibrate the 1,000,000 lb. tup to force magnitude of at least 500,000 lbs. If necessary, we would revise the S&L Report No. SAD-431 to account for the results of the recalibration.

TABLE IV-1 SUMMARY OF ANGULAR CONFIGURATION TEST DATA

No.	Description of Data	SOURCE OF DATA: Test log	ETI-300 output	TEAC-R71 recorder
	Measured Data			
1.	Load Angularity	U		
2.	Drop Weight	U		
3.	Drop Height	U		
4.	Impact Velocity	U		
5.	EAM Temperature	U		
6.	EAM Crush Distance	U		
7.	Saddle Vertical Displacement	U		
8.	Trigger Signal			U
9.	Tup Voltage Time History			U
10.	Impact Velocity		U	
11.	Acceleration Time History			N
	Computed Data			
12.	Theoretical Energy	U		
13.	Load and Energy Versus Displacement Curve		X	U
14.	Load and Energy Versus Time Curve		X	U

U: Data used in evaluation of test results

X: Data discarded

N: Data not available

TABLE IV-2 RATIO OF PEAK TO AVERAGE MEASURED FORCE

SPECIMEN	F_{PEAK}	$F_{AVERAGE}$	RATIO
3 X 3 X 3 WS	79.4	74.4	1.07
3 X 3 X 3 SS	84.1	74.8	1.12
4 X 4 X 2 WS	132.5	120.1	1.10
4 X 4 X 2 SS	181.4	173.7	1.04
4 X 4 X 2 5/16 WS	109.6	104.9	1.05
4 X 4 X 2 5/16 SS	140.5	133.8	1.05
4 X 4 X 3 WS	138.8	126.0	1.10
4 X 4 X 4 WS	131.5	121.9	1.08
4 X 4 X 4 SS	164.7	152.2	1.08
4 X 4 X 4 BT	172.6	171.2	1.01
5 X 5 X 4 WS	232.1	210.0	1.10
5 X 5 X 4 SS	266.7	243.3	1.09
6 X 6 X 3 WS	382.7	353.2	1.08
6 X 6 X 6 SS	420.5	362.3	1.15

TABLE IV-3 DESIGN MARGINS IN TYPE B AND TYPE C RESTRAINTS TO ACCOMMODATE LOAD OSCILLATIONS

RESTRAINT	TYPE	DESIGN MARGIN FACTOR
MS-R4	B	2.16
MS-R33	B	1.32
MS-R48	B	2.08
FWR-2	B	1.98
MS-R1	C	1.43
MS-R2	C	2.19
MS-R9	C	2.75
MS-R10	C	2.75
FWR-3	C	1.73
RH-R1	C	2.84
F[illegible]-R3	C	2.30
SI1R-10B	C	3.33
SI3R-640A	C	2.75
SI4R-15B	C	4.07

TABLE IV-4 COMPARISON BETWEEN COMPUTED AND MEASURED DISPLACEMENTS

TEST ID	DISPLACEMENTS (IN) MEASURED	CALC.	DEV(%)
* 3 X 3 X 3 SS	2.85	2.90	1.9
* 3 X 3 X 3 WS	2.90	2.95	1.9
* 4 X 4 X 2 SS	1.33	1.31	-1.7
* 4 X 4 X 2 WS	1.84	1.90	4.0
* 4 X 4 X 2 5/16 SS	2.13	2.11	-0.8
* 4 X 4 X 2 5/16 WS	2.80	2.75	-1.7
*** 4 X 4 X 3 SS	-	-	-
* 4 X 4 X 3 WS	2.72	2.36	-13.6
* 4 X 4 X 4 SS	3.52	3.61	2.6
* 4 X 4 X 4 WS	3.67	3.50	-4.8
** 5 X 5 X 4 SS	3.23	2.65	-18.1
** 5 X 5 X 4 WS	3.74	3.01	-19.6
** 6 X 6 X 3 SS	2.28	1.71	-24.8
** 6 X 6 X 3 WS	2.35	1.93	-17.9
** 4 X 4 X 4 BT	2.78	2.64	-5.0

* Using 350,000 Tup

** Using 1,000,000 Tup

*** Data Lost

TABLE IV-5 COMPARISON BETWEEN COMPUTED AND MEASURED DISPLACEMENTS FOR 1,000,000 LBS TUP AFTER 30% ADJUSTMENT IN LOAD

TEST ID	DEFLECTION (IN) MEASURED	CALC.	DEV(%)
5 X 5 X 4 SS	3.23	3.25	0.7
5 X 5 X 4 WS	3.74	3.84	2.8
6 X 6 X 3 SS	2.28	2.33	2.0
6 X 6 X 3 WS	2.35	2.40	2.0
4 X 4 X 4 BT	2.78	3.07	10.4

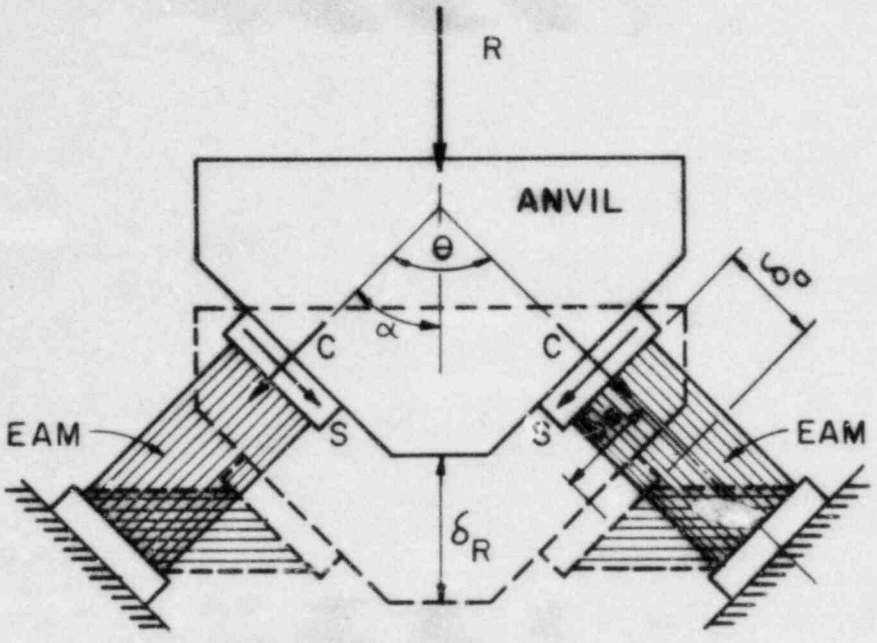

TEST SET UP FOR EAM BEHAVIOUR UNDER IMPACT LOADING IN ANGULAR CONFIGURATION

FIGURE IV-1

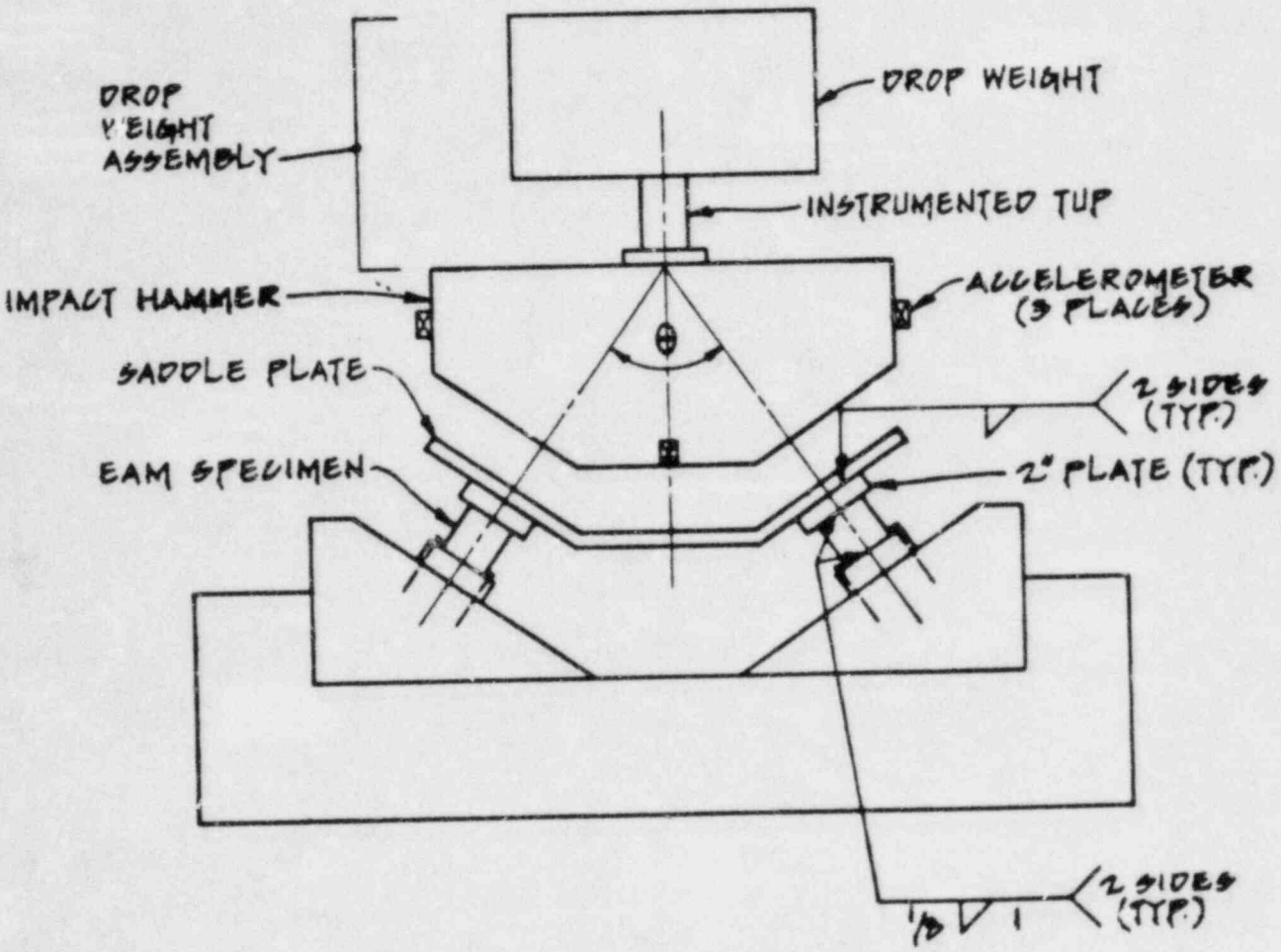

IV-2 BYRON ANGULAR CONFIGURATION TEST SETUP

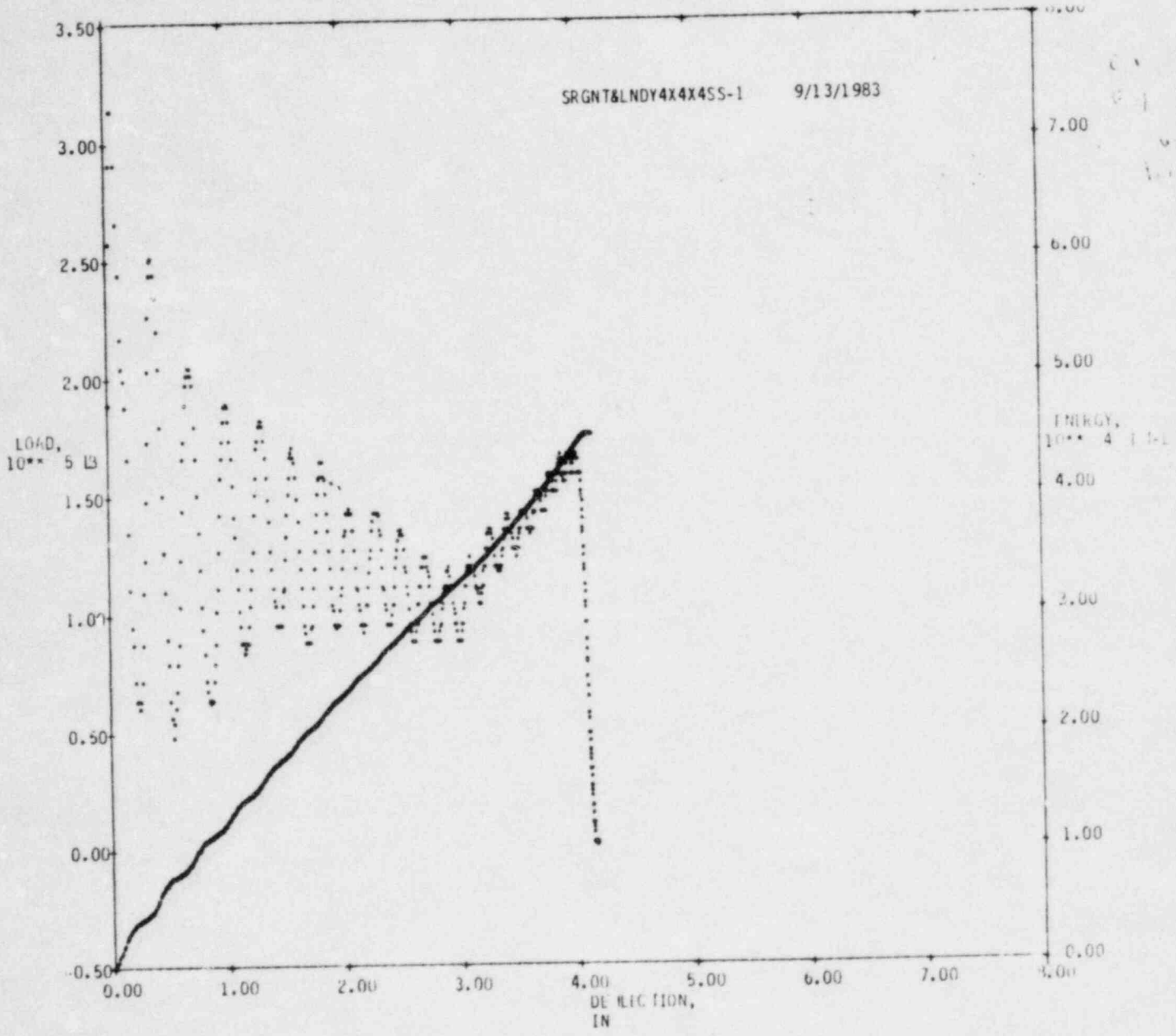

TEST	TEMP F	IMPACT VELOCITY FT/S	ENERGY FT-LB	TIME,10** 1 MSEC INIA	TOTAL	LOAD,10** 2LB MAX	ENERGY,10** 3 FT-LB INIA	PROP	TOTAL
4X4X4SS-1	119.9	26.04	43739.10	0.01	2.65	3144	1.1	43.8	44.9

IV-3 ETI-300 LOAD AND ENERGY VERSUS DISPLACEMENT CURVES FOR 4X4X4 SS TEST

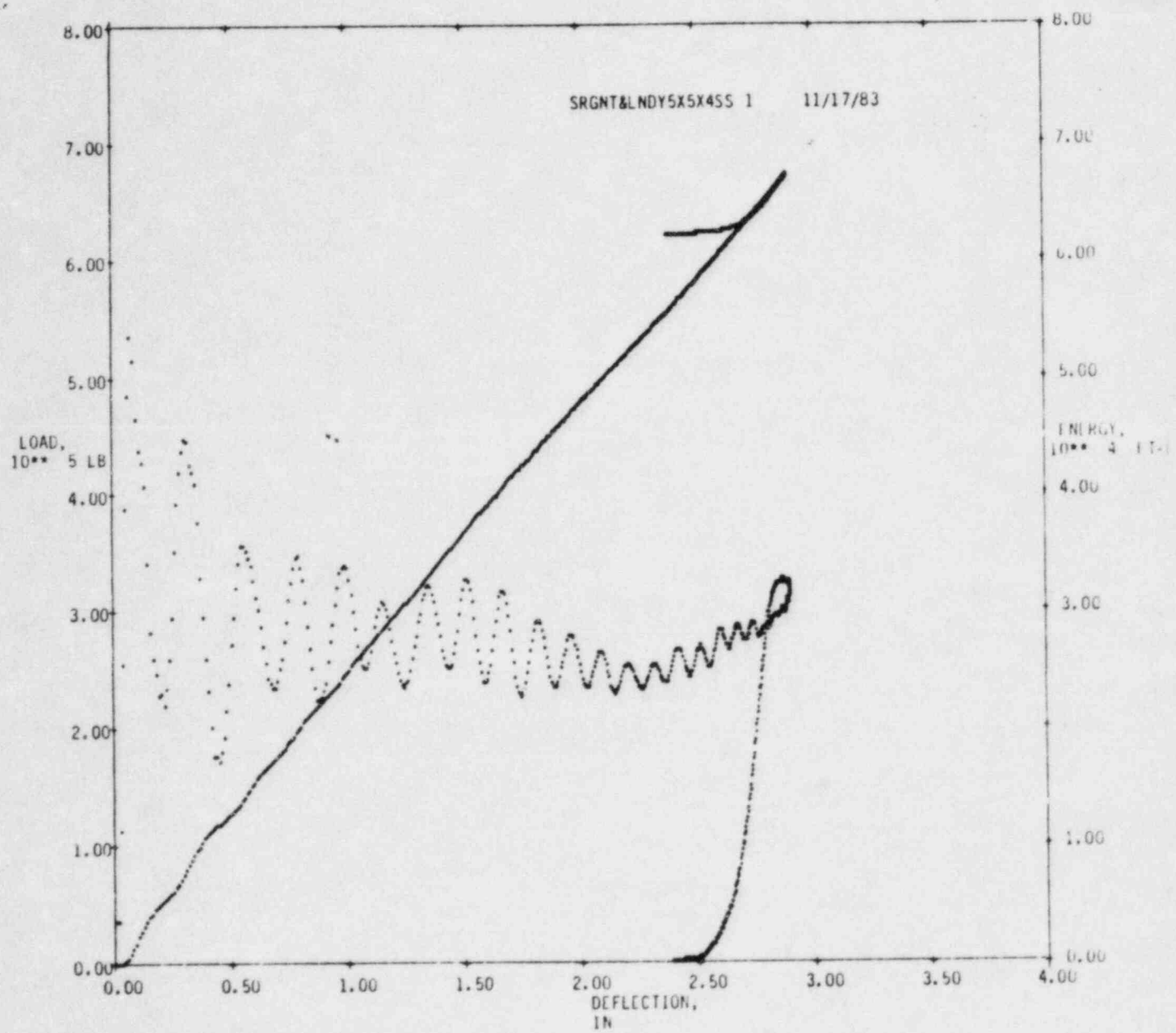

TEST	TEMP F	IMPACT VELOCITY FT/S	ENERGY FT-LB	TIME,10** 1 MSEC INIA	TOTAL	LOAD,10** 2LB MAX	ENERGY,10** 3 FT-LB INIA	PROP	TOTAL
5X5X4SS 1	119.9	25.37	65527.60	0.02	2.75	5361	1.3	60.7	62.0

IV-4 ETI-300 LOAD AND ENERGY VERSUS DISPLACEMENT CURVES FOR 5X5X4 SS TEST

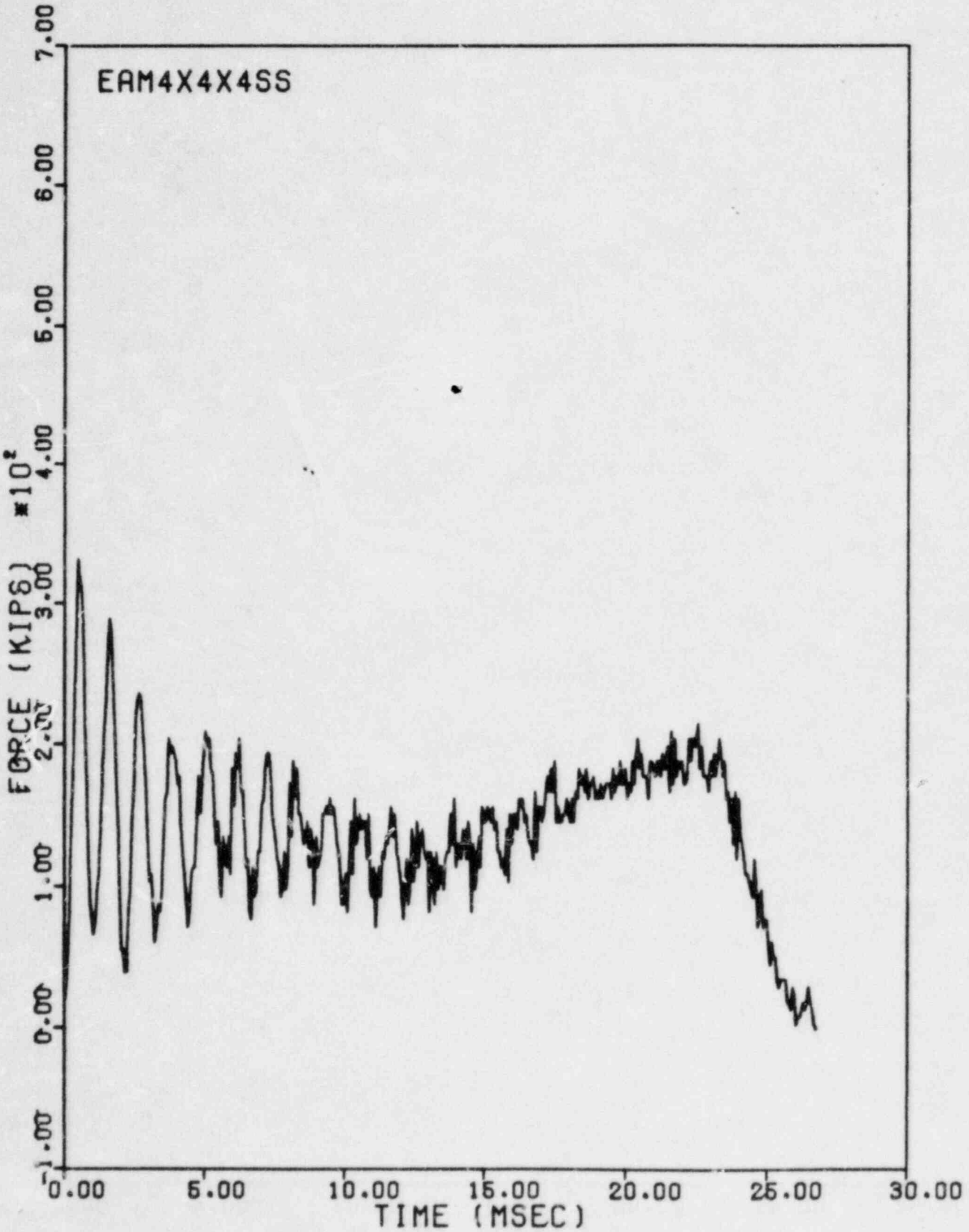

IV-5 MEASURED LOAD TIME HISTORY FOR 4X4X4 SS TEST

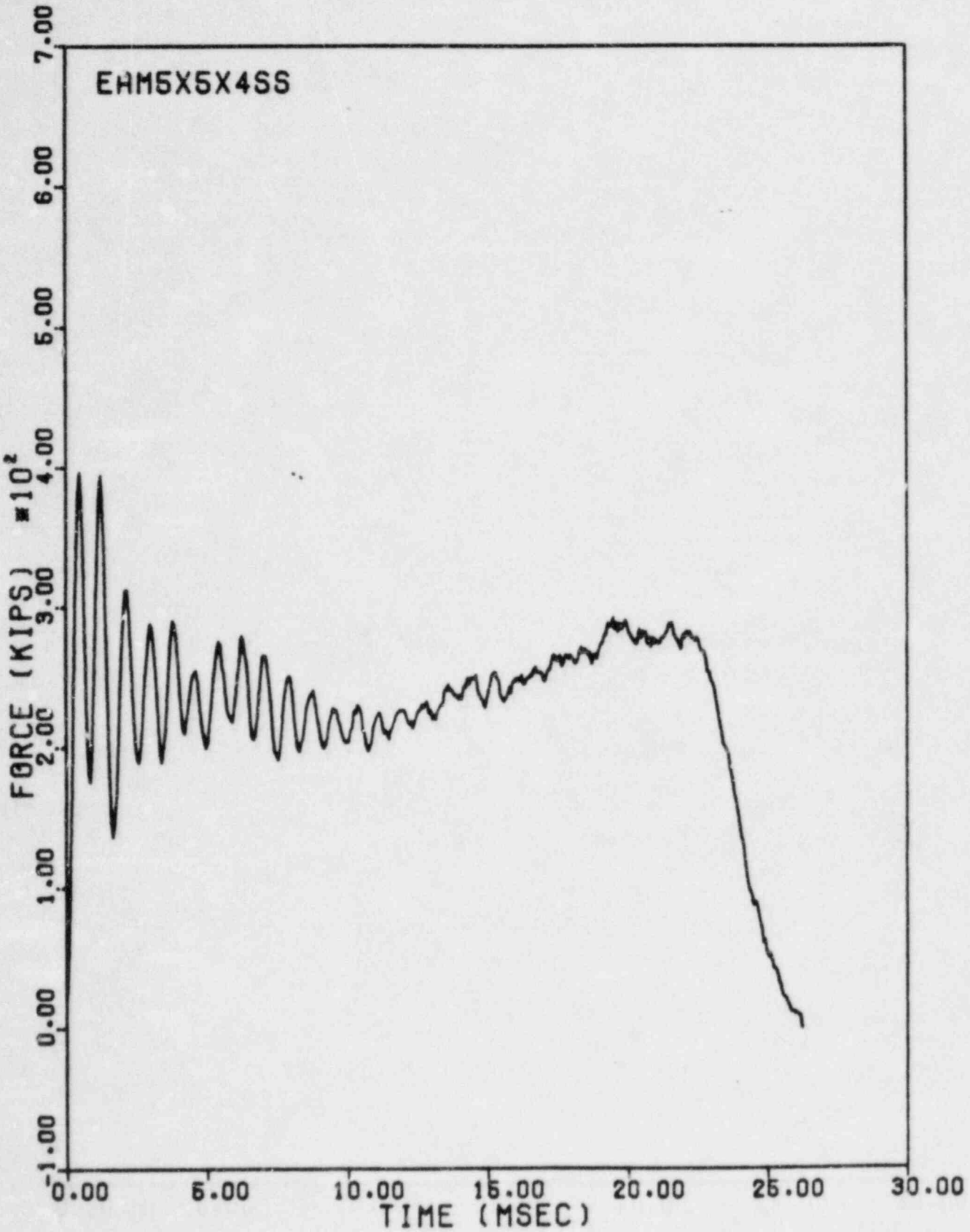

17-6 MEASURED LOAD TIME HISTORY FOR 5X5X4 SS TEST

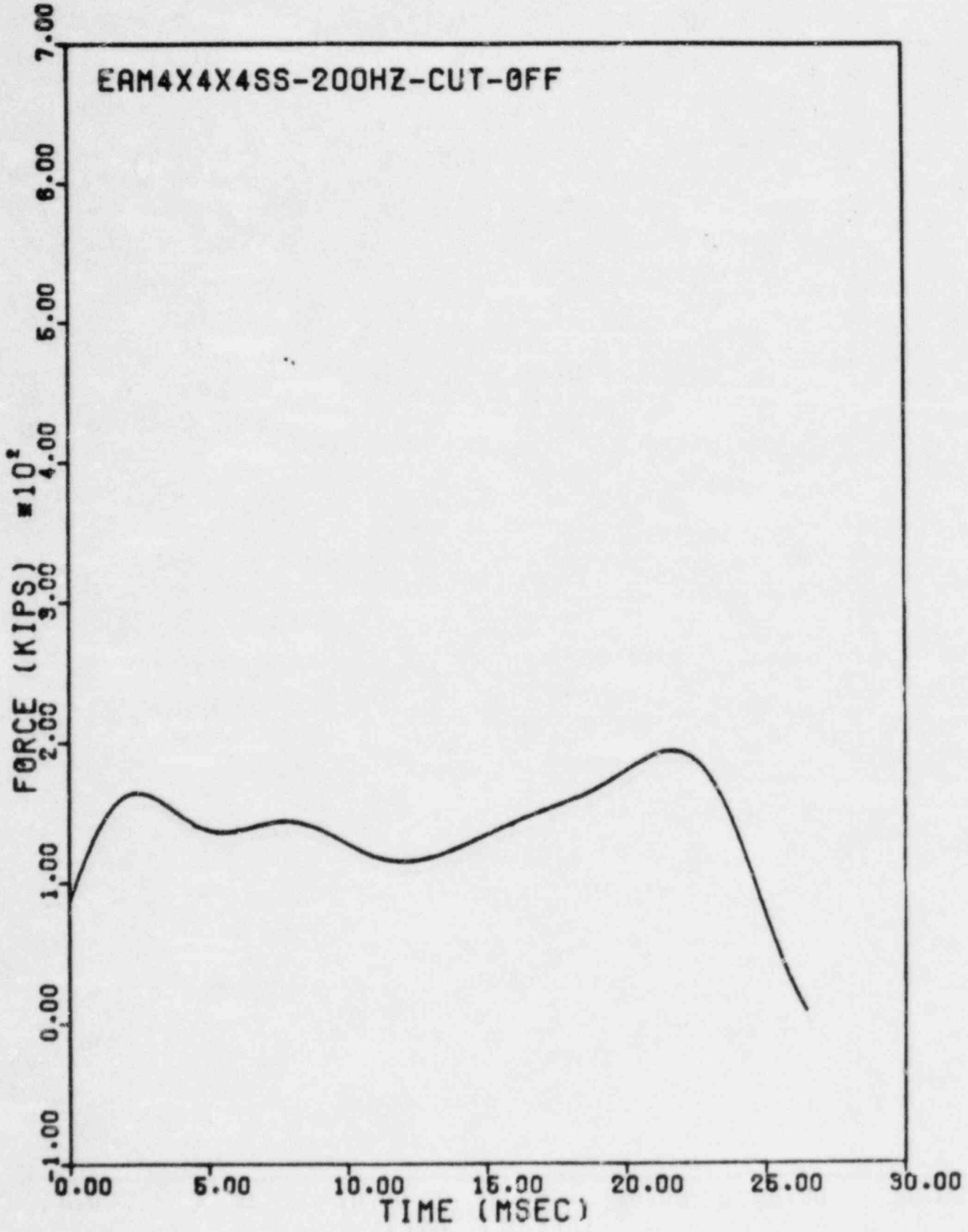

IV-7 200 HZ FILTERED LOAD TIME HISTORY FOR 4X4X4 SS TEST

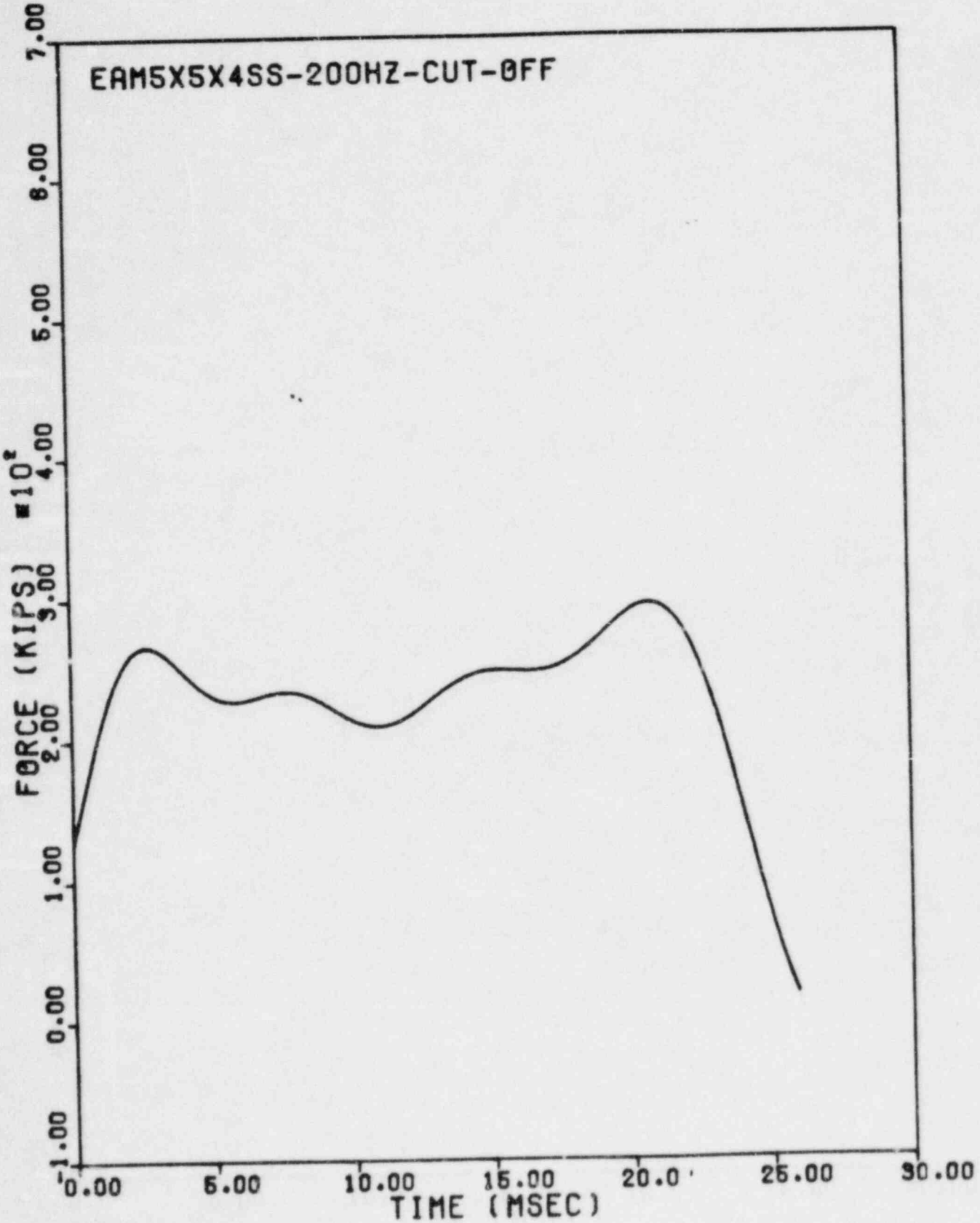

IV-8 200 HZ FILTERED LOAD TIME HISTORY FOR 5X5X4 SS TEST

V. HEIGHT GREATER THAN WIDTH TESTS

This section describes the tests performed by Hexcel in 1981 to study the behavior of the EAM for various height-to-width ratios of the EAM.

A. Test Description

The purpose of these tests was to determine the effects of height-to-width (H/W) ratio on the crush strength of Hexcel/Solarib material. The test results are summarized in the Hexcel test report entitled, "Hexcel/Solarib with Height Greater Than Width," dated August 1981. Hexcel has also provided Sargent & Lundy with the raw test data, including the dynamic load versus deflection and energy versus deflection curves.

To evaluate the effect of height-to-width ratio on the crush strength of EAM, test samples of various sizes were subjected to an impact loading to determine the dynamic crush strength and the load deflection curve. In these tests the specimens were dynamically loaded in axial compression. The test impact velocity was approximately 15.5 feet/sec. The tests were performed by Hexcel to study EAM behavior. The tests meet their technical quality assurance requirements. However, the test paper work was not signed for QA review and acceptance. Based on the review of the raw test data and conversations with Hexcel personnel, it is our judgment that the test represents reliable technical information.

For these tests, Hexcel's ETI-300 Instrumented Impact System was used to record the test results and to generate the loads and energy versus displacement plots. The ETI-300 system and its calibration are briefly described in Appendix A.

B. Test Results

The results of these tests are summarized in the following table.

Test Group	EAM Size (IN) L	W	H	Average Crush Strength at 50% Strain (PSI)
A	4	4	4	3870
	4	4	4	3720
B	4	2	4	3600
	4	2	4	3760
C	4	4	8	3790 (*)
	4	4	8	4030
D	6	2	6	3600 (**)
	6	2	6	3930
E	4	2	2	3660
	4	2	2	3920

* Specimen started to buckle.

** Specimen buckled.

The test results show that all samples, including the 6 x 2 x 6 sample (H/W = 3.0), absorbed the design energy even though one of these samples buckled during the test. Based on these tests, we have concluded that

the EAM H/W ratio should be limited to a maximum of 2.0. The H/W ratio of 2.0 is being established because one sample of H/W ratio of 3.0 buckled. In addition, the load deflection curve load oscillation for this H/W ratio sample was larger than those for the other samples. This can be observed by comparing the load versus deflection plots for a 4 x 4 x 4 inch specimen shown in Figure V-1 to the corresponding plot for the 6 x 2 x 6 inch sample shown in Figure V-2.

The tests also show that the size of the test sample has no effect on the average crush strength of the EAM, thus the test results from small specimens are applicable to the full-size EAM used in the pipe whip restraints.

C. Conformance With SRP Requirements

The test impact velocity was approximately 15.5 feet/sec and all the specimens (except the 4 x 4 x 8") were loaded to at least 125% of their design capacity. The 4 x 4 x 8" samples were loaded to approximately 90% of design capacity due to limitation of the testing machine. The load deformation curve shows that strain hardening starts at loadings greater than 125% of design capacity.

These tests meet the SRP (1981) requirements.

D. Applicability to Byron EAM

It is Hexcel's judgment that the test results are applicable to the Byron project even though they were performed on 3800 psi material as compared to the 6000 psi material used on Byron. This judgment is based on the fact that the manufacturing process and the raw

materials used for the two EAMs are similar. The difference in crush strength is achieved by varying the spacings of the rib. Based on the evaluation of the test data, the resulting load deflection curves, and the fact that buckling for a material with a greater equivalent Young's Modulus (because of the closer rib spacings for Byron EAM) is less likely than for the material tested, it is our judgment that the test results are applicable to the Byron project.

These test results and conclusions were presented to the NRC Region III staff in July 1982 .

E. Additional Tests

The fact that the tests were performed on a nominal 3800 psi material, and the largest H/W ratio of EAM used on Byron is 2.09, we will conduct an additional test with H/W ratio of 2.10 using EAM specimens either cut at the Byron site or at Hexcel's shop from Byron type 6000 psi EAM core block. This test will also confirm our engineering judgment that EAM will perform its intended function for H/W ratios of 2.10 and less.

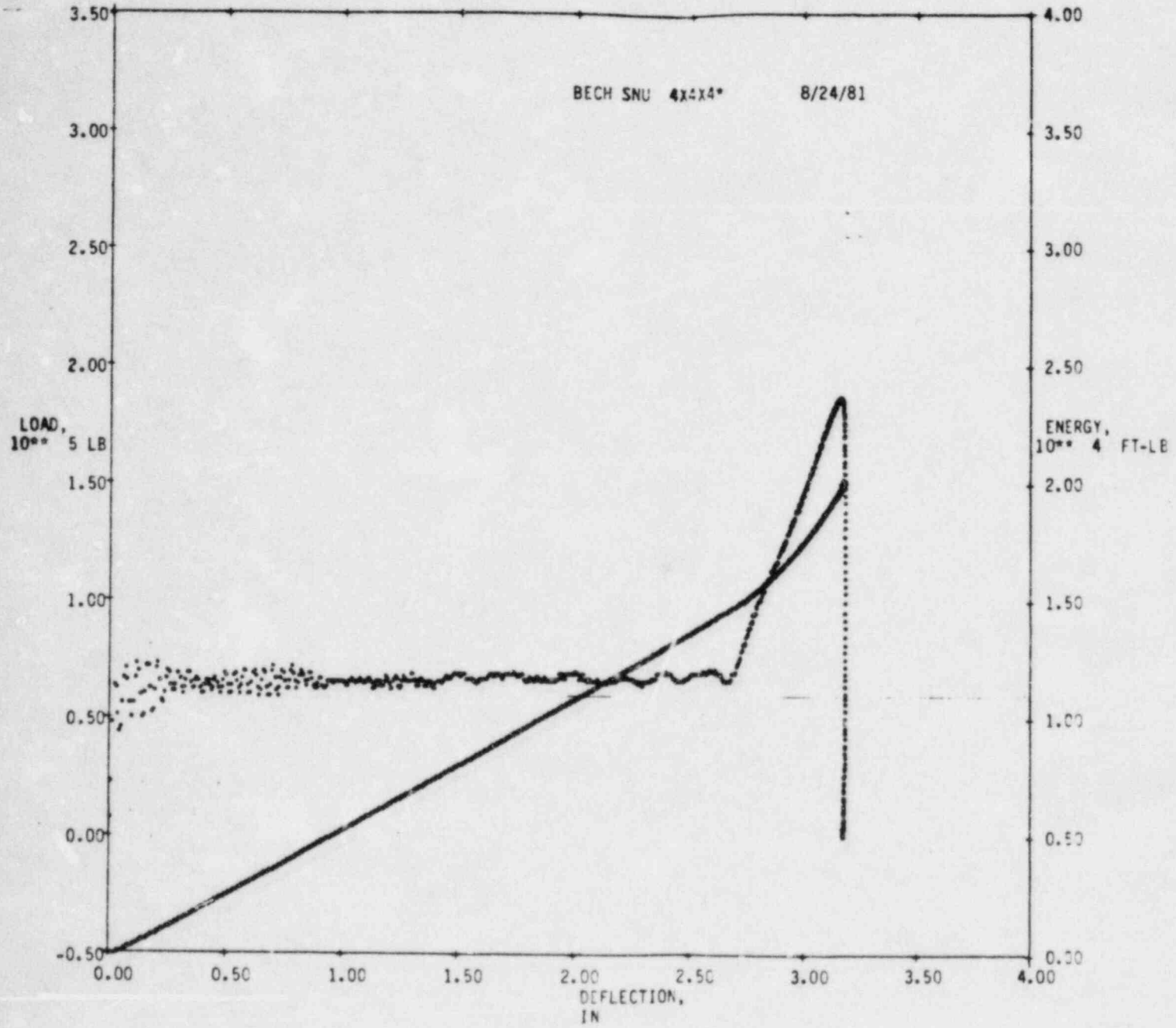

Figure V-1: Load Deflection Curve for 4x4x4 inch Specimen

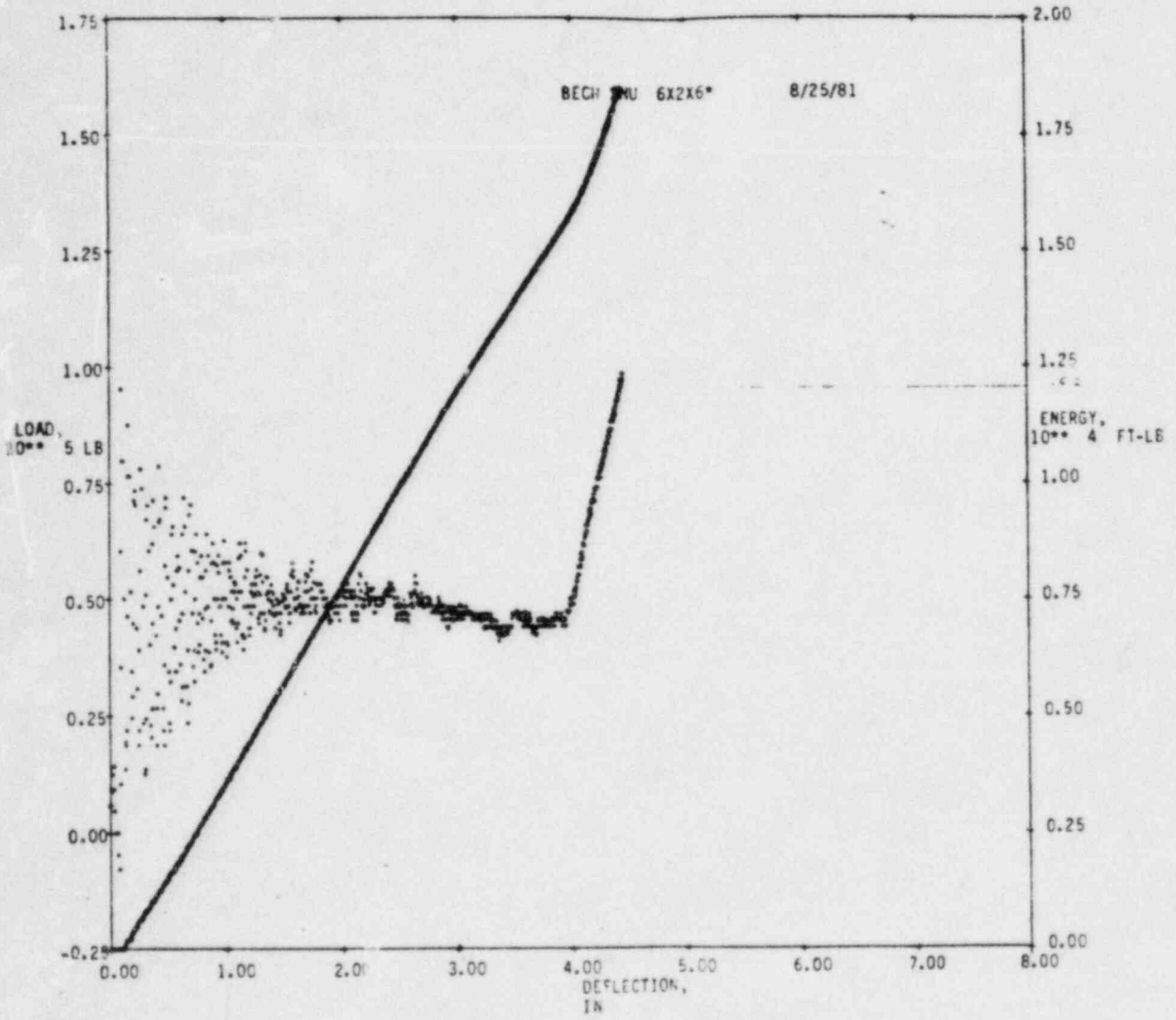

Figure V-2: Load Deflection Curve for 6x2x6 Inch Specimen

VI. TESTS ON STACKED EAM SPECIMENS

This section describes the tests performed by Hexcel in 1982 to study the behavior of the EAM when two or three EAM specimens are stacked on top of one another.

A. Test Description

The purpose of these tests was to determine the effect on the average dynamic crush strength of the EAM specimens when these EAM specimens are vertically stacked. The test results are summarized in the Hexcel Technical report entitled, "Test Program for Hexcel/Solarib Stacked EAM Specimens," dated June 1982. Hexcel has provided Sargent & Lundy with the raw test data, including the dynamic load versus deflection curves and the energy versus deflection curves.

The specimens were taken from one core block of material with an average crush strength of approximately 1000 psi. Each of the specimens had the following nominal dimensions:

Length 4 inch
Width 4 inch
Height 2 inch after a precrush of 1/8 inch

In the test, the specimens were dynamically loaded in direct compression by an impact hammer with an impact velocity of approximately 15.5 feet/sec. The following tests were conducted:

1. Two tests using one specimen at a time.

2. One test with two specimens stacked on top of each other and separated with a 0.02-inch-thick s/s plate, brazed to both specimens.

3. One test with three specimens stacked on top of each other separated with two 0.02-inch-thick s/s plates. These plates were not brazed to the specimens.

For these tests Hexcel's ETI-300 Instrumented Impact System was used to record the test results and to generate the load and energy versus displacement curves. The ETI-300 system and its calibration are briefly described in Appendix A.

The tests were performed by Hexcel to study the EAM behavior. The tests meet their technical quality assurance requirements. The test paper work was signed by the preparer but was not signed for QA review and approval. Based on the review of the raw test data and conversations with Hexcel personnel, it is our judgment that the test represents reliable technical information.

B. Test Results

The test results can be summarized as follows:

Number of Specimen Stacked	Average Dynamic Crush Strength (psi)
One	1040
One	932
Two	960
Three	1150

The tests show that stacking more than one specimen on top of the other has no significant effect on the average dynamic crush strength. The load deflection curves for the three specimens stacked vertically show a somewhat larger than normal oscillation when compared to the two-stacked or unstacked specimens. This can be observed by comparing the load versus deflection curves for the unstacked specimen shown in Figure VI-1, the two-stacked specimens load deflection curve shown in Figure VI-2 and the three-stacked specimens load deflection curve shown in Figure VI-3. In the Byron design, a maximum of two pieces of EAM are stacked and thus the load oscillation for the three-stacked specimens test is not applicable.

C. Conformance to SRP Requirements

The test impact velocity was approximately 15.5 feet per second and all the specimens were loaded to 125% of their design capacity. The load deformation curve shows that significant strain hardening does not start until after energy input is greater than 125% of the design capacity. Thus, the SRP (1981) requirements are met for the purposes of the test.

D. Applicability to Byron EAM

It is Hexcel's judgment that the test results are applicable to the Byron project even though the tests were performed on a 1000 psi material versus 6000 psi material used on Byron. This is based on the fact that the manufacturing process and the raw materials for the two EAMs are the same. The difference in crush strength is achieved by varying the spacings of the ribs. Based on the evaluation of the test data, we concur with the Hexcel judgment.

E. Additional Tests

Because of the large difference in crush strength between the material tested and Byron EAM and the absence of the 0.02-inch separator plate between the field-fabricated stacked EAM for restraints MS-R18, MS-R44 and MS-P26, we will perform two additional dynamic tests using two 4 x 4 x 2" stacked specimens to confirm the applicability of the test results to the Byron station. The specimens for these tests would be cut either at the Byron site or at Hexcel's shop using Byron type 6000 psi EAM material. The EAM test specimens will not be precrushed. One test will be conducted with a 0.02-inch separator plate between the stacked EAM pieces. The other test will be conducted without the 0.02-inch separator plate, this will determine whether or not it is necessary to modify the installed EAM in pipe whip restraints MS-R18, MS-R44 and MS-P26 by adding a 0.02-inch separator plate between the vertically stacked EAM pieces.

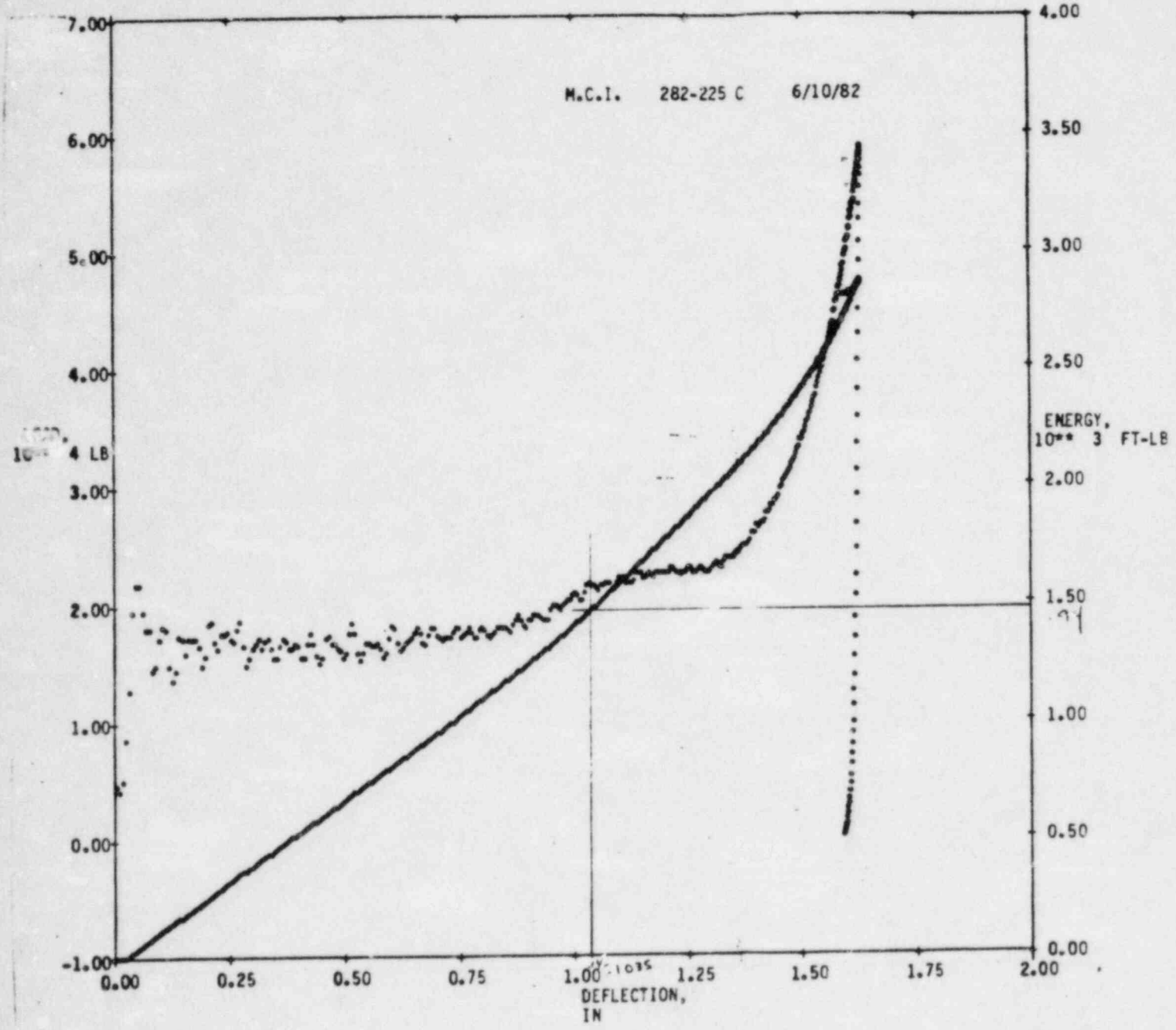

Figure VI-1: Load Deflection Curve for Unstacked Specimen

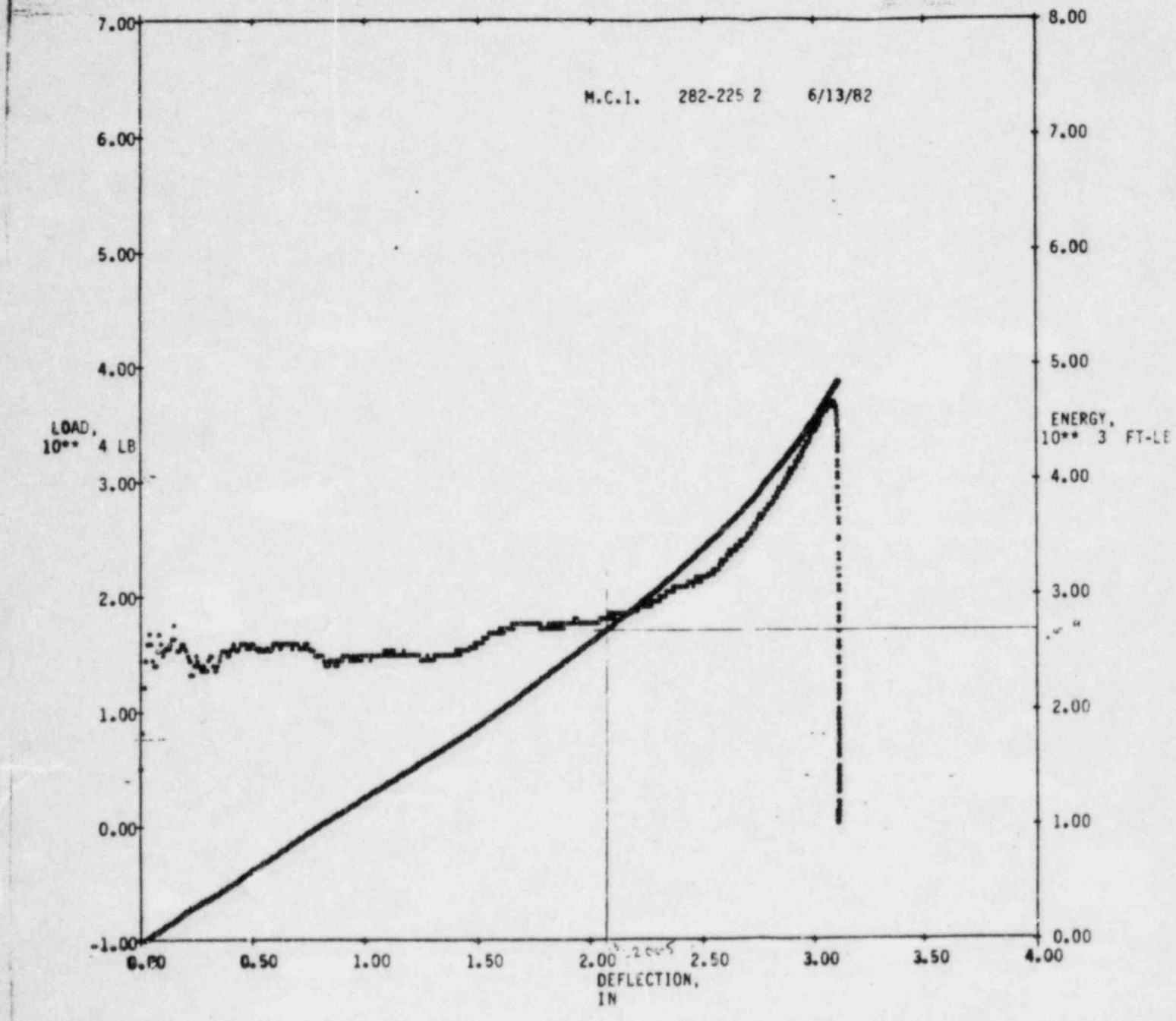

Figure VI-2: Load Deflection Curve for Two-Stacked Specimens

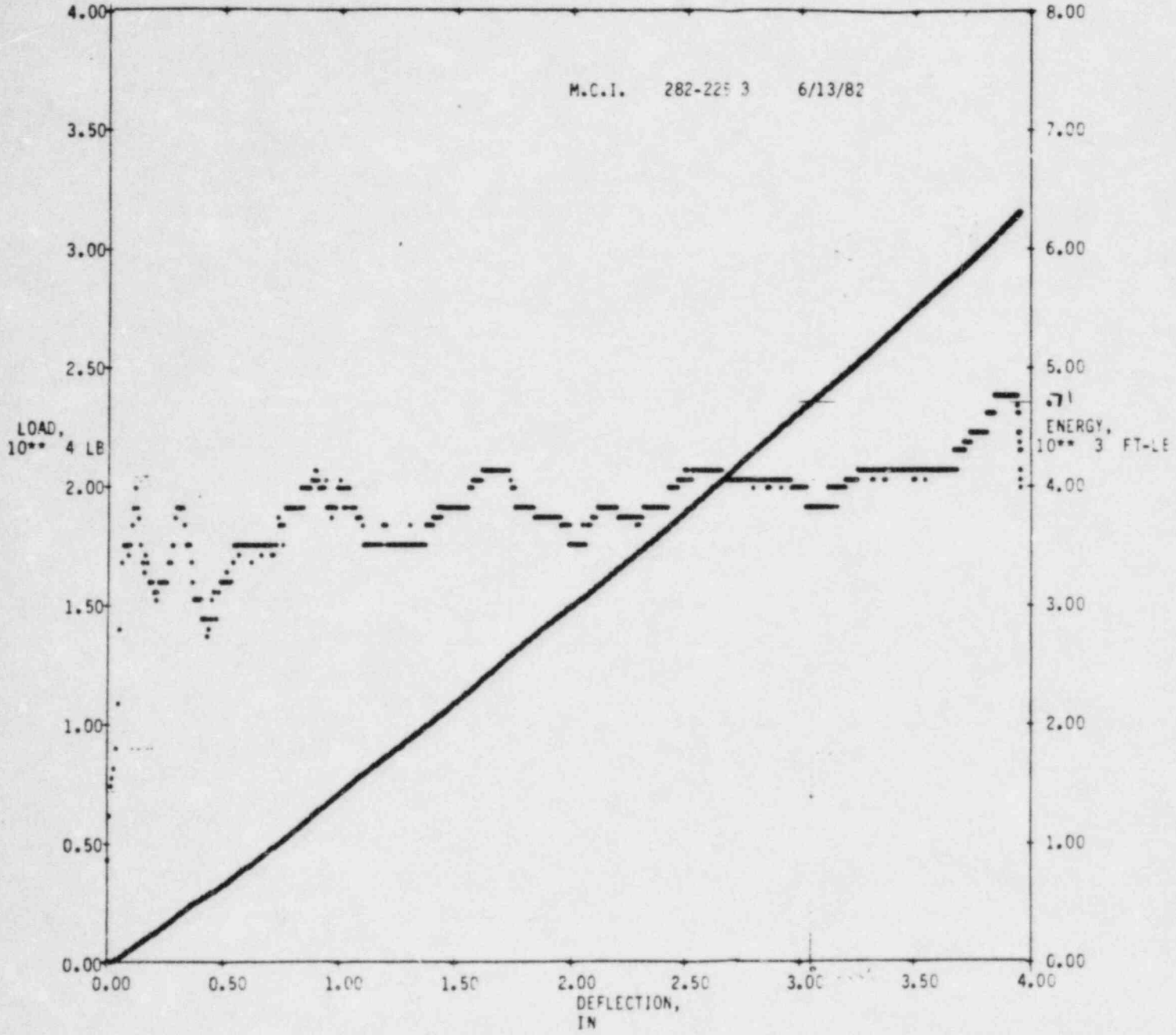

Figure VI-3: Load Deflection Curves for Three-Stacked Specimens

VII. TEST TO DETERMINE EFFECT OF PRECRUSH

This section describes the tests performed by Hexcel in 1983 to study the behavior of the EAM with and without initial precrush.

A. Test Description

The purpose of these tests was to determine the effect of precrush on the peak force during crushing of the Hexcel/Solarib energy absorption material. The tests are summarized in the Hexcel Technical report entitled, "Test Program for Precrush Studies," dated January 1983 and revised in September 1984. Hexcel has provided Sargent & Lundy with the raw test data, including the dynamic load versus deflection curves and the energy versus deflection curves.

In the test, the EAM specimens were dynamically loaded in direct compression with an impact hammer with an impact velocity of 15.5 feet/sec. The following tests were conducted:

1. One specimen without any precrush
2. One specimen with 1/16 to 1/8 inch precrush with peaks
3. One specimen with 1/8 inch precrush with peaks
4. One specimen with 1/8 inch precrush then flattened
5. One specimen with 1/4 inch precrush then flattened
6. One specimen with 1/4 inch precrush and flattened within 1/8 inch

7. One specimen with 1/4 to 5/16 inch precrush with peaks

The "precrush with peaks" refers to the process where a round head hammer is used to precrush the EAM. This process results in an uneven precrush. The "precrush then flattened" refers to the process where a round head hammer is used for initial precrush and then the peaks are flattened with a plate.

The specimens were taken from six separate core blocks with specimens 5 and 6 taken from the same core block. Each of the specimens had the following nominal dimensions:

Length 4 inch
Width 4 inch
Height 3 to 4 inch

For these tests Hexcel's ETI-300 Instrumented Impact System was used to record the test results and to generate the load and energy versus displacement curves. The ETI-300 system and its calibration are briefly described in Appendix A.

The tests were performed by Hexcel to study the behavior of EAM. These tests meet their technical quality assurance requirements. However, the test paper work was not signed. Based on the review of the raw test data and conversations with Hexcel personnel, it is our judgment that the test represents reliable technical information.

B. Test Results

The test results can be summarized as follows:

Specimen	Average Crush Strength (psi)	Average Crush Force (kip)	Peak Crush Force (kip)	Peak to Average Ratio
No precrush	7071	113.1	139.4	1.23
1/16" to 1/8" precrush with peaks	5839	93.4	109.5	1.17
1/8" precrush with peaks	5737	91.8	110.0	1.21
1/8" precrush then flattened	6542	104.7	125.5	1.20
1/4" precrush then flattened	5812	93.0	114.0	1.23
1/4" precrush then flattened to within 1/8"	5794	92.7	114.4	1.23
1/4" to 5/16" precrush with peaks	6440	103.0	123.9	1.20

These tests show that lack of precrush does not significantly increase the peak force during crushing of the EAM. The load deflection curves which were obtained show that the peak force is 17% to 23% greater than the average force during crushing. This increase is predominantly due to load oscillation during crushing and not because of any initial peak. This can be observed by comparing the load deflection

curves for specimen 1 with no precrush, shown in Figure VII-1, and the load deflection curve for specimen 7 with greater than 1/4" precrush, shown in Figure VII-2. The relatively large range of average crushing force for the seven specimens (91,800 lbs. to 113,135 lbs.) is attributed to the fact that these specimens were taken from six different core blocks.

C. Conformance with SRP Requirements

The tests were dynamic impact tests with an impact velocity of approximately 15.5 feet/seconds. The specimens were crushed to at least 80% of the design capacity for these tests. The lower percentage of crushing is acceptable because the effect of precrush is only significant during the initial phases of EAM crushing. Thus for the purpose of the test, the SRP (1981) requirements were met.

D. Applicability to Byron EAM

In Hexcel's judgment, the test results are applicable to Byron EAM because the manufacturing process and raw materials for the two EAMs are the same. Based on the above evaluation and the fact that the tests were performed on material very similar to that used at Byron (average crush strength 6000 psi), it is our judgment that the test results are applicable to the Byron project.

E. Additional Tests

To confirm our judgment that the existing test results are applicable to Byron EAM, we will conduct one additional test to evaluate the effect of the lack of precrush on peak crushing force of EAM specimens. The

material for this test will either be cut at the Byron site or at Hexcel's shop using Byron type 6000 psi EAM.

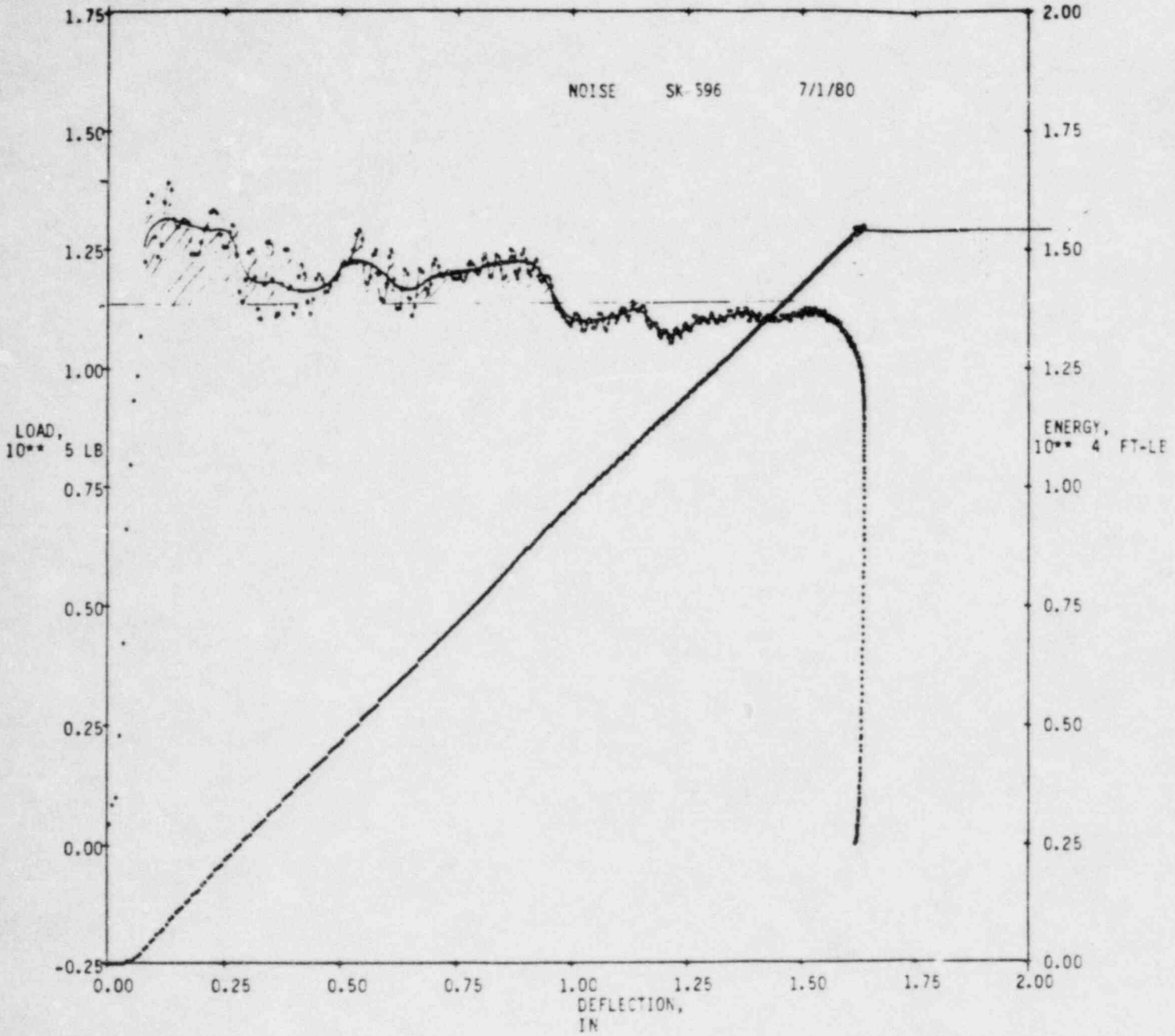

Figure VII-1: Load Deflection Curve for Specimen with No Precrush

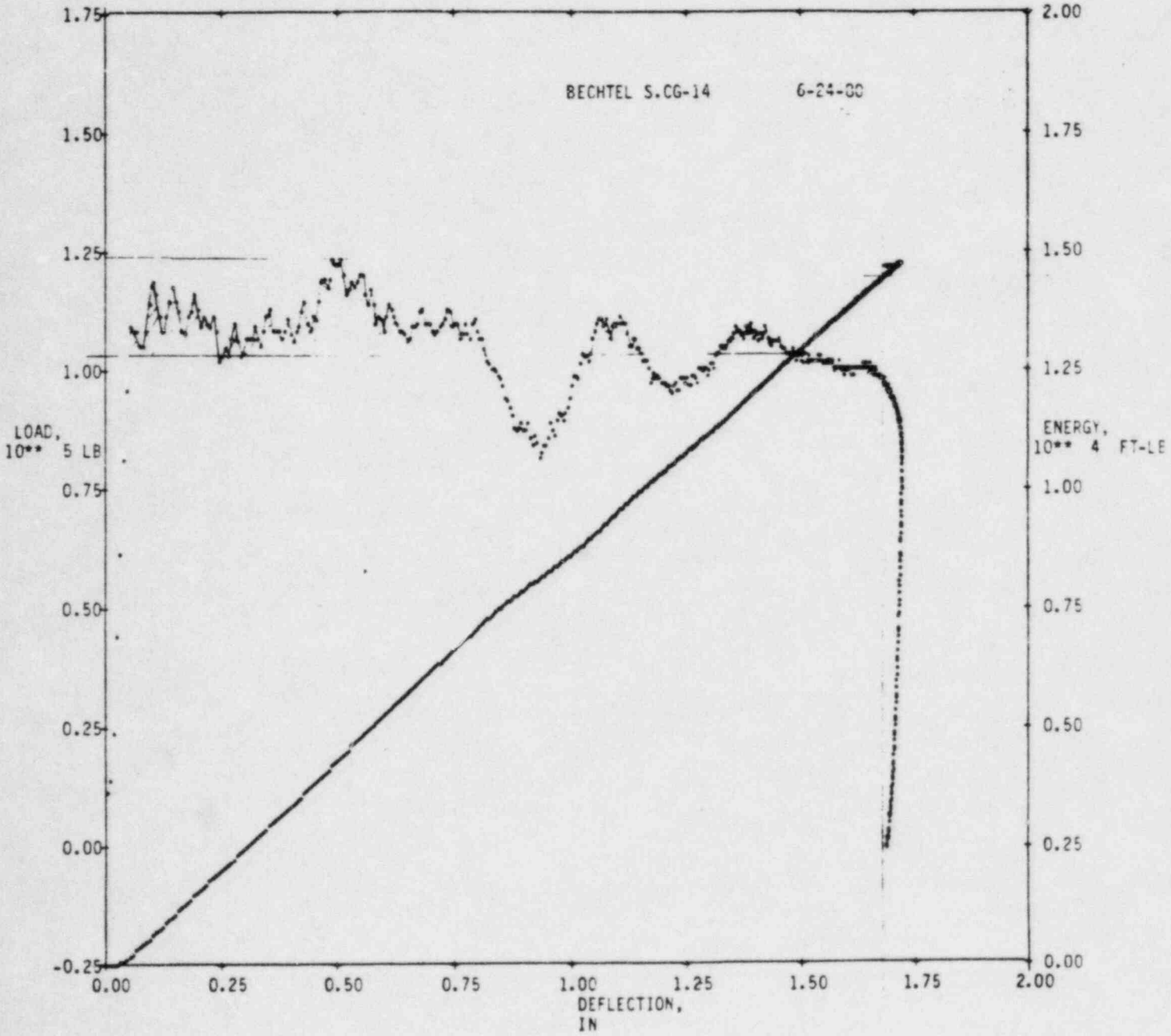

Figure VII-2: Load Deflection Curve for Specimen with Greater than 1/4 Inch Precrush

VIII. TESTS TO DETERMINE MATERIAL VARIABILITY

This section describes the tests performed by Hexcel in 1983 to study the variability of EAM properties within a single core block of material. The variability of EAM properties as a function of different core blocks of material is also presented based on the Byron production tes data.

A. Test Description

The purpose of these tests was to study the variability in the crush strength of the energy absorption material from one single core block of material. The tests are summarized in the Hexcel Technical Report entitled, "Test Program for Checking Material Variability," dated February 1983. Hexcel has provided Sargent & Lundy with the raw test data, including the dynamic load versus deflection curves and the energy versus deflection curves.

In the test, stacked EAM specimens were dynamically loaded in direct compression with an impact hammer with an impact velocity of 25 feet/sec. The following describes the tests conducted.

1. A total of 36 specimens were cut from one core block of nominal 3200 psi crush strength. The locations of the specimens in the core block are shown in Figure VIII-1.

2. All the specimens had the following nominal dimensions:

   Length 4 inch
   Width 4 inch
   Height 1 1/8 inch

3. For each of the 12 dynamic tests, three specimens stacked on top of each other with a 0.50-inch-thick plate separating them were used.

For these tests Hexcel's ETI-300 Instrumented Impact System was used to record the test results and to generate the load and energy versus displacement curves. The ETI-300 system and its calibration are briefly described in Appendix A.

The tests were performed by Hexcel to study the EAM behavior. The tests meet their technical quality assurance requirements. The paper work was signed by the preparer, but was not signed for QA review and acceptance. Based on the review of the raw test data and conversations with Hexcel personnel, it is our judgment that the test represents reliable technical information.

B. Test Results

The test results can be summarized as follows:

Specimen	Average Crush Strength (psi)	Specimen	Average Crush Strength (psi)
1, 2 & 3	3290	19, 20 & 21	3110
4, 5 & 6	3240	22, 23 & 24	3400
7, 8 & 9	3140	25, 26 & 27	3050
10, 11 & 12	3140	28, 29 & 30	3180
13, 14 & 15	3110	31, 32 & 33	3150
16, 17 & 18	3260	34, 35 & 36	3400

Design Average Crush Strength = 3200 psi
Maximum Average Crush Strength = 3400 psi
Minimum Average Crush Strength = 3050 psi

The tests show that the variation in material average crush strength within a single core block of material is +6.25% on the plus (higher) side and -4.69% on the negative (lower) side. The review of the load versus deflection curves for these twelve tests shows that the curves for these tests are very similar. This can be observed by comparing the load versus deflection curves for the lowest crush strength test (test #9) and the highest crush strength test (test #12) shown in Figures VIII-2 and VIII-3, respectively. The tests show a larger than normal load oscillation. This oscillation is attributed to the vertical stacking of three EAM specimens and the 0.50-inch spacer plate between each. Normally a 0.02-inch spacer plate is used when EAM pieces are stacked. The 0.5"-thick plate was used to assure that crushing of all three specimens is uniform. As the purpose of the tests was to study the variability of the material, the load oscillations are not significant to the conclusions. Similar larger than normal load oscillations were also observed in the tests on the three-stacked EAM specimens discussed in Section VI. Notes that the

spacer plate for the three-stacked specimens tests was only 0.02 inches thick compared to the 0.5 inch thick pla[illegible] used in the material variability tests.

C. Conformance to SRP Requirements

The tests were dynamic impact tests with an impact velocity of approximately 25 feet/seconds. All the specimens were crushed with an energy greater than 125% of their design capacity. The load deformation curves showed no significant strain hardening up to the level of 125% of design capacity. Thus the requirements of the SRP (1981) are met for the purposes of this test.

D. Applicability to Byron EAM

The tests were performed on 3200 psi material compared to 6000 psi material used on Byron; however, the two EAMs are made from the same raw material and using the same manufacturing process. The variation in crush strength is achieved by making the spacings of the ribs closer or farther apart. In Hexcel's judgment, the material variability test data is applicable to Byron.

In addition to the test results described above, the Byron production tests also provide an independent check of the material variability. As stated in Section III, a total of 123 dynamic tests were performed in the Byron production tests. In these tests, one 3-3/4" x 3-3/4" x 4" specimen was tested from each core block of material used to fabricate Byron EAMs. The variability of the EAM from this data can be summarized as follows:

Average Dynamic Crush Strength Range (psi)	Range (percent)	Number of Specimen Tested in Range
5700-6300	±5%	43/123
5400-6600	±10%	116/123
6601-7200	+10% to +20%	7/123

This data shows that the EAM material is fairly uniform, with almost 95% of the material within the ±10% limits. The fact that the material variability is likely to be larger in specimens taken from different core blocks than specimens taken from the same core block leads us to conclude that the material variability within one core block is less than ±10%.

Based on the above evaluation of the Byron production test and the Hexcel material variability test data, it is our judgment that the Byron EAM has a fairly uniform average crush strength and that the requirement that one specimen from each core block be tested is an adequate means of controlling the average crush strength of all material supplied to the Byron site.

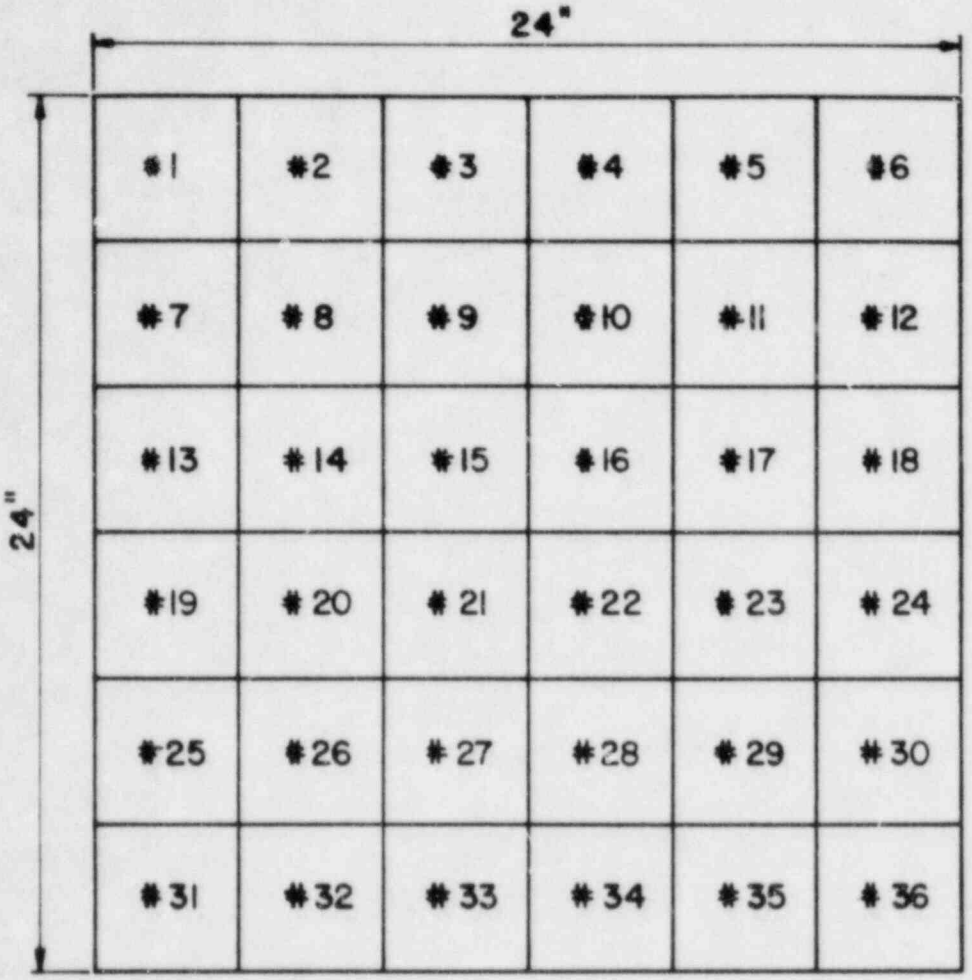

LOCATIONS FROM WHICH TEST SPECIMEN WERE CUT

FIGURE VIII - 1

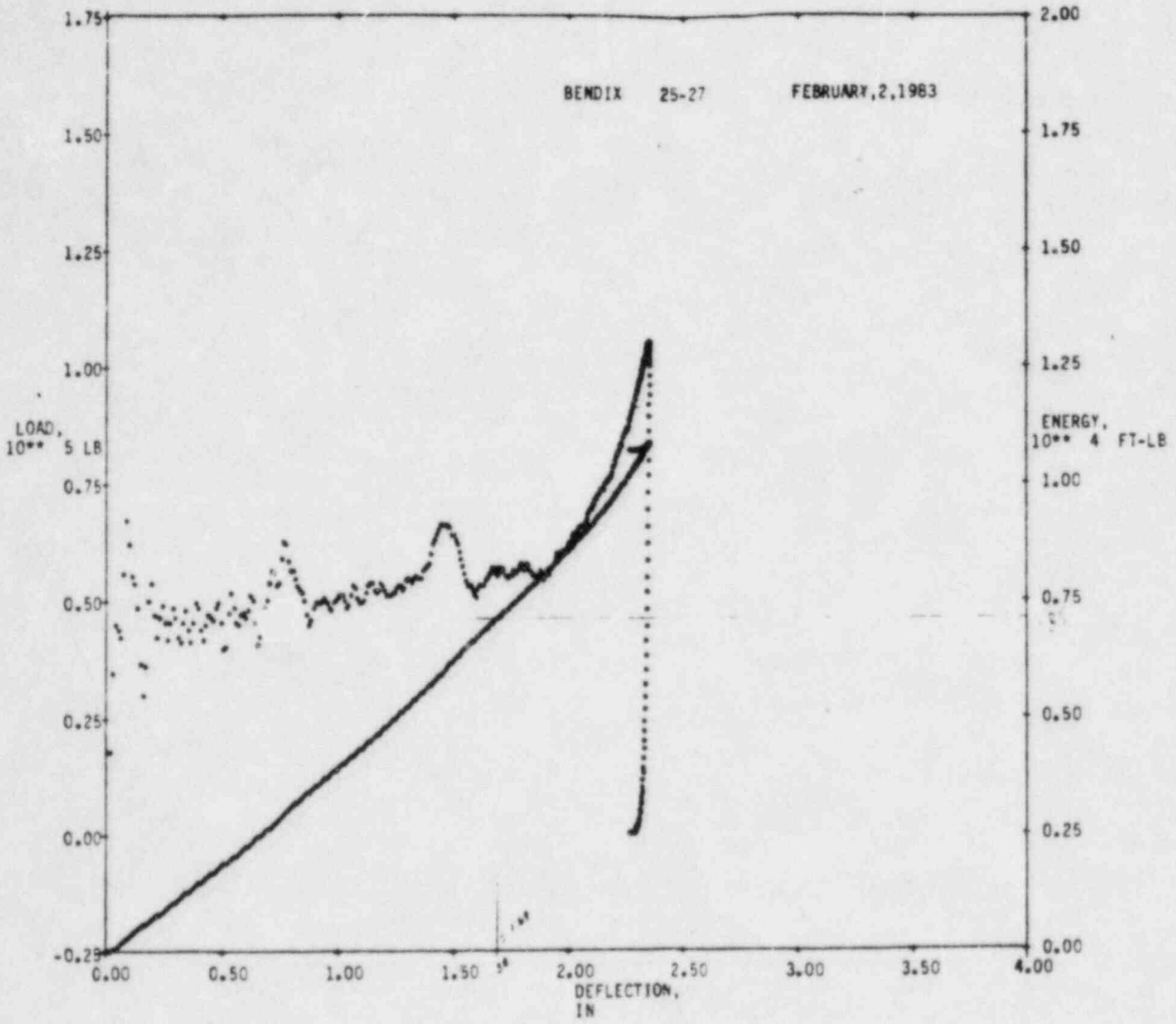

Figure VIII-2: Load Deflection Curve for Test #9, ADCS = 3050 PSI

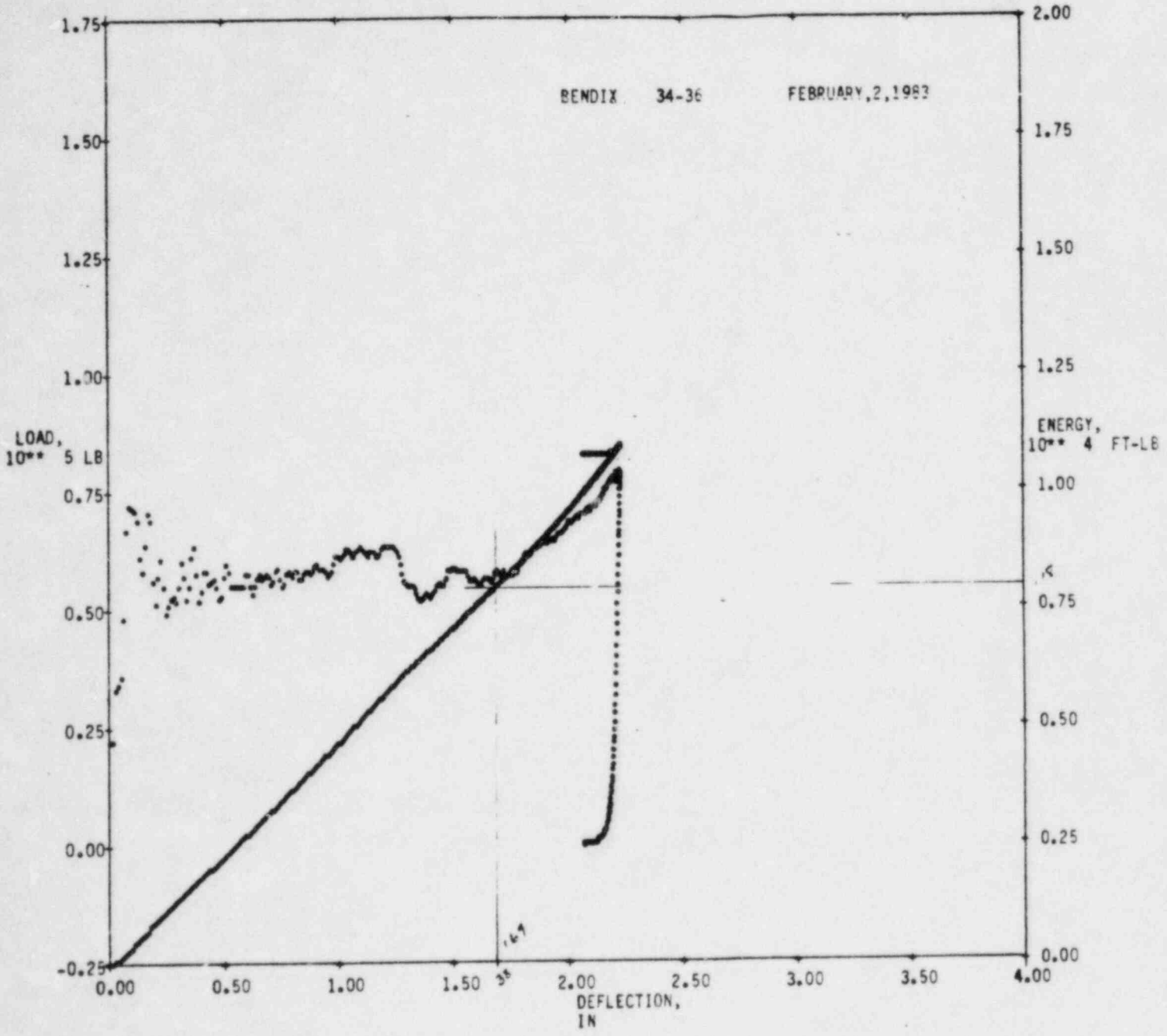

Figure VIII-3: Load Deflection Curve for Test #12, ADCS = 3400 PSI

APPENDIX A: ETI-300 INSTRUMENTED IMPACT SYSTEM

A.1 Instrumentation System and Output

The system, depicted by a block diagram in Figure A-1, consists of the following key elements:

- o Impact Mass and Instrumented Tup - The tup is a strain-gauge type load cell. The impact load is measured by this tup. A load signal conditioning is provided to generate output voltage.

- o Velocity Detector and Trigger - This device provides the inputs for computing velocity and a command signal to start acquiring test data.

- o Transient Signal Recorder - This is digital recorder which records a total of 1024 points of data for each of the force and velocity inputs.

- o Microprocessor System - The system consists of the following components:

  - System Controller
  - 24 K Byte RAM
  - 3.6 K Byte ROM
  - Floppy Disc Controller and Drive

- o Printer Plotter Keyboard - This unit provides user inputs and quick-look plots after each test.

In addition, the system provides load and trigger outputs in the rear panel via two BNC sockets. These outputs could be externally recorded by providing connecting cables at these points.

After each test, two plots may be generated:

a. Load & Energy versus Time Plot

b. Load & Energy versus Displacement Plot

A typical load and energy versus displacement plot produced by the instrumentation system is shown in Figure A-2.

In addition to the above plots, the instrumentation system output also provides the following information:

- o Temperature - Test temperature
- o Impact Velocity - A quantity derived from the inputs of the velocity sensor.
- o Impact Energy - A quantity obtained from the drop weight and the impact velocity. The drop weight is keyed into the system prior to testing.
- o Initial Time - The time at which the load reaches its maximum after impact.
- o Total Time - Total impact duration.
- o Crush Load - Maximum crushing load measured
- o Total Energy - The calculated energy based on measured load and EAM displacement

A.2 Calibration of Instrumentation Setup

The calibration of the instrumentation package and software was performed by General Research for Hexcel. Hexcel purchased the instrumentation package and software from General Research. The calibration results are summarized in a letter from General Research to Hexcel dated January 1984. The calibration results can be summarized as follows:

The load and energy results show good agreement with the theoretical values as shown in Table A-1. The maximum difference between the ETI-300 and the theoretical values is 2.5%. The calibration standard for pendulum machines (AMMRC) calls for absorbed energy value agreement within 5%. The Hexcel tup and the ETI-300 system are easily within this amount.

The calculated deflection values did not agree as well as the energy values. However the maximum difference in deflection values was 11%. This discrepancy is due to an accumulation of small errors. The microprocessor calculates the test results using a real number format (5 decimal place precision). Therefore, roundoff errors can be introduced into calculations involving sums of small numbers. When this sum is subtracted from a large number, the error can be magnified by the ratio of the two numbers. Roundoff error in the ETI-300 system only becomes significant when the majority of the available energy is absorbed, since a 1% error in total energy can cause a much larger error in the deflection values. The roundoff error usually causes the calculated energy values to be slightly smaller than the actual energy values, which in turn causes the calculated velocity values to be larger. The higher velocity values in turn cause the calculated deflection values also to be greater than measured after a test.

In our judgment, the accuracy of the ETI-300 impact system is acceptable for the dynamic and axial tests of EAM specimens.

TABLE A1: MC1/Hexcel Crush Test Results (*)

	Crush Distance (in)			Absorbed Energy (ft-lb)		
Test I.D.	Calculated	Measured	% Diff.	Calculated	Theoretical	% Diff.
Hexcel B	1.89	1.702	11	9990	9955	0.3
Hexcel C	1.91	1.769	8	9960	9961	0.0
Hexcel D	1.92	1.722	11	10200	9952	2.5
Hexcel E	1.96	1.814	8	9960	9964	0.0
Hexcel F	1.86	1.733	7	9940	9954	0.1

* Prepared by General Research for Calibration of the Hexcel Instrumentation Setup

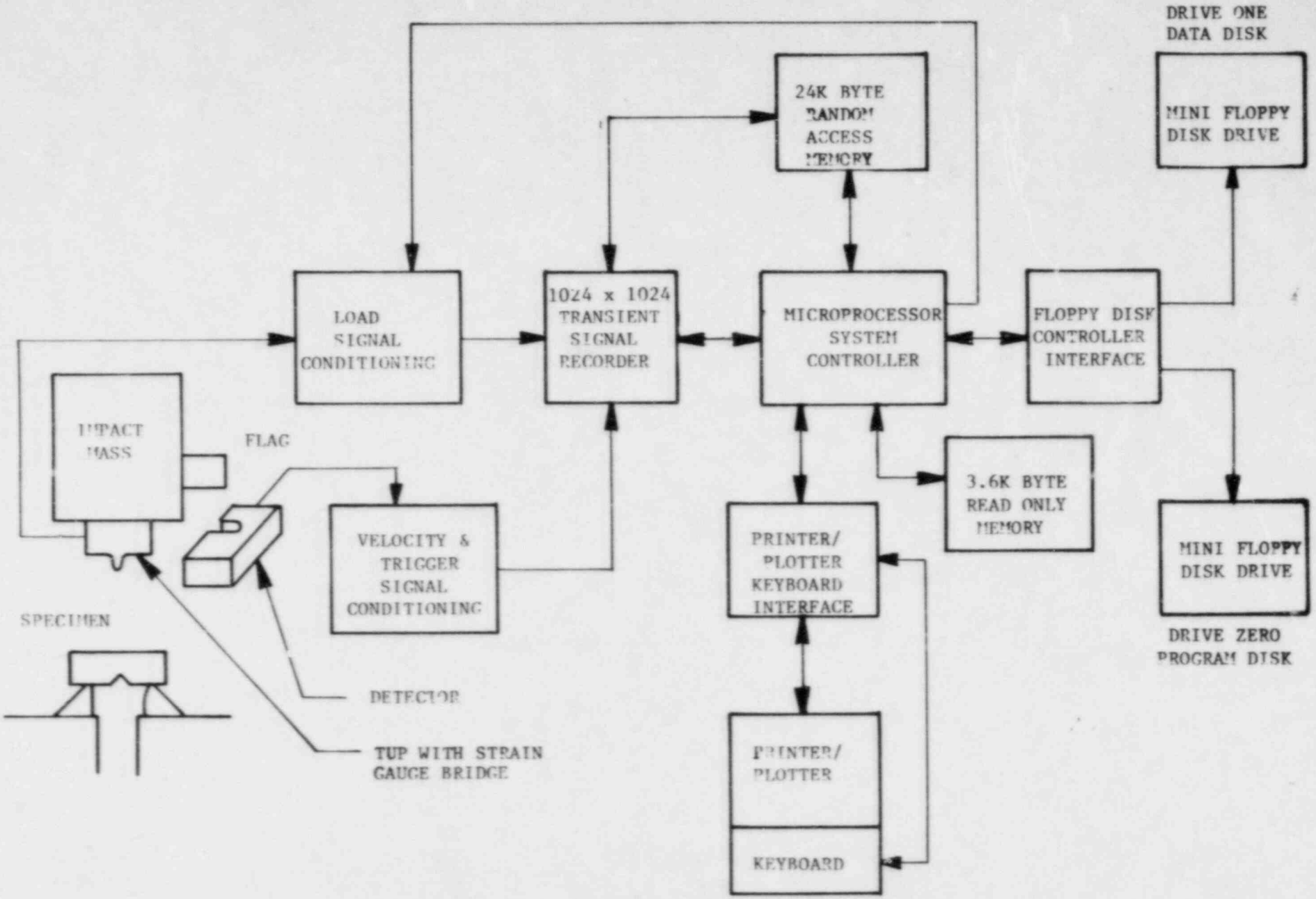

ETI-300 INSTRUMENTED IMPACT SYSTEM

FIGURE A-1

SAD-443
Rev. 0
September 1984

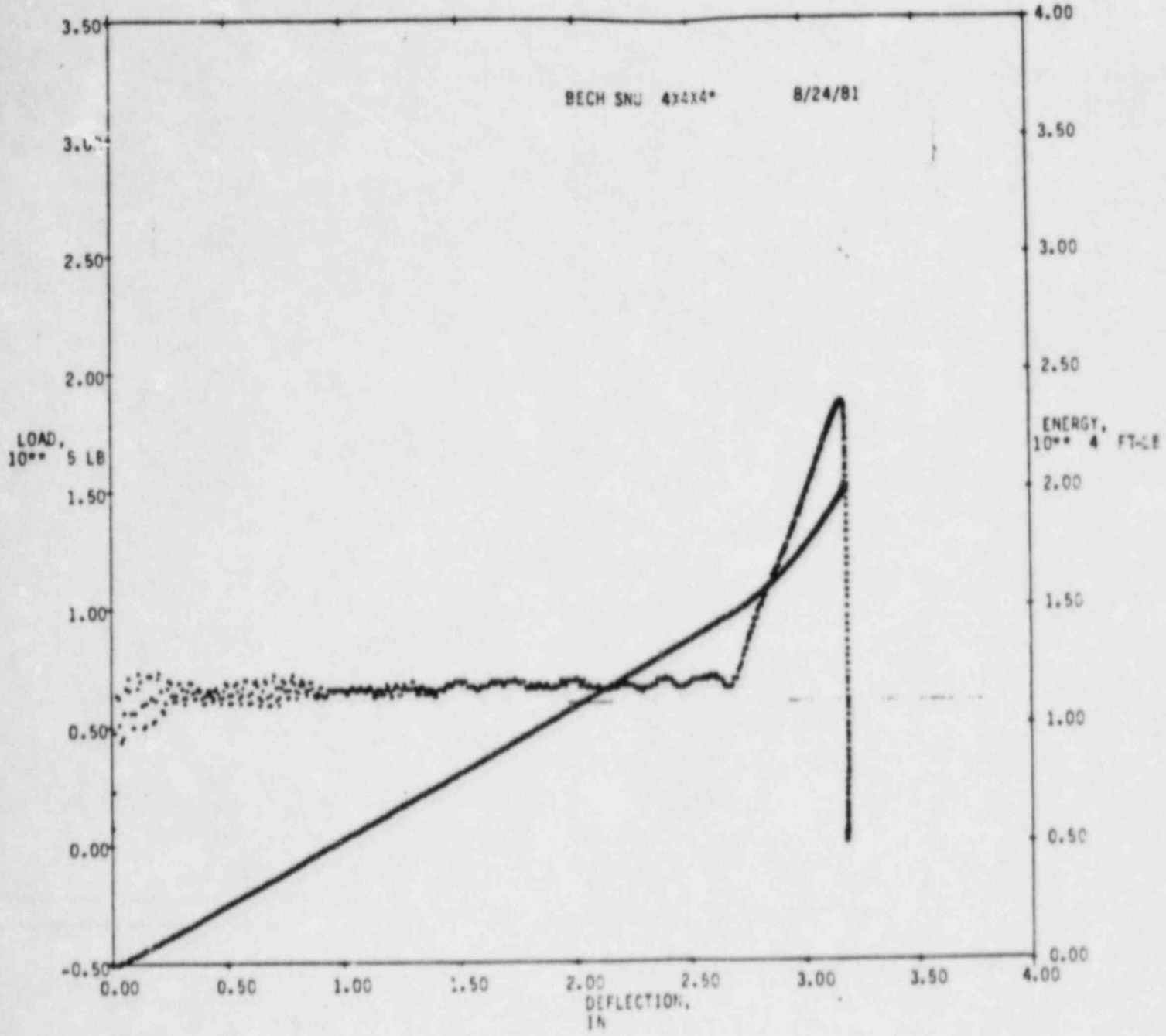

TEST	TEMP F	IMPACT VELOCITY FT/S	ENERGY FT-LB	TIME,10** 1 MSEC INIA	TOTAL	LOAD,10** 2LB MAX	ENERGY,10** 3 FT-LB INIA	PROP	TOTAL
4X4X4*	80.0	14.75	18588.03	2.72	3.21	1871	19.7	0.3	20.0

Figure A2: Typical Load and Energy Versus Deflection Plot

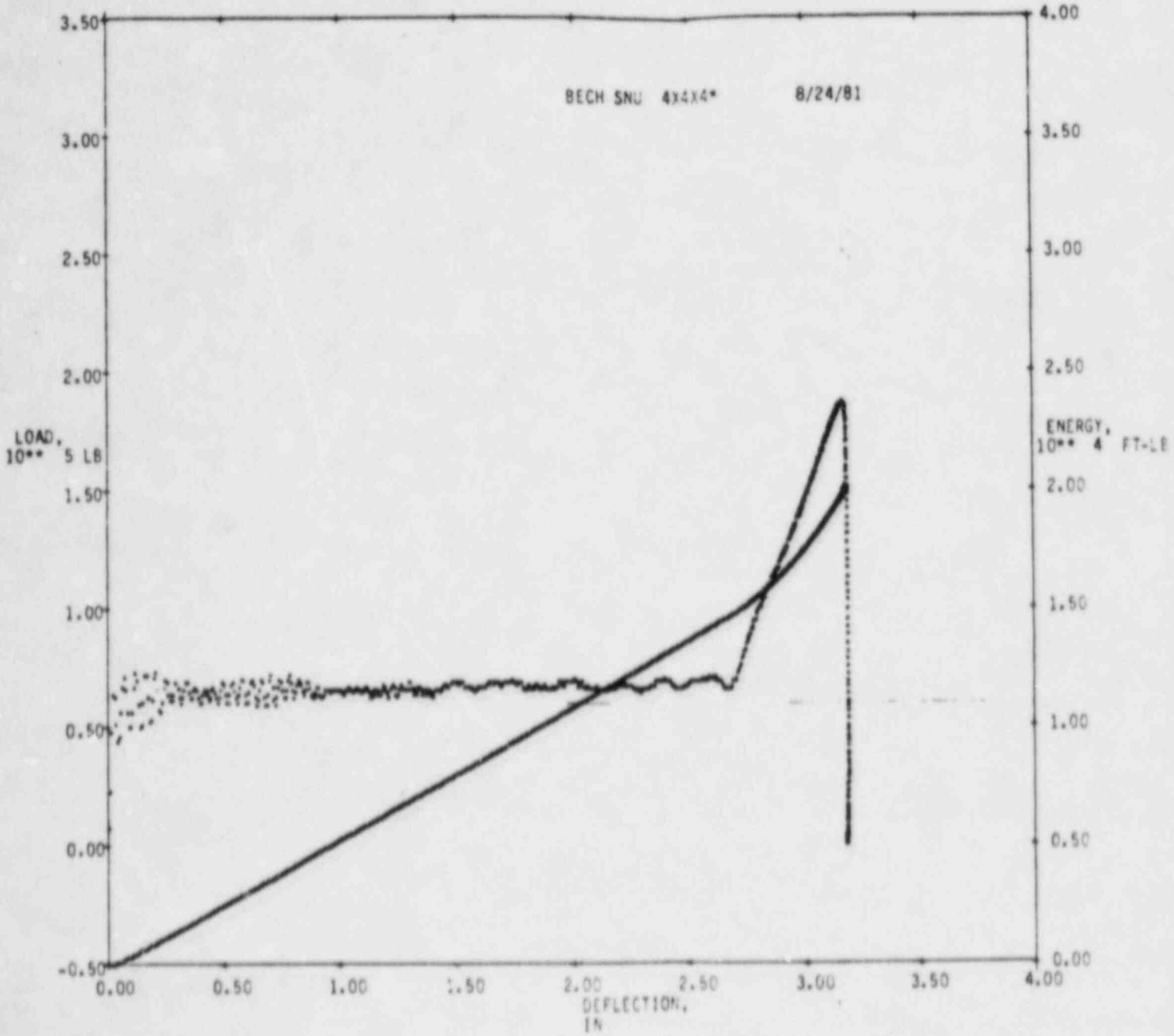

TEST	TEMP F	IMPACT VELOCITY FT/S	ENERGY FT-LB	TIME,10** 1 MSEC INIA	TOTAL	LOAD,10** 2LB MAX	ENERGY,10** 3 FT-LB INIA	PROP	TOTAL
4X4X4*	80.0	14.75	18588.03	2.72	3.21	1871	19.7	0.3	20.0

Figure A2: Typical Load and Energy Versus Deflection Plot